
Theses and Dissertations

2012

Covalent modification and inhibition of tyrosine hydroxylase by 3,4-dihydroxyphenylacetaldehyde, an endogenously produced neurotoxin relevant to Parkinson's disease

Lydia Maria Mexas Vermeer
University of Iowa

Copyright 2012 Lydia Maria Mexas Vermeer

This dissertation is available at Iowa Research Online: <http://ir.uiowa.edu/etd/1923>

Recommended Citation

Vermeer, Lydia Maria Mexas. "Covalent modification and inhibition of tyrosine hydroxylase by 3,4-dihydroxyphenylacetaldehyde, an endogenously produced neurotoxin relevant to Parkinson's disease." PhD (Doctor of Philosophy) thesis, University of Iowa, 2012. <http://ir.uiowa.edu/etd/1923>.

Follow this and additional works at: <http://ir.uiowa.edu/etd>

 Part of the [Pharmacy and Pharmaceutical Sciences Commons](#)

COVALENT MODIFICATION AND INHIBITION OF TYROSINE HYDROXYLASE
BY 3,4-DIHYDROXYPHENYLACETALDEHYDE, AN ENDOGENOUSLY
PRODUCED NEUROTOXIN RELEVANT TO PARKINSON'S DISEASE

by

Lydia Maria Mexas Vermeer

An Abstract

Of a thesis submitted in partial fulfillment of the requirements for the Doctor of
Philosophy degree in Pharmacy (Medicinal and Natural Products Chemistry) in the
Graduate College of The University of Iowa

July 2012

Thesis Supervisor: Associate Professor Jonathan A. Doorn

ABSTRACT

Parkinson's disease (PD) is a prevalent neurodegenerative disorder which affects over a million people in the United States. This disease is marked by the selective loss of dopaminergic neurons in the substantia nigra, leading to a decrease in the important neurotransmitter dopamine (DA), which is essential for the initiation and execution of coordinated movement. Currently, the exact pathogenesis behind PD is unknown, but there is evidence that both exogenous causes, such as pesticides and metals, as well as endogenous causes, such as reactive oxygen species or reactive metabolism intermediates, may play a role in the onset and progression of the disease. DA is catabolized by monoamine oxidase to 3,4-dihydroxyphenylacetaldehyde (DOPAL), which is further metabolized by aldehyde dehydrogenase and aldehyde reductase to the acid and alcohol products, respectively. Studies have demonstrated the reactivity of DOPAL with peptides and proteins, leading to covalent modification which may be detrimental to protein action. Furthermore, studies have shown that DOPAL is toxic, leading to a decrease in cell viability. Due to this, it was of interest to further study DOPAL and how it may play a role in the onset and progression of PD.

It was of particular interest to determine protein targets of DOPAL modification. Until recently, no protein targets were identified and the cellular consequence of elevated DOPAL had not been fully studied. It has been previously shown that the important enzyme, tyrosine hydroxylase (TH) is inhibited by other catechols, including DA. This enzyme catalyzes the rate-limiting step in DA synthesis, oxidizing tyrosine to L-DOPA which is further metabolized to DA. Therefore, it was of interest to determine the effect of DOPAL on TH activity. It was hypothesized that DOPAL modifies and inhibits TH,

leading to a decrease in the production of L-DOPA and DA. This work employed the use of a dopaminergic cell model (PC6-3 cells), to positively identify TH as a protein target of DOPAL modification. It also used both cell lysate as well as PC6-3 cell studies to investigate the effect of DOPAL modification on TH activity. Mass spectrometry was also utilized to determine sites of protein modification on TH.

Results show that TH is potently inhibited by DOPAL modification, leading to a significant decrease in both L-DOPA and DA. Furthermore, DOPAL inhibition appears to be slowly-irreversible, with enzyme activity showing a time- and concentration-dependent recovery after preincubation with DOPAL. A novel cloning and purification procedure was used to obtain human recombinant TH, which was used in mass spectrometry studies in which five sites of DOPAL modification were discovered. Furthermore, a real-time assay for TH activity was developed using a plate reader to spectrophotometrically observe the formation of L-DOPA over time. These data demonstrate the toxicity and potent enzyme inhibition by DOPAL and implicate DOPAL as a neurotoxin relevant in the pathogenesis of PD.

Abstract Approved _____
Thesis Supervisor

Title and Department

Date

COVALENT MODIFICATION AND INHIBITION OF TYROSINE HYDROXYLASE
BY 3,4-DIHYDROXYPHENYLACETALDEHYDE, AN ENDOGENOUSLY
PRODUCED NEUROTOXIN RELEVANT TO PARKINSON'S DISEASE

by

Lydia Maria Mexas Vermeer

A thesis submitted in partial fulfillment of the requirements for the Doctor of Philosophy
degree in Pharmacy (Medicinal and Natural Products Chemistry) in the Graduate College
of The University of Iowa

July 2012

Thesis Supervisor: Associate Professor Jonathan A. Doorn

Copyright by

LYDIA MARIA MEXAS VERMEER

2012

All Rights Reserved

Graduate College
The University of Iowa
Iowa City, Iowa

CERTIFICATE OF APPROVAL

PH.D THESIS

This is to certify that the Ph.D. thesis of

Lydia Maria Mexas Vermeer

has been approved by the Examining Committee for the thesis requirement for the Doctor of Philosophy degree in Pharmacy (Medicinal and Natural Products Chemistry) at the July 2012 graduation.

Thesis Committee: _____

Jonathan A. Doorn, Thesis Supervisor

Robert J. Kerns

Michael W. Duffel

Larry Robertson

David L. Roman

To Edna, Beulah, Blanche, Colbert, Steve, and Gary

Success is to be measured not so much by the position that one has reached in life as by the obstacles which he has overcome.

Booker T. Washington
1856-1915

ACKNOWLEDGEMENTS

I would first like to thank my thesis advisor, Dr. Jonathan A. Doorn, for his guidance and direction over the course of my graduate studies. I would also like to thank both past and current Doorn lab members; David, Erin, Jennifer, Natalie, Jinsmaa, Josie, Andy, Brigette, and especially Laurie and Virginia, who have been there with me the entire time. Thanks also to Sentinel Velociraptor and Jedi Duck for keeping the lab safe and providing entertainment when it was needed.

Special thank you to the members of my thesis committee, Dr. Robert J. Kerns, Dr. Michael W. Duffel, Dr. Larry Robertson, and Dr. David L. Roman, who offered valuable advice during my data sessions, as well as throughout my graduate career.

I can't thank my family and friends enough for all of their support, love and endless encouragement as I completed my doctorate degree. Special thanks to my parents, Kelle and Dan, who always believed I could do anything and always provided a listening ear, laughter, and love. To my sister and nephew, Melina and Danny, thank you. Also to my parents-in-law, Jim and Kim, and brother-in-law, Jake, I very much appreciate your support in pursuing my goals.

To my husband, Brant, thank you for your unwavering support. You never once questioned my decision to go to graduate school, even if it would take us to two different states, and gave more support and encouragement than I can ever thank you for. Thanks for spending so much time in Hawkeye country, even if we are Cyclone fans. I love you.

TABLE OF CONTENTS

LIST OF TABLES	ix
LIST OF FIGURES	x
LIST OF SCHEMES.....	xvi
LIST OF ABBREVIATIONS.....	xvii
CHAPTER ONE. INTRODUCTION.....	1
Parkinson's Disease	1
Etiology.....	2
Environmental or Exogenous Factors.....	3
Endogenous or Genetic Factors	6
Oxidative Stress	7
Dopamine Hypothesis.....	8
The Role of 3,4-Dihydroxyphenylacetaldehyde in Parkinson's Disease	10
Tyrosine Hydroxylase.....	11
CHAPTER TWO. STATEMENT OF HYPOTHESIS.....	13
Introduction.....	13
Hypothesis.....	14
Specific Aims.....	14
CHAPTER THREE. DOPAL AS A NEUROTOXIN CAPABLE OF PROTEIN MODIFICATION	15
Introduction.....	15
Experimental Procedures	16
Materials	16
PC6-3 Cell Culture.....	16
Mitochondrial Dysfunction (MTT Assay)	17
Trypan Blue Assay.....	18
PC6-3 Cell Lysate Collection	18
DOPAL Metabolism Studies	18
HPLC Analysis of Metabolism.....	19
DOPAL Modification of Tyrosine Hydroxylase in Cell Lysate.....	19
Western Blot Analysis of Tyrosine Hydroxylase	19
Isolation of DOPAL Modified Proteins Using An Aminophenylboronic Acid Resin	20
Proteomic Analysis of DOPAL Modified Proteins	21

Quantification of Reactive Oxygen Species	
Using Flow Cytometry.....	21
Statistical Analysis.....	22
Results.....	22
Elevated DOPAL Leads to Cell Morphological Changes	22
Elevated DOPAL Leads to Mitochondrial Dysfunction.....	24
DOPAL Elevation Causes Cell Death	25
DOPAL is Metabolized in PC6-3 Cells.....	26
DOPAL Modifies Tyrosine Hydroxylase	28
Proteomic Identification of Tyrosine Hydroxylase	
as a DOPAL Target.....	29
Elevated DOPAL Leads to Reactive Oxygen Species Production	31
Discussion.....	34
CHAPTER FOUR. INHIBITION OF TYROSINE HYDROXYLASE	
BY DOPAL.....	39
Introduction.....	39
Experimental Procedures	40
Materials	40
PC6-3 Cell Culture and Tyrosine Hydroxylase Collection.....	40
Tyrosine Hydroxylase Activity in Cell Lysate	41
Tyrosine Hydroxylase Activity in PC6-3 Cells	41
HPLC Analysis of Activity Assays.....	42
Mechanism Studies in Cell Lysate.....	42
Statistical Analysis.....	43
Results.....	44
Tyrosine Hydroxylase is Potently Inhibited in Cell Lysate	44
Tyrosine Hydroxylase is Inhibited by DOPAL in PC6-3 Cells.....	46
DOPAL Inhibition Exhibits Slow-Irreversible Element.....	47
Discussion.....	50
CHAPTER FIVE. STRUCTURE-ACTIVITY RELATIONSHIP OF DOPAL	
ANALOGUES: MECHANISM OF TOXICITY AND ENZYME	
INHIBITION.....	54
Introduction.....	54
Experimental Procedures	56
Materials	56
Mitochondrial Dysfunction (MTT Assay)	56
Tyrosine Hydroxylase Activity Assay in Cell Lysate.....	57
Tyrosine Hydroxylase Activity Assay in PC6-3 Cells	57
Relative Protein Reactivity	58
HPLC Analysis of Tyrosine Hydroxylase Activity Assays.....	58
Novel Cloning and Purification of Human Recombinant	
Tyrosine Hydroxylase (hTH) using <i>E. coli</i>	59

hTH Activity Assay and HPLC Analysis	62
Methanol-Chloroform-Water Precipitation of Tyrosine Hydroxylase	62
Mass Spectrometry Analysis to Identify DOPAL Adducts on Tyrosine Tyrosine Hydroxylase	63
Novel Real-Time Assay to Monitor Tyrosine Hydroxylase Activity	64
High-Throughput Screening Assay.....	65
Statistical Analysis	66
Results.....	67
Structure-Activity Relationship of DOPAL Analogues	67
Phenylacetaldehyde Toxicity and Tyrosine Hydroxylase Inhibition.....	69
3-Methoxy-4-hydroxyphenylacetaldehyde Toxicity and Tyrosine Hydroxylase Inhibition	70
3,4-Dimethoxyphenylacetaldehyde Toxicity and Tyrosine Hydroxylase Inhibition	72
3,4-Dihydroxyphenylacetone Toxicity and Tyrosine Hydroxylase Inhibition	74
Summary of Structure-Activity Relationship Studies.....	76
Novel Cloning and Purification of hTH.....	79
Mass Spectrometry Identification of DOPAL Adducts	84
Novel Plate Reader Assay to Monitor Tyrosine Hydroxylase Activity	94
High-Throughput Screening Assay.....	96
Discussion.....	98
 CHAPTER SIX. RESEARCH SUMMARY	 105
Restatement of Hypothesis	105
Discussion of Specific Aims	106
Specific Aim 1: Investigate DOPAL as a Neurotoxin and Identify Protein Targets of Modification.....	106
Specific Aim 2: Determine the Effect of DOPAL on Tyrosine Hydroxylase Activity	107
Specific Aim 3: Elucidate Mechanisms by Which DOPAL Inhibits Tyrosine Hydroxylase	108
Conclusions and Implications for Parkinson's Disease	109
Future Direction of the Project	111
Circular Dichroism Studies of Structural Changes	111
Investigation of DOPAL Trafficking.....	112
Effect of Tyrosine Hydroxylase Phosphorylation on DOPAL-Mediated Inhibition	112
Determine the Structure of DOPAL Adduct.....	113
Identification of Other DOPAL Protein Targets.....	113

APPENDIX A.	THE SYNTHESIS OF 3,4-DIMETHOXYPHENYLACETALDEHYDE	115
	Introduction.....	115
	Experimental Procedures	116
	Materials	116
	Synthesis Method.....	116
	Results.....	117
APPENDIX B.	THE SYNTHESIS OF 3,4-DIHYDROXYPHENYLACETONITRILE	118
	Introduction.....	118
	Experimental Procedures	119
	Materials	119
	Synthesis Method.....	119
	Results.....	119
APPENDIX C.	THE BIOSYNTHESIS OF 3-METHOXY-4-HYDROXYPHENYLACETALDEHYDE.....	121
	Introduction.....	121
	Experimental Procedures	122
	Materials	122
	Synthesis Method.....	122
	MOPAL Extraction.....	122
	HPLC Analysis	123
	Results.....	123
APPENDIX D.	SPECTRA	124
REFERENCES	126

LIST OF TABLES

Table 5.1	Summary of key structural features of DOPAL and analogues, and their relative protein reactivity with BSA as determined by the NBT assay.....	68
Table 5.2	Summary of DOPAL and Analogue Toxicity, and TH Inhibition in Lysate and PC6-3 Cells.....	77
Table 5.3	hTH protein recovery per step and enzyme characterization.....	83
Table 5.4	hTH+DOPAL adducted peptides determined via mass spectrometry	86
Table 5.5	Comparison of average specific activities between previously published HPLC method and the plate reader assay.....	96

LIST OF FIGURES

Figure 1.1	Loss of staining in the substantia nigra indicates decreased DA neuron presence, as occurs in PD.....	1
Figure 1.2	The organochlorine pesticide dieldrin. Evidence shows this compound may play a role in the selective dopaminergic cell death observed in PD.....	4
Figure 1.3	Structure of molinate (A) and molinate sulfone (B). The sulfone metabolite has been shown to inhibit ALDH activity.....	5
Figure 1.4	Structures of the products of lipid peroxidation, 4-HNE, which inhibits AKR activity, and MDA which inhibits both ALDH and AKR activity. Both lead to an increase in the reactive intermediate of DA metabolism, DOPAL	7
Figure 3.1	Images of PC6-3 cells after 1 h incubation with 5, 10, 25, or 50 μM DOPAL. Arrows indicate cellular blebbing and loss of uniform cellular shape (10, 25, and 50 μM). These signs are indicative of early cell dysfunction.....	23
Figure 3.2	PC6-3 cells 2 h after addition of varying concentrations of DOPAL. Arrows indicate significant blebbing and loss of cell shape (5, 10 μM) and the introduction of apoptotic bodies (25, 50 μM). This demonstrates the highly potent toxicity DOPAL induces in cells after just a 2 h incubation.....	24
Figure 3.3	PC6-3 cells incubated with varying concentrations of DOPAL for 2 h. Mitochondrial function was assessed using the MTT assay and cells display a concentration-dependent decrease in function. The low, pathologically relevant concentration of just 10 μM leads to significant dysfunction as compared to controls. All values shown represent the mean \pm SEMs ($n = 4$). **indicates significance from control cells.....	25
Figure 3.4	PC6-3 cells incubated with DOPAL for 2 h. Trypan blue used to assess cell viability, with cells exhibiting a concentration-dependent decrease in viability. Low concentrations of only 5 μM DOPAL lead to significant cell death as compared to controls. All values shown represent the mean \pm SEMs ($n = 3$). **indicates significance from control cells.....	26

Figure 3.5	DOPAL metabolism in dopaminergic PC6-3 cells. (A) DOPAL is taken up by cells as indicated by a decrease in concentration in the extracellular media over time. (B) DOPAC is produced from ALDH metabolism of DOPAL. (C) DOPET is produced by AKR metabolism of DOPAL. For all graphs all values shown represent the mean \pm SEMs ($n = 3$). DOPAC and DOPET graph symbols are the same as shown in the DOPAL graph	27
Figure 3.6	TH from PC6-3 cells was incubated with DOPAL for 4 h at 37°C. Western blot analysis reveals a concentration-dependent decrease in antibody recognition of TH indicating DOPAL interferes with ability of antibody to bind to protein.....	28
Figure 3.7	Chemistry of APBA reactivity with vicinal diols (i.e. such as those found on catechols). The resin reacts specifically with diols in basic conditions (pH > 8.0) with a bond strong enough to withstand wash conditions in neutral pH. Acid release steps (pH = 2) lead to separation of the boronic acid and vicinal diol.	30
Figure 3.8	Cells treated with either no DOPAL or 50 μ M for two h and then subjected to APBA resin for separation were then run on SDS-PAGE for western blot analysis of TH. (A) The control cells (i.e. no DOPAL) exhibit no staining for TH in the release fractions, indicating there was no major DOPAL modification of TH. (B) Cells treated with DOPAL demonstrate DOPAL-modified TH in the release fractions (lanes 5-8), as denoted by arrows.	31
Figure 3.9	Representative scatter plots of flow cytometry data on DOPAL-treated cells. Data demonstrates a slight increase in fluorescence of DHE in 5 and 10 μ M DOPAL-treated cells as compared to controls, indicative of increased super oxide anion, while fluorescence of DCFDA decreases in both DOPAL treated conditions, indicating less hydrogen peroxide production.	33
Figure 3.10	PC6-3 cells incubated with 5 or 10 μ M DOPAL for 1 h and then subjected to flow cytometry to determine levels of superoxide anion and hydrogen peroxide. Elevated DOPAL leads to increased superoxide anion and decreased hydrogen peroxide production. All values shown represent the mean \pm SEMs ($n = 3$). **indicates significance from control cells where no DOPAL was added.....	34

Figure 4.1	<p>Treatment of PC6-3 cell lysate with varying concentrations of DOPAL leads to TH inhibition and a decrease in L-DOPA production. (A) L-DOPA production over 2 h shows significant inhibition by DOPAL. (B) Enhancement of 4.1A showing DOPAL treatment experiments. (C) Comparison of initial linear slopes shows the concentration-dependent decrease in L-DOPA production. Values shown represent the mean \pm SEMs ($n = 4$). **Significantly different from the control ($p < 0.05$). In all graphs: (●) control, (▽) 0.1 μM DOPAL, (□) 0.5 μM DOPAL, (▲) 1.0 μM DOPAL, (◇) 2.5 μM DOPAL, (◆) 5.0 μM DOPAL, and (○) 10.0 μM DOPAL.....</p>	45
Figure 4.2	<p>NGF-differentiated PC6-3 cells incubated with 10 μM tyrosine and MDA, and 5 μM DOPAL for 2 h. Cells were lysed and subjected to HPLC analysis to determine L-DOPA and DA production. (A) L-DOPA production over time; elevation in DOPAL leads to ~44% TH inhibition. (B) Concomitantly, DA production is decreased by a similar percent due to a decrease in L-DOPA. Values shown represent the mean \pm SEMs ($n = 3$)</p>	47
Figure 4.3	<p>TH activity assays to determine recovery of L-DOPA production after inhibition by DOPAL (5, 10, 20 μM) for 30, 60, or 90 min preincubation. Upon removal of DOPAL, there was re-introduction of tyrosine and BH₄ (100 μM, 0.5 mM, respectively) and time points were taken as shown in the figure. (A), (B), and (C) demonstrate recovery of activity which displays time and concentration-dependent elements and 30, 60 and 90 min, respectively. (D) Indicates a linear decrease in recovery of TH as preincubation time and DOPAL concentration increase as determined by HPLC analysis. ($n = 3$ for all studies). In all graphs: (●) control, (*) 5 μM DOPAL, (▲) 10 μM DOPAL, (■) 20 μM DOPAL</p>	49
Figure 5.1	<p>PAL toxicity and TH inhibition profile. (A) PC6-3 cells incubated with increasing concentrations of PAL for 2 h. MTT analysis of mitochondrial function showed concentration-dependent increase in dysfunction. (B) Cell lysate activity assay in the presence of PAL; increased PAL demonstrated decreased L-DOPA production. (C) 20 μM PAL on PC6-3 cells lead to ~56% decrease in L-DOPA production. All values shown represent the mean \pm SEMs ($n = 3$). **indicates significant mitochondrial dysfunction as compared to control cells ($p < 0.05$).....</p>	70

Figure 5.2	MOPAL toxicity and TH inhibition. (A) PC6-3 cells incubated with MOPAL for 2 h demonstrated minimal toxicity, with significance from the controls only seen at 50 μ M. (B) TH inhibition in cell lysate. 20 μ M MOPAL lead to ~44% inhibition. (C) MOPAL lead to ~50% inhibition of TH in PC6-3 cells when 10-12 μ M MOPAL was found intracellularly. All values shown represent the mean \pm SEMs ($n = 3$). **indicates significance from control cells ($p < 0.05$).....	72
Figure 5.3	DMPAL toxicity and TH inhibition in lysate and PC6-3 cells. (A) MTT results demonstrating no toxicity to PC6-3 cells in the presence of DMPAL after 2 h. (B) TH+ cell lysate incubated with 20 μ M DMPAL exhibited ~28% inhibition as compared to controls. (C) PC6-3 cells with 9-10 μ M DMPAL intracellularly showed a little over 30% inhibition of TH activity. All values shown represent the mean \pm SEMs ($n = 3$).....	74
Figure 5.4	DHPAN toxicity and TH inhibition in lysate and cells. (A) MTT results when investigating varying low concentrations of DHPAN after 2 h. Cells show no significant toxicity compared to controls. (B) Pilot studies studying the effect of high concentrations of DHPAN. 200 μ M DHPAN exhibits mitochondrial dysfunction similar to that of 50 μ M DOPAL. (C) DHPAN shows inhibition of TH in cell lysate (~25% at 20 μ M). (D) DHPAN leads to no significant inhibition in PC6-3 cells. Concentrations of DHPAN were found to be only 0-1 μ M intracellularly. All values shown represent the mean \pm SEMs ($n = 3$ for A, C and D) ($n = 2$, for B). **indicates significant from the control ($p < 0.05$).....	76
Figure 5.5	TH inhibition by DOPAL and analogues (PAL, MOPAL, DMPAL, and DHPAN) in cell lysate. Analogues show decreased inhibition of TH, indicating DOPAL is a more potent inhibitor of TH activity. All values shown represent the mean \pm SEMs ($n = 3$ for all) ** indicates significant from the control ($p < 0.05$).....	78
Figure 5.6	TH inhibition in PC6-3 cells by DOPAL and analogues. DOPAL shows more potent inhibition of TH activity than analogues at lower intracellular concentrations. The table shows the levels of each compound in the cells as determined by HPLC analysis. All values shown represent the mean \pm SEMs ($n = 3$ for all) ** indicates significant from DOPAL incubated cells ($p < 0.05$).....	79
Figure 5.7	Construct used for the cloning of hTH. This pMal vector contained a maltose-binding protein which was used in the purification process later	80

Figure 5.8	SDS-PAGE analysis of each step in the purification of hTH using the novel cloning and purification technique developed. (A) Typical gel obtained after amylose resin. Lane 1: Load (Crude protein); Lane 2: Flow (unbound proteins); Lanes 3-6: Wash, Lanes 7-20: Eluted proteins with competing concentration of maltose. 100 kDa band is indicative of hTH-MBP protein, which was collected. (B) Gel after TEV cleavage for 8 h; upper band is hTH, lower band is MBP. (C) After anion exchange column. MBP elutes first, hTH is second (lane 3). (D) Western blot analysis of pure hTH; band at ~60 kDa is indicative of hTH.....	82
Figure 5.9	TH activity over the purification process using HPLC analysis. L-DOPA production increases as the enzyme is purified, indicating the process does not impede or negatively affect the enzyme, and leads to higher tyrosine turnover as TH is purified.....	83
Figure 5.10	Typical MS spectra of hTH digest by trypsin for 8 h at 37°C. (A) depicts hTH with no DOPAL, while (B) is the incubation of hTH with 50 µM DOPAL for 4 h prior to the addition of trypsin. All samples were run through a Bio-Rad spin column to remove excess DOPAL in order to ensure adducts were on whole hTH. Gradient separation was 40 min, this figure demonstrates the first 30 min of the run; no significant peptides were found after 30 min.	85
Figure 5.11	NCBI macromolecular structure view of hTH (1) (A). One subunit has been expanded to better visualize the adducts. (B) shows adducts R481, R320, and R226, while (C) shows K238 as well as R320, and R226. As mentioned in the text, this model does not contain the adducts on the peptide from 39-51, which are hypothesized to be the reason behind the decrease in antibody recognition of TH incubated with DOPAL.....	88
Figure 5.12	Y- and b-ions corresponding to 5 DOPAL adducts found on hTH upon MS/MS analysis of the protein after trypsin. (A) aa220-226 with one DOPAL adduct (R 226). (B) aa312-320 with one DOPAL adduct (R320). (C) aa39-51 with 2 DOPAL adducts (R43, R51). (D) aa227-238 with one DOPAL adduct (K238). (E) aa464-481 with one DOPAL adduct (R481).	89
Figure 5.13	Enlarged view of the adduct on peptide 220-226 (1), which contains a DOPAL adduct on R226. Leu206 has been demonstrated to be an important residue to the overall structure of the protein. Furthermore, R226 is a part of an important structural salt bridge and adduction is predicted to lead to destabilization of hTH.....	91

Figure 5.14	An enlargement of the adduct on R320 (1), which is in close proximity to the site of iron binding (gray ball). F300 and F309 are shown due to their importance in the coordinating of the iron atom in each subunit. DOPAL adduction in this location is predicted to lead to structural changes which may cause incomplete or improper binding of iron, partially explaining the dramatic loss of enzyme activity in the presence of DOPAL.....	92
Figure 5.15	L-DOPA production as measured by the plate reader assay. L-DOPA is oxidized by sodium periodate, and then further cyclizes to dopachrome which can be measured at 475 nm. Low micromolar concentrations of DOPAL lead to decreased TH activity, and higher levels of DOPAL 3IT, and CoCl ₂ lead to almost complete inhibition of L-DOPA production. All values shown represent the mean ± SEMs (<i>n</i> = 5 for Control, DOPAL, 3IT, <i>n</i> = 3 for CoCl ₂). **indicates significance from control wells.	95
Figure 5.16	High-throughput screening (HTS) of hTH plate reader assay. 48 wells were used for positive (no inhibition) and 48 wells used for negative control (100 μM CoCl ₂). Assay was performed for 180 min at 90 sec read intervals. (A) depicts spectra obtained, exhibiting high signal-to-noise (S/N) ratio, and a long stable screening time (between 75-180 min). (B) Z-factor over time of assay shows stability over the course of the assay well above the accepted threshold of 0.5. Z-factor values ranged between 0.825 and 0.925, a robust value which makes this ideal for HTS.....	97
Figure D.1	300 MHz ¹ H NMR of compound 1; 3,4-dimethoxyphenylacetaldehyde (DMPAL), CDCl ₃	124
Figure D.2	300 MHz ¹ H NMR of compound 1; 3,4-dihydroxyphenylacetoneitrile (DHPAN), DMSO-d ₆	125

LIST OF SCHEMES

Scheme 1.1	DA synthesis starting with TH which oxidizes tyrosine to L-DOPA. DA is metabolized by MAO to DOPAL, which is further oxidized to DOPAC or reduced to DOPET	9
Scheme 1.2	DA auto-oxidation to a quinone, which has the potential to interact with and modify protein through Cys residues	10
Scheme 5.1	Tyrosine is metabolized to L-DOPA by TH. The resulting L-DOPA is oxidized by sodium periodate (NaIO ₄), and subsequently rearranges to dopachrome, a chromophore which absorbs at 475 nm.....	93
Scheme 6.1	DOPAL is hypothesized to be a neurotoxin, capable of causing mitochondrial dysfunction and cell death. Oxidative stress may lead to inhibition of DOPAL metabolism. The data presented here predicts elevated DOPAL would modify and inhibit intracellular TH (and possibly other proteins), leading to a decrease in DA production	111
Scheme A.1	1-step synthesis of DMPAL (1) using 4-allyl-1,2-dimethoxybenzene (2).	115
Scheme B.2	Synthesis of DHPAN (3) from 3,4-methylenedioxyphenylacetonitrile (4).....	118
Scheme C.1	Biosynthesis of MOPAL (5) from 3-methoxytyramine (6)	121

LIST OF ABBREVIATIONS

6,7-Dimethyl-5,6,7,8-tetrahydropterine Hydrochloride	DMPH ₄
2'-7'-Dichlorodihydrofluorescein diacetate	DCFDA
3-(4,5-dimethylthiazol-2-yl)-2,3-diphenyltetrazolium bromide	MTT
3,4-Dihydroxyphenylacetaldehyde	DOPAL
3,4-Dihydroxyphenylacetic acid	DOPAC
3,4-Dihydroxyphenylacetonitrile	DHPAN
3,4-dihydroxyphenylethanol	DOPET
3,4-Dimethoxyphenylacetaldehyde	DMPAL
3-Hydroxy-4-methoxyphenylacetaldehyde.....	MOPAL
4-hydroxy-2-nonenal.....	4-HNE
Acetonitrile	ACN
Aldehyde dehydrogenase	ALDH
Aldehyde reductase	AKR
Amino acid decarboxylase	AADC
Aminophenylboronic acid.....	APBA
Ampicillin	Amp
β-D-1-thiogalactopyranoside	IPTG
Bovine serum albumin	BSA
Catechol-o-methyl transferase	COMT
Dihydroethidium	DHE
Dimethylsulfoxide.....	DMSO

Dopamine	DA
Electrospray ionization mass spectrometry	ESI-MS
High performance liquid chromatography	HPLC
High-throughput screening	HTS
Human recombinant tyrosine hydroxylase	hTH
L-3,4-dihydroxyphenylalanine.....	L-DOPA
Leucine-rich repeat kinase 1	LRRK2
Malondialdehyde.....	MDA
Monoamine oxidase	MAO
Nerve growth factor	NGF
Nitroblue tetrazolium	NBT
Parkinson's disease	PD
Phenylacetaldehyde.....	PAL
Reactive oxygen species	ROS
Sodium cyanoborohydride	NaCNBH ₃
Sodium dodecylsulfate polyacrylamide gel electrophoresis	SDS-PAGE
Structure-activity relationship.....	SAR
Tetrahydrobiopterin	BH ₄
Tris-buffered saline with Tween.....	TBST
Trifluoroacetic acid.....	TFA
Tyrosine hydroxylase.....	TH
Vesicular monoamine transporter 2	VMAT2

CHAPTER ONE

INTRODUCTION

Parkinson's Disease

First described by James Parkinson in 1817, Parkinson's disease (PD) is a neurodegenerative disorder which affects over a million people in the United States today (2). PD has a number of symptoms, including both cognitive and motor disruptions. Affecting the pars compacta of the substantia nigra region in the midbrain, this disease leads to the selective loss of dopaminergic neurons, causing a decrease in the important neurotransmitter dopamine (DA) (3). DA is necessary for the initiation and execution of coordinated movement. Figure 1.1, as adapted from A.D.A.M. Navigator, depicts the location of the midbrain, and demonstrates decreased staining in the substantia nigra in PD brains, indicating the loss of DA neurons.

Substantia nigra located in the midbrain

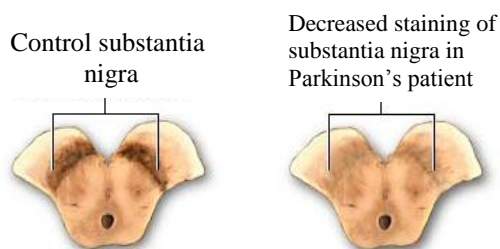


Figure 1.1 Loss of staining in the substantia nigra indicates decreased DA neuron presence, as occurs in PD.

Furthermore, evidence indicates the presence of protein aggregation in postmortem brains of PD patients, which are known as Lewy bodies, and contain a variety of proteins, including α -synuclein (2). Early symptoms of PD include a decrease in sense of smell, sleep disturbances, as well as digestive disruptions (4). Motor symptoms include a resting tremor, which usually begins on one side of the body, as well as muscle stiffness, and bradykinesia, or slowness in the initiation of movement (3).

Current treatments are varied, but the most common is the administration of levodopa (L-DOPA), which is the direct precursor to DA, and can help alleviate motor symptoms. L-DOPA is generally given in conjunction with carbidopa to help decrease peripheral metabolism; but unfortunately, this drug does not halt the progression of the disease. Patients tend to develop tolerance over time (4-6 years) and the remaining DA neurons are no longer able to properly store or metabolize the DA produced (5). Other treatments include the use of monoamine oxidase (MAO) inhibitors to decrease the metabolism of DA, as well as surgical treatments such as performing a pallidotomy in which an electrode is used to destroy a small part of the globus pallidus. This helps decrease involuntary movement associated with PD. Recent work has been done into deep-brain stimulation of the substantia nigra in order to help regain smooth movement (6). Furthermore, there are drug treatments which act as agonist of the D2 receptor, which have been shown to help alleviate symptoms associated with the disease (7).

Etiology

Currently, the pathogenesis behind PD is unknown; however, there are a variety of factors that are hypothesized to play a role, including both genetic or heredity factors, as well as both exogenous and endogenous toxins.

Environmental or Exogenous Factors

There are a number of environmental toxins, including a variety of pesticides, that are thought to play a role in the onset of PD. Dieldrin, an organochlorine pesticide was used frequently from the 1950's until the 1970's as an insecticide to control soil pests such as termites and grasshoppers (8). Figure 1.2 shows the structure of dieldrin, which contains six chlorines and an epoxide ring, and is very lipophilic. Surprisingly, this compound is quite stable, and persists in nature even though it has been banned from use since the 1970's (9, 10). Studies have shown dieldrin to be present in the post-mortem brains of PD patients as compared to age-matched control groups with no PD diagnosis (11, 12). The exact mechanism of action of dieldrin is unknown, but studies have been conducted to determine how increased levels of the pesticide affect dopaminergic neurons. Animal models, including rats and ducks, when chronically fed dieldrin exhibited significantly depleted levels of DA, as well as altered vesicular monoamine transporter 2 (VMAT2), which is responsible for DA transport into vesicles after synthesis (13, 14). Furthermore, there is evidence that dieldrin exposure leads to an increase in reactive oxygen species (ROS) production, as well as apoptotic cell death in PC12 and N27 dopaminergic cell lines (15, 16).

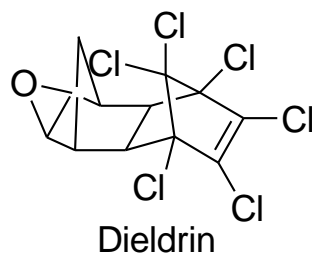


Figure 1.2 The organochlorine pesticide dieldrin. Evidence shows this compound may play a role in the selective dopaminergic cell death observed in PD.

There is also some evidence implicating the herbicide molinate, which was used in the United States until 2009. Studies in our lab and others have shown this compound to inhibit the action of ALDH, leading to an increase in the reactive product of MAO metabolism of DA, 3,4-dihydroxyphenylacetaldehyde (DOPAL) (17, 18). It is hypothesized that the metabolites of molinate are primarily responsible for the toxic effects that are observed in cell models; mainly, oxidation of the thiol moiety. Figure 1.3 depicts the structure of molinate and the oxidized product (19). It was concluded in our lab findings that the sulfone metabolite was a potent inhibitor of ALDH activity, leading to an alteration in the DA metabolism pathway (17).

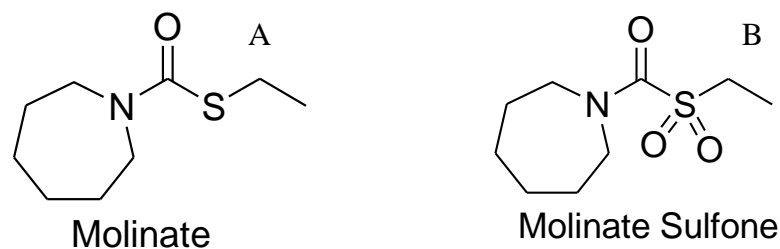


Figure 1.3 Structure of molinate (A) and molinate sulfone (B). The sulfone metabolite has been shown to inhibit ALDH activity.

Other exogenous factors may include exposure to metals, such as manganese, copper and iron, all of which are known to cross the blood-brain barrier and have been implicated as being factors that may lead to the onset of the disease. There are studies that demonstrate an increased level of metal ions in the brains of patients with PD, particularly in the substantia nigra (20, 21). Accumulation of free iron in the substantia nigra can lead to the production of reactive oxygen species (ROS), which could lead to a decrease in cell viability and ultimately death. It is important to note that copper has been shown to play a role in the aggregation of α -synuclein, through the binding of a specific site in the N-terminus, leading to conformational changes and protein aggregation. A-synuclein is known to be a large part of Lewy bodies, or protein aggregates, which are found in the post-mortem brains of PD patients (22). Furthermore, exposure to manganese leads people to display parkinson-like symptoms, even though it affects a different part of the brain than typical PD patients, leading to death of the pallidial system as opposed to the striatal region (23)

Endogenous or Genetic Factors

There are also a variety of possible endogenous and genetic factors that are hypothesized to play a role in the onset of PD. While the percentage of genetically related PD cases is low (10%, (24)), several genes have been identified that when mutated, lead to early-onset PD; including, *parkin*, leucine-rich repeat kinase (LRRK2), and the previously mentioned, α -synuclein.

Mutations in the *parkin* gene are generally associated with early-onset PD, and can lead to significant changes to mitochondrial function and cause cell vulnerability to oxidative stress. Furthermore, *parkin* is involved in the ubiquitin proteasome pathway; therefore, mutations to this gene could lead to changes in the ability of the cell to properly dispose of aged or incorrectly folded proteins (25).

LRRK2 mutations are the most commonly associated genetic factor behind autosomal dominant PD. Generally, the pathogenesis behind this mutated gene is varied; patients will demonstrate Lewy bodies, as well as striatal degeneration, and sometimes neurofibrillary tangles. This gene mutation prevalence among different ethnicities varies, and while the function of LRRK2 is currently not known, it is hypothesized the toxicity behind mutation is due to kinase activity (26-29).

Finally, α -synuclein has been shown to be the major protein component in Lewy bodies. While the exact function of this protein in the cell is unknown, there is evidence that α -synuclein interacts directly with lipids and membranes (30). Furthermore, studies have shown that overexpression of α -synuclein impairs macroautophagy, a process by which cells degrade cytoplasmic proteins (31). Combined, these genetic factors are

thought to play a role in the onset and progression of PD, especially in cases of early onset Parkinson's, where patients are well below the median age of 70.

Oxidative Stress

Reactive oxygen species (ROS) and products of lipid peroxidation are known to cause detrimental effects *in vivo*; including, protein modification, oxidation of amino acids, and a decrease in cell viability when levels of ROS are elevated. Examples of lipid peroxidation products include, 4-hydroxy-2-nonenal (4-HNE), and malondialdehyde (MDA) depicted in Figure 1.4, both of which have been shown to have cellular consequences (32). MDA in particular has demonstrated the ability to inhibit the important enzymes aldehyde dehydrogenase (ALDH) and aldehyde reductase (AKR), which in turn leads to a decrease in metabolism of DOPAL, a reactive DA metabolite (33). Furthermore, 4-HNE has also been implicated in inhibition of ALDH, as well as protein modification and inhibition (34, 35). There is also evidence of elevation in 4-HNE levels in the brains of PD patients, indicating these could play a role in disease pathogenesis (36, 37).

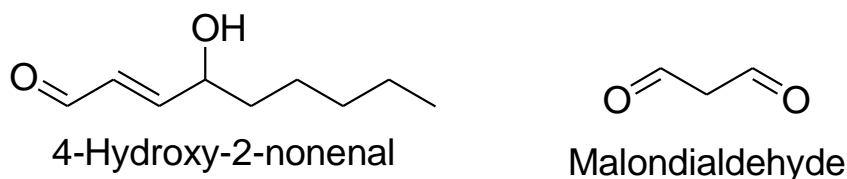
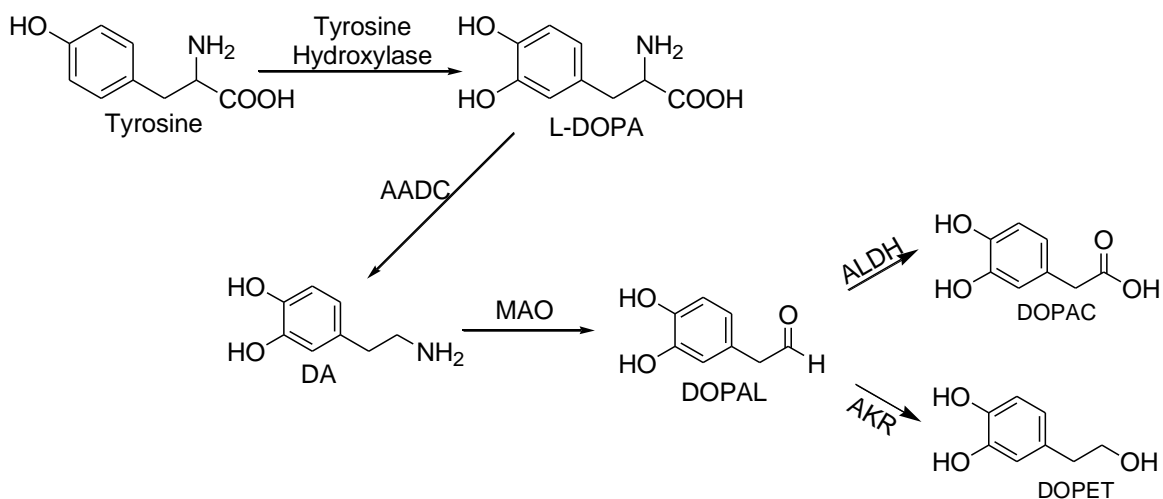


Figure 1.4 Structures of the products of lipid peroxidation, 4-HNE, which inhibits AKR activity, and MDA which inhibits both ALDH and AKR activity. Both lead to an increase in the reactive intermediate of DA metabolism, DOPAL.

ROS include superoxide anion, hydrogen peroxide, and a hydroxyl radical. While ROS production is important to cell viability, over production of these species can lead to lipid peroxidation and protein modification. Cells have mechanisms to decrease some ROS, including superoxide dismutase (SOD), and catalase, which metabolize superoxide anion and hydrogen peroxide, respectively (38). It is important to note the brain is known to be highly susceptible to oxidative stress because it has a high metabolic rate, as well as lower levels of antioxidants and a large number of polyunsaturated lipids, which are targets of peroxidation by ROS (39).

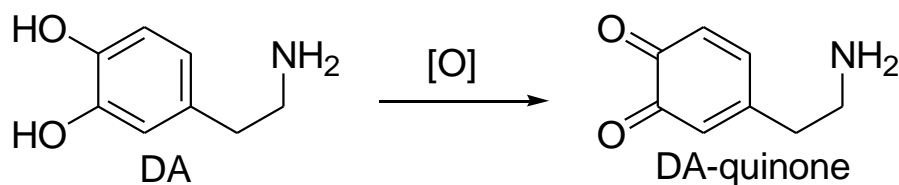
Dopamine Hypothesis

DA synthesis begins with the hydroxylation of tyrosine to L-DOPA catalyzed by the rate-limiting tyrosine hydroxylase (TH). L-DOPA is further metabolized to DA by L-aromatic amino acid decarboxylase (AADC) (40). DA is then transported into vesicles by vesicular monoamine transporter 2 (VMAT2), or is metabolized in a reaction catalyzed by MAO to the reactive intermediate, 3,4-dihydroxyphenylacetaldehyde (DOPAL), which is further oxidized by ALDH to 3,4-dihydroxyphenylacetic acid (DOPAC), or reduced by AKR to 3,4-dihydroxyphenylethanol (DOPET) as seen in Scheme 1.1.



Scheme 1.1 DA synthesis starting with TH which oxidizes tyrosine to L-DOPA. by MAO to DOPAL, which is further oxidized to DOPAC or reduced to DOPET.

It was previously hypothesized that DA could be a causative factor behind PD. This was due to a variety of reasons; including, DA has the potential to auto-oxidize, leading to the formation of a DA-quinone (Scheme 1.2), as well as lead to the production of ROS (41). Furthermore, the DA-quinone is a soft electrophile, which has the potential to lead to protein modification by interacting with soft nucleophiles such as those containing thiol groups. There are studies that demonstrate the reactivity of the DA-quinone with Cys residues in proteins, and some that also show there are adducts on Cys residues in the brains of PD patients (42, 43).



Scheme 1.2 DA auto-oxidation (i.e. [O]) to a quinone, which has the potential to interact with and modify protein through Cys residues

It is important to note, that recent work has demonstrated that while DA is reactive with proteins upon auto-oxidation, it rapidly rearranges to form dopaminochrome in the absence of thiols (44, 45), and furthermore, DA has been shown to be significantly less toxic and reactive than its MAO metabolite, DOPAL (46). It requires many times the concentration of DOPAL to cause cellular toxicity, and is significantly less reactive with proteins than DOPAL is. Combined, these results indicate that DA does not play a large role in cytotoxicity and protein modification.

The Role of 3,4-Dihydroxyphenylacetaldehyde in Parkinson's Disease

As described above, DOPAL is the MAO metabolite of DA. This reactive intermediate contains two functional groups: a catechol and an aldehyde. As previously mentioned, this metabolite has been found to be several orders of magnitude more toxic than DA (46). Physiological concentrations of DOPAL have been measured to be 2-3 μ M, and it was demonstrated that when levels are slightly elevated (~6.6 μ M), there is a decrease in TH-positive cells, indicating dopaminergic cell death (47-49). Furthermore, there is significant evidence implicating DOPAL in protein modification (50-54). Studies

have demonstrated the ability of DOPAL to covalently modify residues such as Lys and Arg, forming Schiff base-like structures (34). While exact targets of DOPAL modification were previously unknown, studies have revealed that catechols and other DA metabolism products interact with and inhibit tyrosine hydroxylase. Furthermore, DOPAL is structurally analogous to DA, it therefore is predicted to have the ability to interact with proteins that contain DA-binding sites, such as tyrosine hydroxylase. DOPAL modification of proteins may lead to aggregation and loss of function, which may lead to dopaminergic cell death, a hallmark of PD.

Tyrosine Hydroxylase

As previously described, tyrosine hydroxylase (TH, E.C. 1.14.16.2) catalyzes the rate-limiting step in DA synthesis and requires oxygen, tetrahydrobiopterin (BH₄), iron and tyrosine in order to function properly. As Scheme 1.1 displays above, tyrosine is oxidized by TH to L-DOPA, which is further metabolized to DA (40). This 56 kDa enzyme exists in tetrameric form, and has been determined to be a loosely packed helical structure containing an N-regulatory region, a catalytic domain, and a tetramerization domain (55). The catalytic site where tyrosine binds is the only tightly packed portion of the enzyme, and the catalytic domain as a whole is key to enzyme function and activity (55). TH is tightly controlled due to the important role DA plays in controlling movement as well as mood. In particular, the phosphorylation of three key Ser residues appears to play a large role in the activity of TH. Ser 19, Ser 31, and Ser 40 are a part of the N-regulatory region, and studies have demonstrated that phosphorylation of these residues can dramatically alter the activity of TH (56, 57). As mentioned above, TH activity is also controlled by DA synthesis, with DA acting as a negative feedback inhibitor of the

enzyme through the DA-binding site (58). This enzyme is used frequently in immunostaining for dopaminergic neurons due to the role it plays in DA synthesis. Furthermore, the rate-limiting step produces L-DOPA, which has also been shown to have trophic properties in the cell, leading to an increase in cell viability (59, 60). There is also evidence that TH is inhibited by other catechols, such as DOPAC and norepinephrine (61, 62).

Combined, these results indicate TH to be a potential protein target of DOPAL modification, and it was of interest to determine how DOPAL affected TH activity, and consequently, the production of L-DOPA and DA. Elucidation of a protein target of DOPAL will help provide insight into a possible mechanism of toxicity behind the selective dopaminergic cell death exhibited in PD. Completion of these studies may help with future work focused on determining a means of halting the progression of the disease, or leading to better treatments for patients suffering from PD.

CHAPTER TWO

STATEMENT OF HYPOTHESIS

Introduction

Parkinson's disease (PD) is a neurodegenerative disorder which affects over 1% of the population. This disease results from the selective loss of dopaminergic neurons, leading to a decrease in the important neurotransmitter, dopamine (DA), which is necessary for the initiation and execution of coordinated movement (2). Currently, the pathogenesis behind this disease is unknown, but there is evidence the aldehyde metabolite of DA may play a role in the onset and progression (34, 46, 49, 50, 63). DA is metabolized by monoamine oxidase (MAO) to 3,4-dihydroxyphenylacetaldehyde (DOPAL), which can be further metabolized to both the acid and alcohol products.

DOPAL has been shown to interact with and modify peptides, and there is evidence of protein modification, although no specific targets have previously been identified (47, 50). Furthermore, evidence shows that DOPAL is toxic to dopaminergic neurons, with elevated concentrations leading to a decrease in tyrosine hydroxylase-positive cells.

Tyrosine hydroxylase (TH) is the rate-limiting step in DA-synthesis, oxidizing tyrosine to L-DOPA, which is further metabolized to DA (40). This enzyme is tightly controlled, and contains a DA-binding site used as a negative feedback mechanism (58). Furthermore, studies have shown TH to be inhibited by other catechols, such as 3,4-dihydroxyphenylacetic acid (DOPAC) and norepinephrine (61, 62).

The goal of this study was to positively identify a protein target of DOPAL modification and determine the effect of DOPAL on TH activity. It was also of interest to further study the toxic properties of DOPAL and how elevated levels affected cell viability, reactive oxygen species production, and mitochondrial function.

Hypothesis

The endogenously produced neurotoxin, 3,4-dihydroxyphenylacetaldehyde, covalently modifies and inhibits tyrosine hydroxylase, leading to a decrease in L-DOPA and dopamine production.

Specific Aims

To test this central hypothesis, three Specific Aims were proposed as follows:

Specific Aim 1: Investigate DOPAL as a neurotoxin and identify protein targets of modification. Completion of this aim will determine the toxicity of DOPAL in a dopaminergic cell model, investigate the production of reactive oxygen species, and for the first time positively identify a protein target of DOPAL modification.

Specific Aim 2: Determine the effect of DOPAL on tyrosine hydroxylase activity. Completion of this aim will elucidate the effect elevated DOPAL has on the production of L-DOPA, and consequently, DA production, which will have implications for PD.

Specific Aim 3: Elucidate mechanisms by which DOPAL inhibits tyrosine hydroxylase. Completion of this aim will accomplish a number of things; including, structure-activity studies to determine the mechanism behind DOPAL inhibition of TH activity as well as mass spectrometry studies to reveal sites of covalent modification of TH.

CHAPTER THREE
DOPAL AS A NEUROTOXIN CAPABLE
OF PROTEIN MODIFICATION

Introduction

Parkinson's disease (PD) is a neurodegenerative disorder characterized by the selective loss of dopaminergic neurons in the substantia nigra. This results in a decrease in the important neurotransmitter dopamine (DA), which is necessary for the initiation and execution of coordinated movement (2). Currently, the pathogenesis behind this disease is not well understood, but there is evidence implicating both environmental toxins, such as pesticides, as well as endogenously produced oxidative stress (12, 64, 65).

Previous evidence has demonstrated DA to be an endogenous neurotoxin, capable of auto-oxidation and protein modification (44, 45, 66). DA is metabolized by monoamine oxidase (MAO) to 3,4-dihydroxyphenylacetaldehyde (DOPAL), which is then further catabolized by aldehyde dehydrogenase (ALDH) and aldehyde reductase (AKR) to 3,4-dihydroxyphenylacetic acid (DOPAC) and 3,4-dihydroxyphenylethanol (DOPET), respectively (67). Recent work has shown DOPAL to be orders of magnitude more toxic than DA, and significantly more reactive with proteins (46, 63). Normal physiologic concentrations of DOPAL are known to be 2-3 μM , with studies demonstrating even slight elevations ($\sim 6.6 \mu\text{M}$) led to significant dopaminergic cell death (47, 48). Furthermore, DOPAL has been established as a reactive intermediate, capable of protein modification via Lys residues (34, 51, 54), leading to the formation of a Schiff base-like structure (50).

While studies have demonstrated DOPAL's ability to interact with peptides and proteins, until recently, no protein targets of DOPAL modification have been identified. The current study was undertaken to study the neurotoxic properties of DOPAL in dopaminergic PC6-3 cells by investigating both mitochondrial function and overall cell viability. Furthermore, a protein target of DOPAL modification was identified using proteomic analysis of PC6-3 cells incubated with DOPAL. To investigate the link between elevated DOPAL and cellular dysfunction and death, flow cytometry was employed to determine levels of reactive oxygen species (ROS) in the presence of elevated DOPAL. Such work will help further the knowledge regarding protein modification by DOPAL and the link between elevated DOPAL and cell dysfunction and death.

Experimental Procedures

Materials

DOPAL was biosynthesized as previously described using enzyme-catalyzed conversion of DA to DOPAL by rat liver MAO (54), and the concentration was determined using an ALDH assay with NAD (52) and HPLC analysis as described below.

3,4-dihydroxyphenylethanol (DOPET) was obtained via reduction of DOPAL using a 10-fold excess of sodium borohydride. DA, DOPAC, and all other chemicals were purchased from Sigma-Aldrich (St. Louis, MO) unless otherwise noted.

PC6-3 Cell Culture

PC6-3 cells were cultured in RPMI 1640 medium supplemented with heat-inactivated 10% horse serum, 5% fetal bovine serum, penicillin (10 IU/mL) and

streptomycin (10 mg/mL). PC6-3 cells are a subline of the pheochromocytoma (rat adrenal medulla) PC-12 cell line. They were chosen due to a decreased tendency from the parent line to aggregate, as well as decreased background cell death, and they are also a homogeneous population that can be easily maintained (68, 69). PC-12 cells are also a widely accepted model for DA synthesis and metabolism (15, 70). Furthermore, PC6-3 cells assume a neuronal cell phenotype in the presence of nerve growth factor, and have important neurochemical processes similar to dopaminergic neurons (71, 72). Cells were grown in a 10 cm tissue culture dish at 37 °C in 5% CO₂ for 3 days. Cells were then seeded into six-well plates (1×10^5) and were incubated at 37 °C in 5% CO₂ for 3 days prior to the addition of nerve growth factor (NGF) (50 ng/mL) to stimulate cell differentiation. PC6-3 cells were kept in the same conditions for 4 days prior to use. For experiments involving treatment with DOPAL, cellular medium was removed in order to eliminate DOPAL interaction with serum proteins and replaced with HEPES-buffered medium containing 115 mM NaCl, 5.4 mM KCl, 1.8 mM CaCl₂, 0.8 mM MgSO₄, 5.5 mM glucose, 1 mM NaH₂PO₄, and 15 mM HEPES (pH 7.4).

Mitochondrial dysfunction (MTT Assay)

To determine the cytotoxicity of DOPAL in PC6-3 cell cultures, cell viability was measured using the 3-(4,5-dimethylthiazol-2-yl)-2,3-diphenyltetrazolium bromide (MTT) reduction assay. In this assay, the conversion of yellow tetrazolium salt MTT to purple formazan is achieved by active mitochondrial reductases found in functional cells. In brief, NGF-differentiated cells were treated with varying concentrations of DOPAL (0, 5, 10, 25, 50 μM) for 2 h at 37 °C. Following this, yellow MTT (0.5 mg/mL) was added to each well, and further incubated for 2 h at 37 °C. The media was then removed, and the

purple formazan crystals were dissolved in DMSO. The formazan product absorbs at 570 nm, and a Molecular Devices Spectra-Max plate reader was used to measure the absorbance in each well. Absorbance values for the experimental wells were compared to controls (no DOPAL).

Trypan Blue Assay

In trypan blue studies with DOPAL, cells were incubated as previously described with DOPAL for 2 h at 37°C in 5% CO₂. Cells were then triturated with a pipette and centrifuged at 10,000 \times g for 3 min. Cells were then resuspended in 200 μ L of HEPES-buffered media and 20 μ L of trypan blue was added and live cells were counted. MTT and trypan blue results are expressed in terms of % control, with controls being cells not exposed to DOPAL (73).

PC6-3 Cell Lysate Collection

PC6-3 cells were grown as previously described (1×10^5) in 10 cm tissue culture dishes and used as a source of TH. Undifferentiated cells, which contain levels of TH several fold higher than NGF-differentiated cells, (71) were washed 3 times with cold 10 mM sodium phosphate buffer (pH 6.4) (74). Cells were scraped and collected in 500 μ L of buffer. They were then sonicated at 3 second intervals 10 times, and the lysate was centrifuged using a Sorvall Discovery SE Ultraspeed centrifuge at 100,000 \times g for 1 h at 4 °C. The cytosolic fraction (i.e. supernatant) was collected to be used in TH activity assays or stored at -80°C until use.

DOPAL Metabolism Studies

PC6-3 cells were grown as described above. Four days after the addition of NGF, cellular medium was removed and cells were washed with 1 mL HEPES-buffered

medium and then preincubated for 15 min in the same buffer. DOPAL (5, 10, 25, 50 μM) was added and cells were incubated for 2 h at 37°C. 100 μL aliquots of extracellular medium were taken at 30 min time points and placed in 5% (v/v) perchloric acid. After spinning at 10,000 $\times g$ for 3 min, samples were subjected to HPLC-ECD detection.

HPLC-ECD Detection of DOPAL and Metabolites

An Agilent 1100 Series Capillary HPLC system was coupled with an ESA Coulochem III electrochemical detector and used for separation and quantification of DOPAL, DOPAC, and DOPET. Electrode potentials were set at -150 and +300 mV. Two μL of sample was injected, and separation was achieved using a Phenomenex Synergy Hydro column (2 x 150 mm, 80 Å) and a mobile phase consisting of 50 mM citrate, 1.8 mM SHS, 0.2% trifluoroacetic acid and 2% (v/v) ACN (pH 3). The flow rate was 250 $\mu\text{L}/\text{min}$ and conversion of area to concentration units was achieved using a calibration curve of standards.

DOPAL Modification of Tyrosine Hydroxylase in Cell Lysate

PC6-3 cell lysate was collected as described below. Lysate was incubated with DOPAL (10, 50, 100 μM) for 4 h at 37 °C. Sodium cyanoborohydride (1 mM) was added to help stabilize Schiff base adducts formed.

Western Blot Analysis of Tyrosine Hydroxylase

Protein (1 μg) from DOPAL modification studies was loaded into a 7.5% acrylamide gel used to separate proteins via sodium dodecylsulfate polyacrylamide gel electrophoresis (SDS-PAGE). After separation, protein was transferred to nitrocellulose

membrane for 1.25 h at 20 V, and blocked over night at 4 °C in 3% BLOTTO (i.e. dried milk in TBTS). Primary rabbit anti-TH antibody was used at a dilution of 1:1000 for 2 h at room temperature, and horseradish-peroxidase-conjugated secondary goat-anti-rabbit antibody was used at a dilution of 1:10000 (Santa Cruz Biotechnology, Santa Cruz, CA, USA) for 1.5 h at room temperature. Between blocking and antibody incubations, membranes were washed 3 times using 0.05 M Tris, 0.9% NaCl containing 0.05% Tween-20 (TBS-T) for 3 minutes at room temperature. Staining for actin was used as a loading control. Primary and secondary antibody dilutions were 1:500 and 1:10000, respectively (Santa Cruz Biotechnology, Santa Cruz, CA, USA). Signal was detected using an Amersham ECL-plus Western Blotting Detection Kit according to manufacturer instructions. Band density was measured using NIH program ImageJ 1.43 μ and compared to control lanes.

Isolation of DOPAL Modified Proteins

Using an Aminophenylboronic Acid Resin

PC6-3 cells were cultured and incubated with DOPAL as previously described above. Control (i.e. no DOPAL) and 50 μ M DOPAL conditions were used in ABPA protein separation. After 2 h, extracellular media was removed and 300 μ L lysis buffer (0.1% Triton-X in 10 mM KH_2PO_4) was added and plates were placed on dry ice for 5 min to rupture cell membranes. Lysate was then collected and supernatant was used in APBA isolation of DOPAL-bound proteins as previously described with some modification (50, 53). Briefly, 100 μ L of resin was washed and equilibrated 3 times in 50 mM sodium phosphate buffer (pH 7.4) and centrifuged at 10,000 $\times g$ for 3 min. After removal of the final wash, 100 μ L of sample (either control or 50 μ M DOPAL lysate)

and 100 μ L of 50 mM sodium phosphate buffer (pH 8.4) were added to the resin and allowed to incubate for 4 h at room temperature on a shaker table. The resin was subsequently washed with 300 μ L of 1:1 acetonitrile:50 mM sodium phosphate (pH 8.4) buffer 3 times, and 300 μ L of distilled water 3 times, centrifuging after each wash fraction ($10,000 \times g$, 3 min). In order to elute protein bound to the APBA resin, the resin was washed with 100 μ L of 1% trifluoroacetic acid (TFA) 2 times, 100 μ L of 1:1 acetonitrile:1% TFA once, and 100 μ L of 1:1 acetonitrile:H₂O once, centrifuging after each release fraction ($10,000 \times g$, 3 min). The pH of the each release fraction was immediately neutralized using 5 μ L of 1 M sodium phosphate buffer (pH 7.4). A 10% gel was used for SDS-PAGE and Coomassie blue staining was used for protein detection.

Proteomic Analysis of DOPAL Modified Proteins

Bands of interest from the APBA resin-bound fractions were excised and digested using trypsin as previously described (75). Samples were then subjected to LC-ESI-MS/MS analysis using a Thermo LTQ-XL linear ion trap mass spectrometer. TH, with a molecular weight of approximately 60 kDa, was identified as a protein of interest using the TrEMBL database for rat. Scaffold (version Scaffold_3_00_05, Proteome Software Inc., Portland, OR) was used to validate MS/MS based peptide and protein identifications. Protein probabilities were assigned by the Protein Prophet algorithm (76).

Quantification of Reactive Oxygen Species

Using Flow Cytometry

PC6-3 cells were cultured and maintained as described above. Four days after the addition of NGF, cells were washed with HEPES-buffered media (pH 7.4) and pretreated

with 2'-7'-dichlorodihydrofluorescein diacetate (DCF-DA, 50 μ M) and dihydroethidium (DHE, 10 μ M) at 37°C for 20 min in the dark. Supernatant was then removed, and new HEPES-buffered media was added. DOPAL (5, 10 μ M) was added to the cells and incubated for 1 h at 37°C. Cells were then removed from the plate by decanting the supernatant. After spinning for 5 min at 4600 \times g, supernatant was removed and cells were resuspended in 1 mL phosphate buffered saline (PBS) to wash. Cells were once again pelleted via centrifugation, and then resuspended in 300 μ L HEPES-buffered media. Prior to analysis by flow cytometry, cells were filtered using a 70 μ m Falcon filter and 4.8 μ L Hoescht 33250 stain was added. A Becton Dickinson LSR II flow cytometer was used with lasers set to 530 and 610 nm.

Statistical Analysis

All linear regression and statistical analyses were performed using the software GraphPad Prism 5.0 (Graph Pad Software, San Diego, CA). Data for cells treated with DOPAL were compared to the controls and significant differences ($p < 0.05$) were determined using an ANOVA with a Tukey post-test (this was also used to analyze % recovery data for reversibility studies).

Results

Elevated DOPAL leads to cell morphological changes

When PC6-3 cells are incubated with varying concentrations of DOPAL (5, 10, 25, 50 μ M) for 2 h significant changes occur to the cell morphology. The images in Figures 3.1 and 3.2 show cells begin to exhibit signs of dysfunction after just 1 h in the presence of elevated DOPAL. The arrows in 3.1 (1 h) are indicative of cell blebbing and

loss of uniform shape, while the arrows in 3.2 (2 h) demonstrate a high level of apoptotic body formation along with blebbing and significant loss of cell shape. These are all signs of cellular dysfunction and the start of apoptosis. Significant changes can be seen at the low concentration of 5 μM DOPAL after just 2 h, and cells exhibit a concentration-dependent increase in dysfunction. These results demonstrate the negative effect DOPAL has on dopaminergic PC6-3 cells at pathologically relevant concentrations. It is clear even slight changes from normal levels of DOPAL (2-3 μM , (46)) lead to detrimental effects on cell morphology.

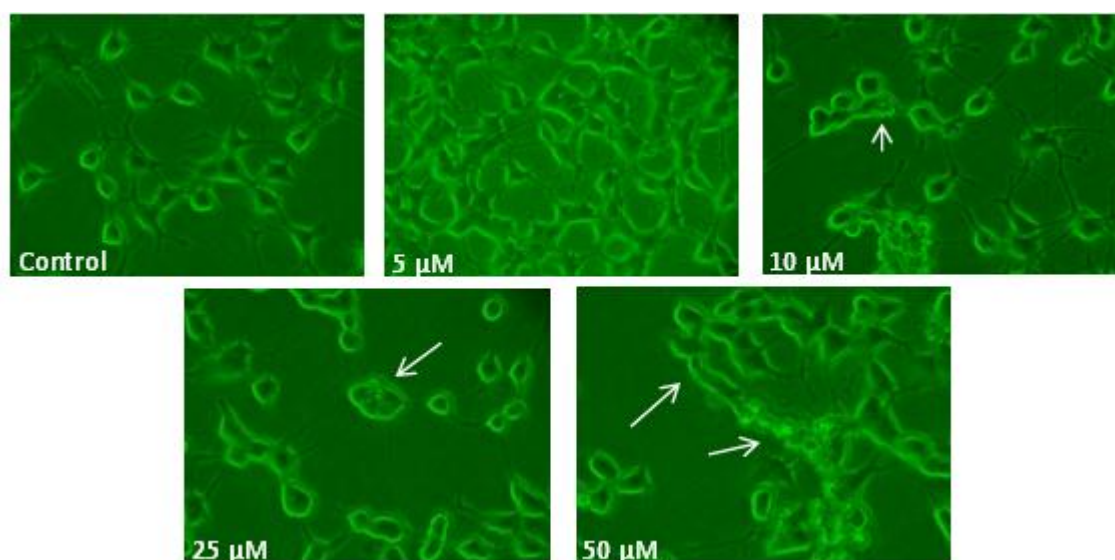


Figure 3.1 Images of PC6-3 cells after 1 h incubation with 5, 10, 25, or 50 μM DOPAL. Arrows indicate cellular blebbing and loss of uniform cellular shape (10, 25, and 50 μM). These signs are indicative of early cell dysfunction.

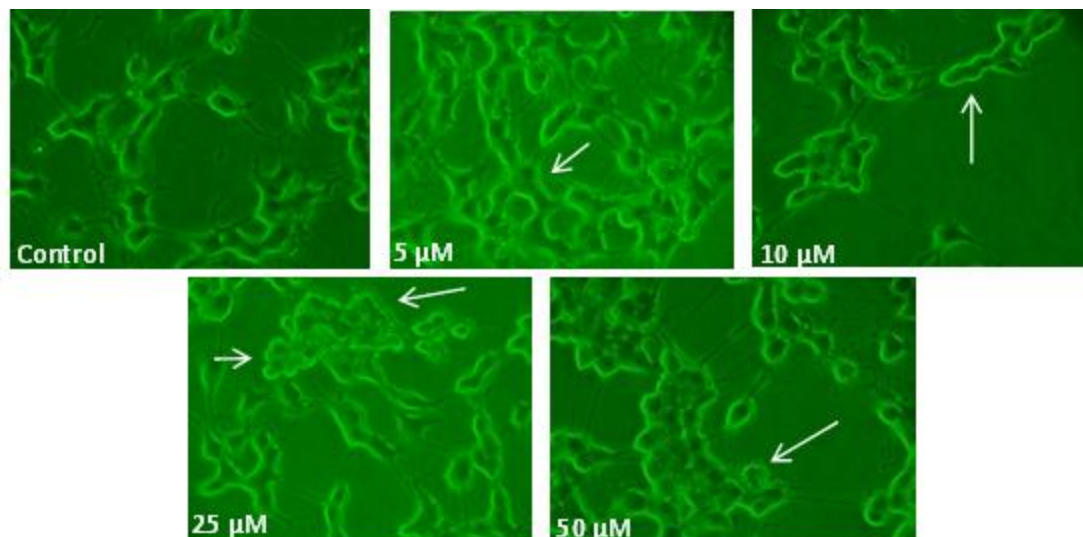


Figure 3.2 PC6-3 cells 2 h after addition of varying concentrations of DOPAL. Arrows indicate significant blebbing and loss of cell shape (5, 10 μM) and the introduction of apoptotic bodies (25, 50 μM). This demonstrates the highly potent toxicity DOPAL induces in cells after just a 2 h incubation.

Elevated DOPAL Leads to Mitochondrial Dysfunction

PC6-3 cells were incubated with varying concentrations of DOPAL (5, 10, 25, 50 μM) for 2 h and then mitochondrial function was assessed using the MTT assay as described in the methods section. After 2 h, the absorbance was measured and cells showed a concentration-dependent increase in mitochondrial dysfunction as compared to controls. Significant dysfunction was exhibited at only 10 μM DOPAL as compared to cells where no DOPAL was present. The data in Figure 3.3 show that as DOPAL levels increase, the mitochondrial function decreases, until ~40% of cells exhibit mitochondrial dysfunction (50 μM DOPAL). These results demonstrate the toxic effect elevated DOPAL has in dopaminergic PC6-3 cells.

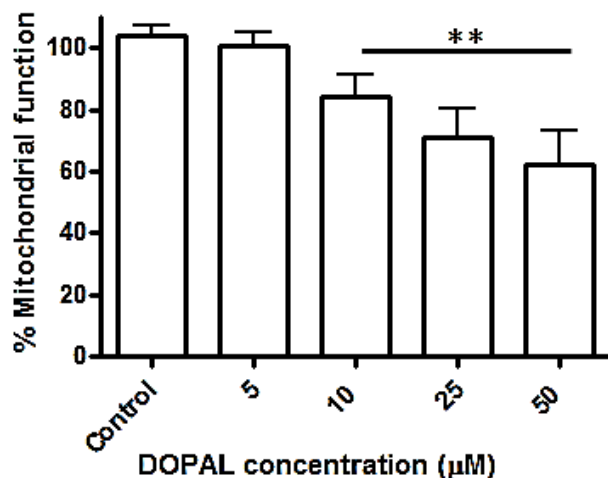


Figure 3.3 PC6-3 cells incubated with varying concentrations of DOPAL for 2 h. Mitochondrial function was assessed using the MTT assay and cells display a concentration-dependent decrease in function. The low, pathologically relevant concentration of just 10 µM leads to significant dysfunction as compared to controls. All values shown represent the mean \pm SEMs ($n = 4$). ** indicates significance from control cells.

DOPAL Elevation Causes Cell Death

NGF-differentiated PC6-3 cells were once again incubated with increasing concentrations of DOPAL (5, 10, 25, 50 µM) for 2 h and cell viability was assessed using the trypan blue method of counting live cells. The dye is excluded from live cells, due to the intact membrane, but cells with compromised membranes will stain blue (73). As the data in Figure 3.4 demonstrate, dopaminergic PC6-3 cells exhibit a concentration-dependent decrease in viability as DOPAL concentrations are elevated. These results indicate that elevation in DOPAL levels leads to both mitochondrial dysfunction as well as significant cell death. Concentrations of only 5 µM DOPAL leads to significant cell death after a 2 h incubation, indicating the potent toxicity of DOPAL.

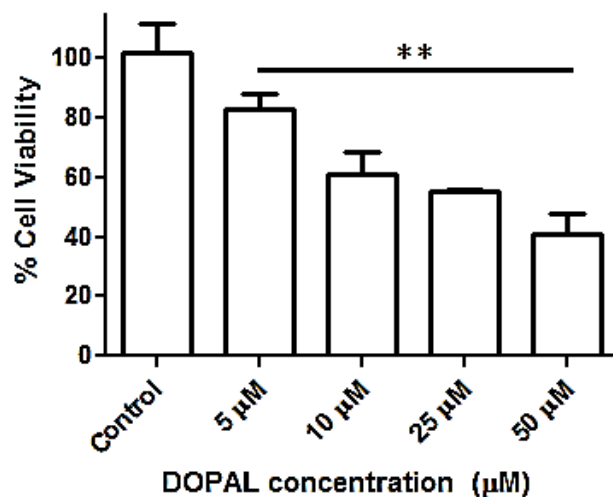


Figure 3.4 PC6-3 cells incubated with DOPAL for 2 h. Trypan blue used to assess cell viability, with cells exhibiting a concentration-dependent decrease in viability. Low concentrations of only 5 µM DOPAL lead to significant cell death as compared to controls. All values shown represent the mean \pm SEMs ($n = 3$). **indicates significance from control cells.

DOPAL is Metabolized in PC6-3 Cells

To study the metabolism of DOPAL in dopaminergic PC6-3 cells, NGF-differentiated cells were incubated with increasing concentrations of DOPAL (5, 10, 25, 50 µM) for 2 h and aliquots of extracellular media were taken at 30 min time points. HPLC analysis of aliquots demonstrated the ability of cells to take up DOPAL, metabolize, and release both DOPAC and DOPET. Metabolism was concentration-dependent, with higher levels of DOPAL leading to higher release of metabolites. As expected, DOPAC was the major metabolite, and DOPET was the minor product. The graphs in Figure 3.5 show the decrease of DOPAL (3.5A) in the extracellular medium as

it is taken up by cells, and the increase in DOPAC (3.5B) through ALDH activity (77), and DOPET (3.5C) over time as metabolism by AKR occurs (78)

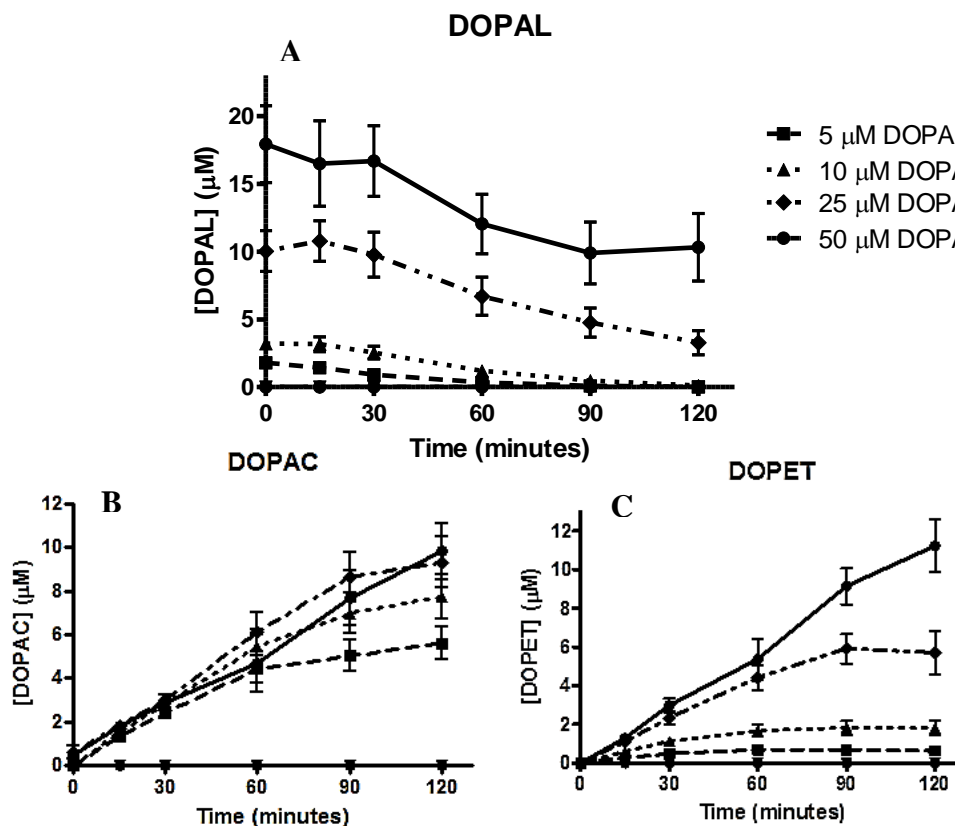
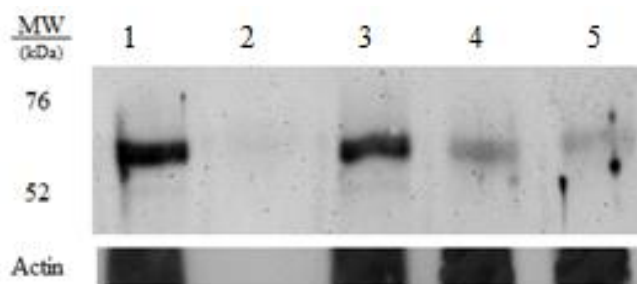


Figure 3.5 DOPAL metabolism in dopaminergic PC6-3 cells. (A) DOPAL is taken up by cells as indicated by a decrease in concentration in the extracellular medium over time. (B) DOPAC is produced from ALDH metabolism of DOPAL. (C) DOPET is produced by AKR metabolism of DOPAL. For all graphs all values shown represent the mean \pm SEMs ($n = 3$). DOPAC and DOPET graph symbols are the same as shown in the DOPAL graph.

DOPAL Modifies Tyrosine Hydroxylase

In order to determine protein targets of DOPAL, PC6-3 cells were lysed and incubated with different concentrations of DOPAL (10, 50, 100 μM) for 4 h at 37°C. Samples were then subjected to western blot analysis probing for TH. Controls included TH+ cell lysate, and BSA as a negative control. Figure 3.6 shows a concentration-dependent decrease in antibody recognition of TH indicating DOPAL interferes with the ability of the antibody to properly bind to the protein. These results indicate DOPAL is interacting with TH and leading to a decrease in staining by the antibody. Actin was used as a loading control.



Lane	Loaded	[DOPAL] (μM)	% Control Staining
1	TH+ lysate	0	100
2	BSA	0	0
3	TH+DOPAL	10	62.9 \pm 4.66
4	TH+DOPAL	50	45.4 \pm 5.91
5	TH+DOPAL	100	29.4 \pm 5.31

Figure 3.6 TH from PC6-3 cells was incubated with DOPAL for 4 h at 37°C. Western blot analysis reveals a concentration-dependent decrease in antibody recognition of TH indicating DOPAL interferes with ability of antibody to bind to protein.

Proteomic Identification of Tyrosine Hydroxylase as a DOPAL Target

To positively identify TH as a protein target of DOPAL modification, PC6-3 cells were incubated with DOPAL (0, 50 μ M) as previously described in the methods section. Lysate was then subjected to an APBA resin, and DOPAL-modified proteins were separated. SDS-PAGE further separated proteins and the most prevalent band at approximately 60 kDa was excised and an in-gel digestion was performed using trypsin. LC-ESI-MS/MS and the TrEMBL database (79) were used, and 6 peptides were matched to identify tyrosine hydroxylase as the band of interest with a 95% confidence interval. Mascot ion scores, which are a measure of probability of a peptide matching the correct protein, ranged from 47.2-141.2 for peptides. Scores above 67, or if the matches can be established with greater than 90% probability, are considered significant (80). These results positively identify tyrosine hydroxylase as a protein target of DOPAL modification.

To further support these results, the collected fractions from the APBA separation of DOPAL-modified proteins were subjected to western blot analysis for TH as described in the methods section. The chemistry behind the APBA resin is described in Figure 3.7. It has been shown that the resin reacts specifically with vicinal diols, such as those found on catechols, under basic conditions. The bond is strong enough to withstand washing, and upon the addition of an acidic solution (pH =2), the bond is broken, leaving DOPAL-modified proteins. The gels depicted in Figure 3.8 demonstrate antibody recognition of TH in samples that contained DOPAL-modified TH. For both gels BSA was used as a negative control for the TH antibody, while TH⁺ cell lysate was used as a positive

control. The supernatant in each gel contains proteins that were not DOPAL-modified. As expected, both groups of cells contain some TH which was not bound by DOPAL. Wash 1 also contains proteins with no DOPAL adducts. The release fractions should contain DOPAL-modified TH. As can be seen from the data, the control cells in which no excess DOPAL was added exhibit no staining, indicating there was no TH bound to the resin. Conversely, when cells were treated with 50 μ M DOPAL, the release fractions demonstrate staining for TH. These results indicate that DOPAL modifies TH in the cells. These adducted proteins then bind to the APBA resin, and are then released with acid. Both proteomic analysis and western blot analysis for TH recognized and identified TH as the modified protein.

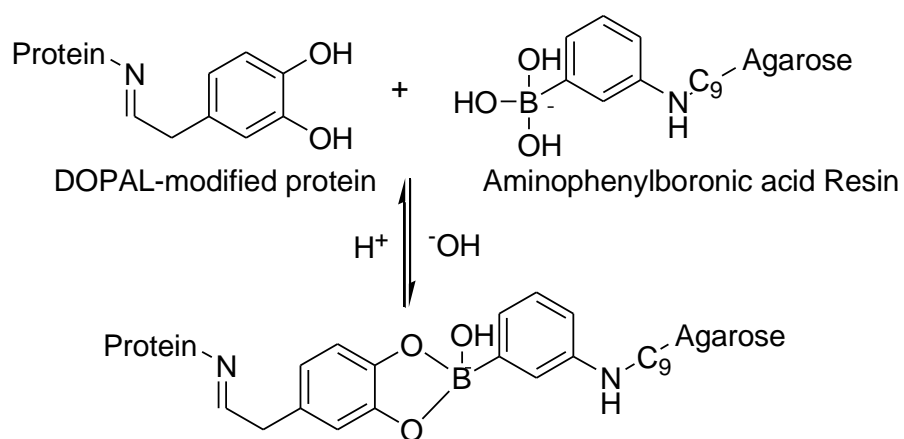


Figure 3.7 Chemistry of APBA reactivity with vicinal diols (i.e. such as those found on catechols). The resin reacts specifically with diols in basic conditions (pH > 8.0) with a bond strong enough to withstand wash conditions in neutral pH. Acid release steps (pH = 2) lead to separation of the boronic acid and vicinal diol.

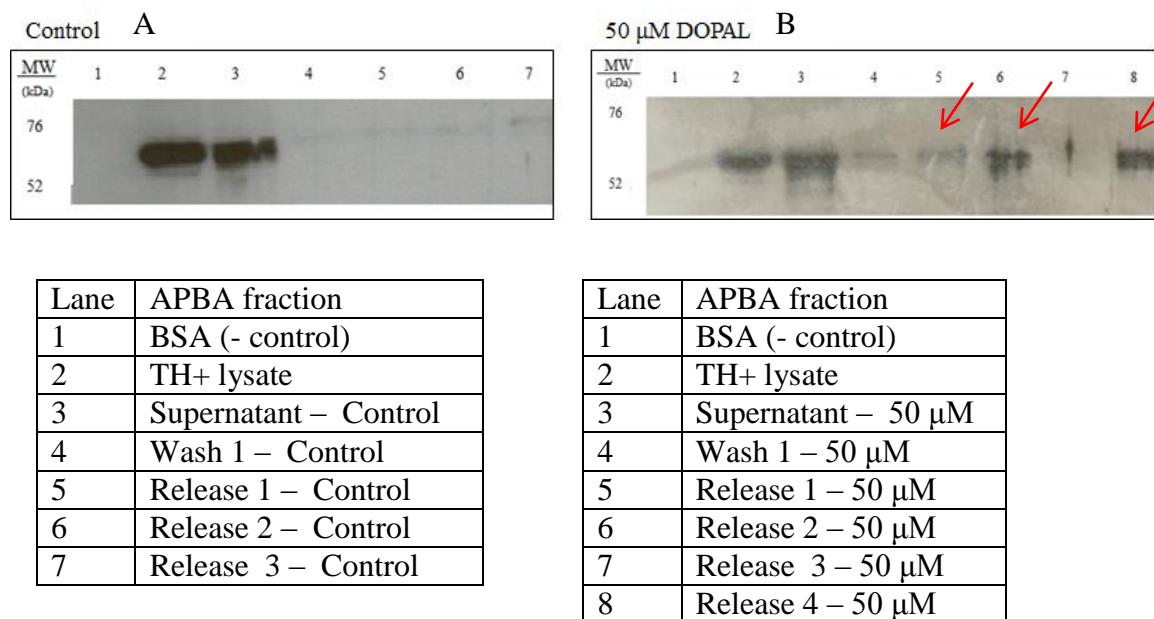


Figure 3.8 Cells treated with either no DOPAL or 50 μ M for two h and then subjected to APBA resin for separation were then run on SDS-PAGE for western blot analysis of TH. **(A)** The control cells (i.e. no DOPAL) exhibit no staining for TH in the release fractions, indicating there was no major DOPAL modification of TH. **(B)** Cells treated with DOPAL demonstrate DOPAL-modified TH in the release fractions (lanes 5-8), as denoted by arrows.

Elevated DOPAL Leads to

Reactive Oxygen Species Production

PC6-3 cells were incubated with DOPAL (5, 10 μ M) and DCFDA and DHE were used to determine the levels of hydrogen peroxide and superoxide anion, respectively. The data in Figure 3.8 show the raw scatter plots acquired. These results demonstrate an increase in cells that show DHE staining, and a slight decrease as compared to controls in cells that show DCFDA staining. Upon further analysis, it can be seen in Figure 3.9 that there is an increase in superoxide anion formation as concentration of DOPAL increases.

On the other hand, there was a decrease in hydrogen peroxide. The increase in superoxide anion indicates there is oxidative stress occurring when levels of DOPAL are elevated from normal (2-3 μM , (49)). In contrast, levels of hydrogen peroxide demonstrated a decreasing trend compared to the control, specifically, cells treated with 5 and 10 μM DOPAL exhibited significantly less hydrogen peroxide than controls (Figure 3.10). While initially surprising, these results have implications for the inhibition of TH by DOPAL and downstream pathways, such as the metabolism of DA (81), which is further commented on in the discussion.

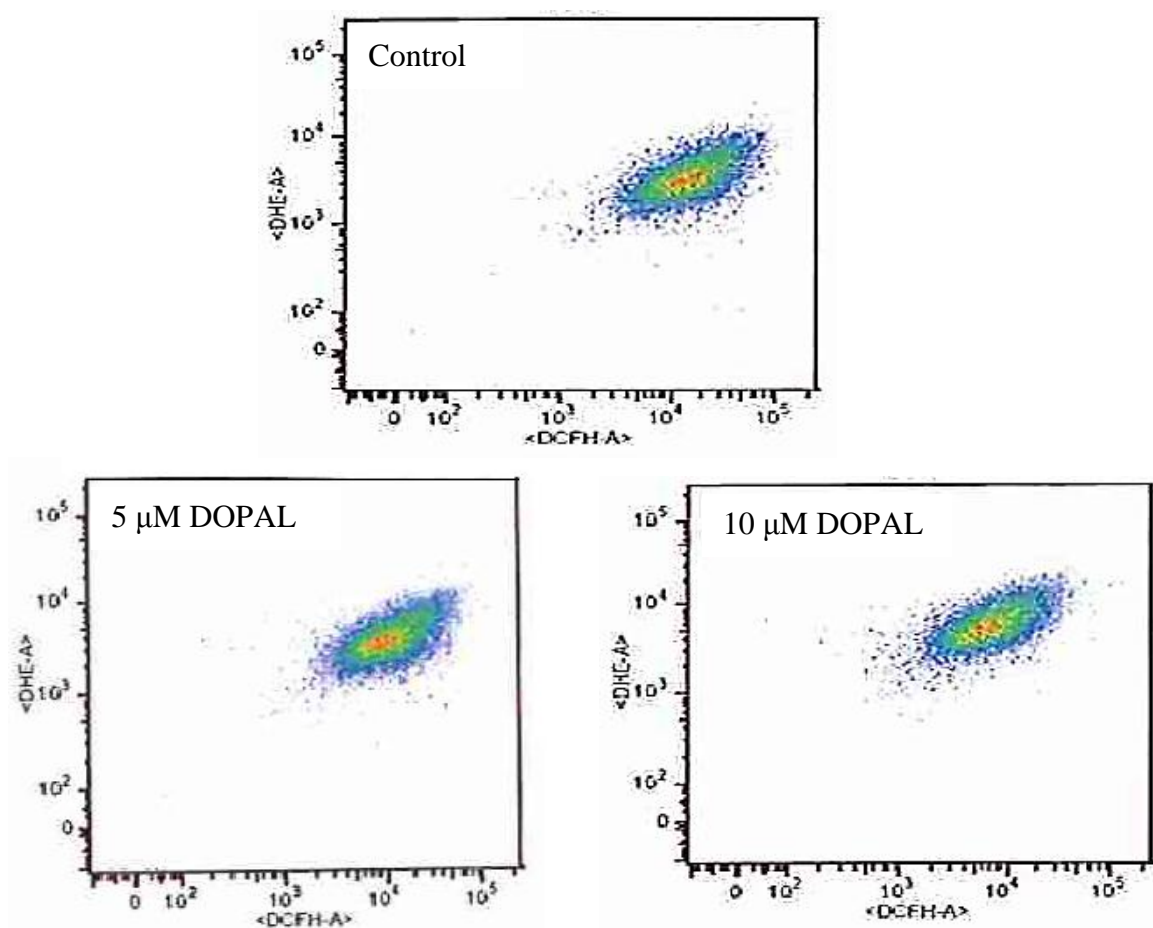


Figure 3.9 Representative scatter plots of flow cytometry data on DOPAL-treated cells. Data demonstrates a slight increase in fluorescence of DHE in 5 and 10 μ M DOPAL-treated cells as compared to controls, indicative of increased super oxide anion, while fluorescence of DCFDA decreases in both DOPAL treated conditions, indicating less hydrogen peroxide production.

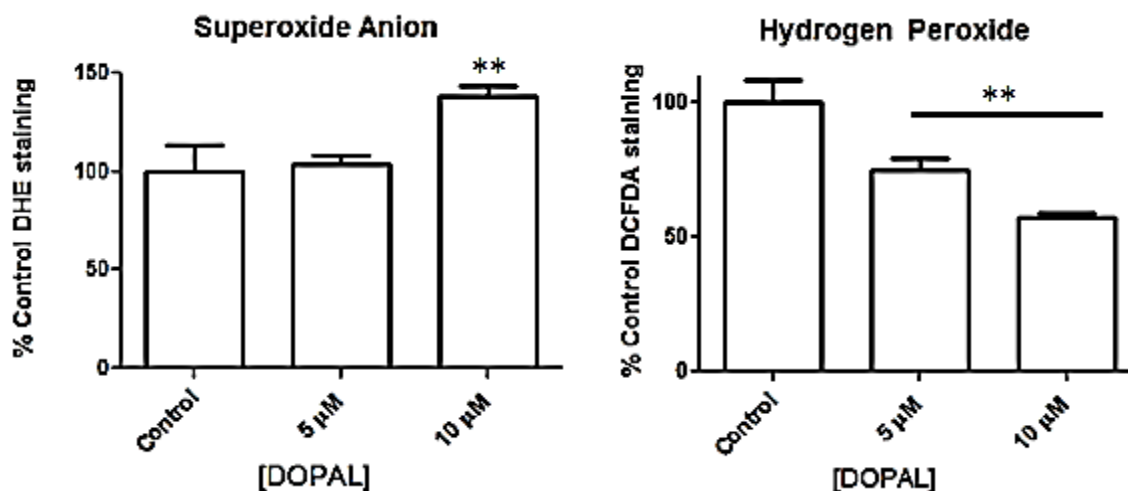


Figure 3.10 PC6-3 cells incubated with 5 or 10 μM DOPAL for 1 h and then subjected to flow cytometry to determine levels of superoxide anion and hydrogen peroxide. Elevated DOPAL leads to increased superoxide anion and decreased hydrogen peroxide production. All values shown represent the mean \pm SEMs ($n = 3$). **indicates significance from control cells where no DOPAL was added.

Discussion

DOPAL, an intermediate of DA catabolism, is an endogenous neurotoxin known to covalently modify proteins (34, 46, 50) and hypothesized to be a factor in the pathogenesis of PD (47, 67). While brain levels of DOPAL were measured to be between 2-3 μM under normal conditions, studies have shown that slight elevations (to $\sim 6.6 \mu\text{M}$) can lead to cell death in dopaminergic cells and a decrease in TH-positive immunostaining indicating dopaminergic cell death (63). The work presented here confirms the neurotoxic properties of DOPAL. This can be seen qualitatively in Figures 3.1 and 3.2 where there are significant morphological changes in PC6-3 cells over the course of a 2 h incubation with elevated DOPAL. Cells begin to exhibit loss of uniform

cell shape, blebbing and the formation of apoptotic bodies, indicating cellular distress and the start of apoptosis.

Furthermore, decreased mitochondrial function and increased cell death in the presence of elevated DOPAL were demonstrated using the MTT assay, looking at mitochondrial function, and the trypan blue method to study overall cell viability. These two studies were chosen to investigate cell function as well as membrane permeability, which can be indicative of cell viability. The results in Figures 3.3 and 3.4 show low micromolar (5 or 10 μM) concentrations of DOPAL lead to significant dysfunction and cell death after only a 2 h incubation.

It was also of interest to determine the metabolism of DOPAL in dopaminergic PC6-3 cells. As can be seen from the data in Figure 3.5, DOPAL added exogenously to cells is taken up and metabolized by both ALDH and AKR, and released as the acid and alcohol products. It is important to note that the metabolism of DOPAL changes as the concentration increases. When low concentrations (5, 10 μM) DOPAL is placed on cells, ALDH is the major metabolism pathway (Figure 3.5B), but upon the addition of higher DOPAL (25, 50 μM), AKR metabolism is seen to be the major pathway (Figure 3.5C). This can be explained by the K_m value of each enzyme; ALDH has a K_m for DOPAL of low micromolar to high nanomolar concentrations, while the K_m of AKR for DOPAL is between 10-30 μM (82-84). These results indicate that as DOPAL concentration increases, ALDH would become overwhelmed, and AKR would compensate to help decrease levels of this reactive intermediate. This is further supported by V_{max} values for both ALDH and AKR, which are 81.8 $\mu\text{mol}/\text{min}/\text{kg}$ and 10 $\mu\text{mol}/\text{min}/\text{kg}$, respectively (85). This indicates that low concentrations of DOPAL would be quickly turned over by

ALDH, while high concentrations of DOPAL would be reduced by AKR over a longer period of time.

For the first time, a protein target of DOPAL modification was identified. Tyrosine hydroxylase was shown to be modified by DOPAL first through western blot analysis in which antibody recognition was decreased in the presence of DOPAL (Figure 3.6); and then through proteomic analysis in which 6 peptides were matched. It is important to note that the APBA resin used to separate DOPAL-modified proteins has previously been used in the separation of DA-modified proteins (53). The boronic acid component of APBA resin is capable of binding to vicinal diols (i.e. catechols) under basic condition, and the catechol can then be released using acidic conditions. DOPAL has been shown to modify proteins through free amines via the aldehyde. It is hypothesized a Schiff base-like structure is formed with the protein, leaving the catechol on DOPAL available for interaction with the APBA resin (50). While it might be argued that TH modification was due to oxidized DA or possibly DOPAC, it was assumed that the major compound present in cells was DOPAL due to loading of the cells (50 μM) at the beginning of the experiment. Furthermore, DOPAL, as described above, is significantly more reactive with proteins than DA or DOPAC. Finally, while DA has been implicated in protein modification, it requires oxidation to the quinone, which is then known to quickly rearrange to dopaminochrome when there are no thiols present (44, 45, 66).

Flow cytometry examination of reactive oxygen species production in cells treated with DOPAL led to interesting conclusions. As predicted, levels of superoxide anion increased when DOPAL (10 μM) was present, as compared to controls (Figure

3.8). These results indicated increased oxidative stress within the cell, leading to higher levels of reactive oxygen species like superoxide anion. Interestingly, hydrogen peroxide levels decreased after a 1 h exposure to elevated DOPAL. While it could be argued that there is the possibility of oxidation of DOPAL by hydrogen peroxide, leading to the formation of a quinone, recent studies employing electron paramagnetic resonance spectroscopy demonstrated this does not occur (64).

Alternatively, there have been previous studies monitoring the production of hydrogen peroxide in the extracellular space of brains of male Sprague-Dawley rats when a variety of conditions were employed. In one study, the application of 250 mg/kg intraperitoneally of alpha-methyltyrosine, a known selective inhibitor of TH, led to a significant decrease in the production of hydrogen peroxide (81). Inhibition of TH would lead to a decrease in the production of DA, in turn causing equally less turnover by MAO. A by-product of MAO metabolism is hydrogen peroxide; therefore, a decrease in DA would mean a decrease in hydrogen peroxide production. As described above, TH is a protein target of DOPAL modification as determined by both western blot and proteomic analysis (Figures 3.6 and 3.7, respectively). These results are the first indication that DOPAL is inhibiting TH activity, leading to decreased DA production overall. This would directly lead to a decrease in hydrogen peroxide formation due to a reduction in DA turnover by MAO, following the results displayed in Figures 3.9 and 3.10.

Overall, DOPAL has been established as a neurotoxin capable of protein modification, causing mitochondrial dysfunction, leading to the production of ROS, and eventual cell death. Furthermore, for the first time, a protein target of DOPAL

modification has been identified using proteomic analysis. Tyrosine hydroxylase is modified by DOPAL, leading to decreased antibody recognition and as the ROS studies indicate, a decrease in DA production. These results demonstrate the high toxicity and high reactivity of DOPAL and have implications for the onset and progression of PD. There is evidence that in the aging process, MAO activity increases, and products of lipid peroxidation (i.e. 4-hydroxy-2-nonenal and malondialdehyde) inhibit the activity of ALDH and AKR (33, 86). Combined, these occurrences would lead to an increased production of DOPAL, thus causing the many problems described in this work. There is also recently published evidence of changes in the ratio of DOPAC to DOPAL in the post-mortem brains of PD patients versus their control counterparts, indicating the disease leads to significant alterations in the production and metabolism of DOPAL (87). All of these results demonstrate how important a balance in the DA synthesis and metabolism systems are, and how slight changes can lead to very significant problems in the brain.

CHAPTER FOUR

INHIBITION OF TYROSINE HYDROXYLASE BY DOPAL

Introduction

3,4-Dihydroxyphenylacetaldehyde (DOPAL) is the monoamine oxidase (MAO) metabolite of dopamine (DA). This catabolism product is a known neurotoxin with the capability of interacting with and modifying proteins (34, 46, 50). Until recently, protein targets of DOPAL were unknown; however, studies in our lab utilizing proteomic analysis revealed tyrosine hydroxylase (TH) to be modified by DOPAL (88).

TH (E.C.1.14.16.2) the rate-limiting step in DA synthesis, oxidizes tyrosine to L-DOPA, which is further metabolized to DA (40). The action of this important enzyme is tightly controlled through a variety of mechanisms. It has been demonstrated that iron and tetrahydrobiopterin are necessary for proper enzyme action, and the order of binding appears to play a role in activity (89). TH also contains a DA-binding site which is used in a negative feedback mechanism of enzyme regulation (90). As discussed in Chapter 3 and in previously published results (88), TH is a protein target of DOPAL modification. Western blot demonstrated a concentration-dependent decrease in antibody recognition of TH in the presence of DOPAL, and proteomic analysis positively identified TH as a protein target (88).

Based on these results, it was of interest to determine how TH activity was affected by elevated DOPAL. It was hypothesized that DOPAL modification would lead to inhibition of enzyme activity, expressed as a decrease in L-DOPA production. The following studies were undertaken to investigate the effect of elevated DOPAL in both cell lysate and a PC6-3 cell model. It was also of interest to elucidate the mechanism of

DOPAL inhibition (i.e. reversible or irreversible). The data presented here will help further the knowledge of DOPAL protein modification. Furthermore, it will directly study the affect modification by DOPAL has on TH activity, and how this impacts the production of L-DOPA and DA.

Experimental Procedures

Materials

DOPAL was biosynthesized as previously described using enzyme-catalyzed conversion of DA to DOPAL by rat liver MAO (54), and the concentration was determined using an ALDH assay with NAD (52) and HPLC analysis as described below. Malondialdehyde (MDA) was obtained by heating 1,1,3,3-tetraethoxypropane in an aqueous solution containing HCl (91). Tyrosine, L-DOPA, DA, and all other chemicals were purchased from Sigma-Aldrich (St. Louis, MO) unless otherwise noted.

PC6-3 Cell Culture and

Tyrosine Hydroxylase Collection

PC6-3 cells were cultured in RPMI 1640 medium supplemented with heat-inactivated 10% horse serum, 5% fetal bovine serum, penicillin (10 IU/mL) and streptomycin (10 mg/mL). PC6-3 cells are a subline of the pheochromocytoma (rat adrenal medulla) PC-12 cell line which are a well-accepted model of a DA neuron (92). Cells were grown in a 10 cm tissue culture dish at 37 °C in 5% CO₂ for 3 days. Cells were then seeded into six-well plates (1×10^5) and were incubated at 37 °C in 5% CO₂ for 3 days prior to the addition of nerve growth factor (NGF) (50 ng/mL) to stimulate cell differentiation. PC6-3 cells were then kept in the same conditions for 4 days prior to use.

To collect cell lysate for some TH studies, cells were left undifferentiated (71) and 10 cm dishes were grown to confluence (4 days). Cells were washed 3 times with cold 10 mM sodium phosphate buffer (pH 6.8) (74), scraped and collected in 500 μ L of the same buffer. Lysate was sonicated 10 times at 3sec intervals, and then centrifuged using a Sorvall Discovery SE Ultraspeed centrifuge at $100,000 \times g$ for 1 h at 4 °C. The cytosolic fraction (i.e. supernatant) was collected to be used in TH lysate activity assays.

Tyrosine Hydroxylase Activity

Assay in Cell Lysate

Cell lysate was collected as previously described and stored at -80 °C until assays were performed. TH activity is stable up to a year when stored in these conditions (62). Activity was assessed using HPLC to monitor L-DOPA production. Control groups contained tyrosine (100 μ M) and tetrahydrobiopterin (0.5 mM), which were combined with lysate (0.2 mg/mL). Time points were taken at 0, 30, 60, 90, and 120 minutes and the reaction was stopped by the addition of 5% (v/v) perchloric acid. In DOPAL inhibition assays, varying concentrations of DOPAL (0.1, 0.5, 1.0, 2.5, 5, and 10 μ M) was also added and time points were taken as described above. After centrifugation to pellet proteins (10,000 $\times g$ for 3 min), all samples were then subjected to HPLC analysis to quantify L-DOPA production.

Tyrosine Hydroxylase

Activity Assay in PC6-3 Cells

In dopaminergic PC6-3 cell assays, NGF-differentiated cells were preincubated in a HEPES-buffered medium (115 mM NaCl, 5.4 mM KCl, 1.8 mM CaCl₂, 0.8 mM MgSO₄, 5.5 mM glucose, 1 mM NaH₂PO₄, and 15 mM HEPES (pH 7.4) for 15 min, and

then 10 μM tyrosine, 5 μM malondialdehyde (MDA, to inhibit aldehyde dehydrogenase and aldehyde reductase) (33), and 5 μM DOPAL were added. At time points of 0, 30, 60, 90, and 120 min, supernatant was removed and cells were lysed using 300 μL of 0.1% Triton-X in potassium phosphate (pH 7.4) buffer. After centrifugation ($10,000 \times g$ for 3 min) the supernatant was analyzed using HPLC analysis as described below for L-DOPA and DA production. It is important to note that MDA does not inhibit or alter tyrosine hydroxylase activity in pilot studies we completed as well as in previous studies (93).

HPLC Analysis of Activity Assays

An Agilent 1200 Series Capillary HPLC system with a photodiode array detector set to absorbance at 202 and 280 nm was used to determine L-DOPA and DA production. 15 μL of sample was injected, and separation was achieved using a Phenomenex Luna C18 column (1 x 150 mm, 100 \AA) and an isocratic flow of mobile phase consisting of 97% 0.1% trifluoroacetic acid (v/v) in HPLC-grade water, and 3% acetonitrile (v/v). The flow rate was 50 $\mu\text{L}/\text{min}$ and retention times were determined for DA, L-DOPA, tyrosine, and DOPAL to be 6.8, 7.9, 10.5, and 11.2 minutes, respectively, using standard samples. Conversion of area to concentration units was achieved using a calibration curve of standards.

Mechanism Studies in Cell Lysate

To determine how DOPAL inhibits TH (i.e. reversibly or irreversibly), cell lysate was used to study the mechanism of inhibition. To lysate (0.2 mg/mL), DOPAL (5, 10, or 20 μM), tyrosine (100 μM), and tetrahydrobiopterin (BH_4 , 0.5 mM) were added and preincubated (30, 60, or 90 min). After preincubation, all reactions were subjected to a Micro Bio-Spin 6 column twice (Bio-Rad, Hercules, CA) in order to entirely remove

excess DOPAL (use of column one time removed ~90% of DOPAL). Control groups (i.e. no DOPAL) were also subjected to the spin columns in order to keep continuity among experiments. Tyrosine and tetrahydrobiopterin were then reintroduced to the system (100 μ M and 0.5 mM, respectively) and time points were taken again at 0, 30, 60, 90, and 120 min. After placing samples in 5% (v/v) perchloric acid to stop the reaction and centrifuging at 10,000 x g for 3 min, samples were analyzed by HPLC as described above. In reversibility assays, the % recovery is defined as the production of L-DOPA in experimental conditions (preincubation with DOPAL) as compared to the controls where no DOPAL was present. Results were subtracted from 100 in order calculate the % recovery of activity after the removal of DOPAL. All assays were performed in 10 mM sodium phosphate buffer (pH 6.4) in a final volume of 275 μ L.

Statistical Analysis

All linear regression and statistical analysis were performed using the software GraphPad Prism 5.0 (Graph Pad Software, San Diego, CA) Data for cells treated with DOPAL were compared to the controls and significant differences ($p < 0.05$) were determined using a one-way ANOVA with a Tukey post-test (this was also used to analyze % recovery data for reversibility studies). Data for TH activity (i.e. L-DOPA formation) was determined using a linear regression.

Results

Tyrosine Hydroxylase is Potently

Inhibited in Cell Lysate

As shown in Figure 4.1A and 4.1B, treatment of PC6-3 cell lysate with tyrosine, BH₄, and varying concentrations of DOPAL (0, 0.1, 0.5, 1.0, 2.5, 5.0, and 10 μM) for 2 h resulted in a concentration-dependent inhibition of enzyme activity. HPLC analysis was used to quantify the production of L-DOPA, and Figure 4.1B is an enlargement of 4.1A to show detail at the higher concentrations of DOPAL.

All concentrations of DOPAL examined yielded inhibition of TH. Controls (i.e. no DOPAL present) showed a time-dependent increase in L-DOPA production, while the presence of DOPAL exhibited significant inhibition of tyrosine hydroxylase activity. It is important to note that TH activity in PC6-3 control cell lysate is similar as compared to activity demonstrated in previous studies using PC-12 cells (62, 71).

Analysis of linear slopes indicated over 80% inhibition of the enzyme at the low concentration of 0.5 μM DOPAL. As the concentration of DOPAL increased to 10 μM greater than 95% inhibition of TH activity was exhibited (Figure 4.1C). Initial studies indicated that 30 μM DOPAL demonstrated complete inhibition of the enzyme (data not shown). These results exhibit the potent inhibition of TH that DOPAL causes in cell lysate, leading to almost complete loss of L-DOPA production at low concentrations of DOPAL.

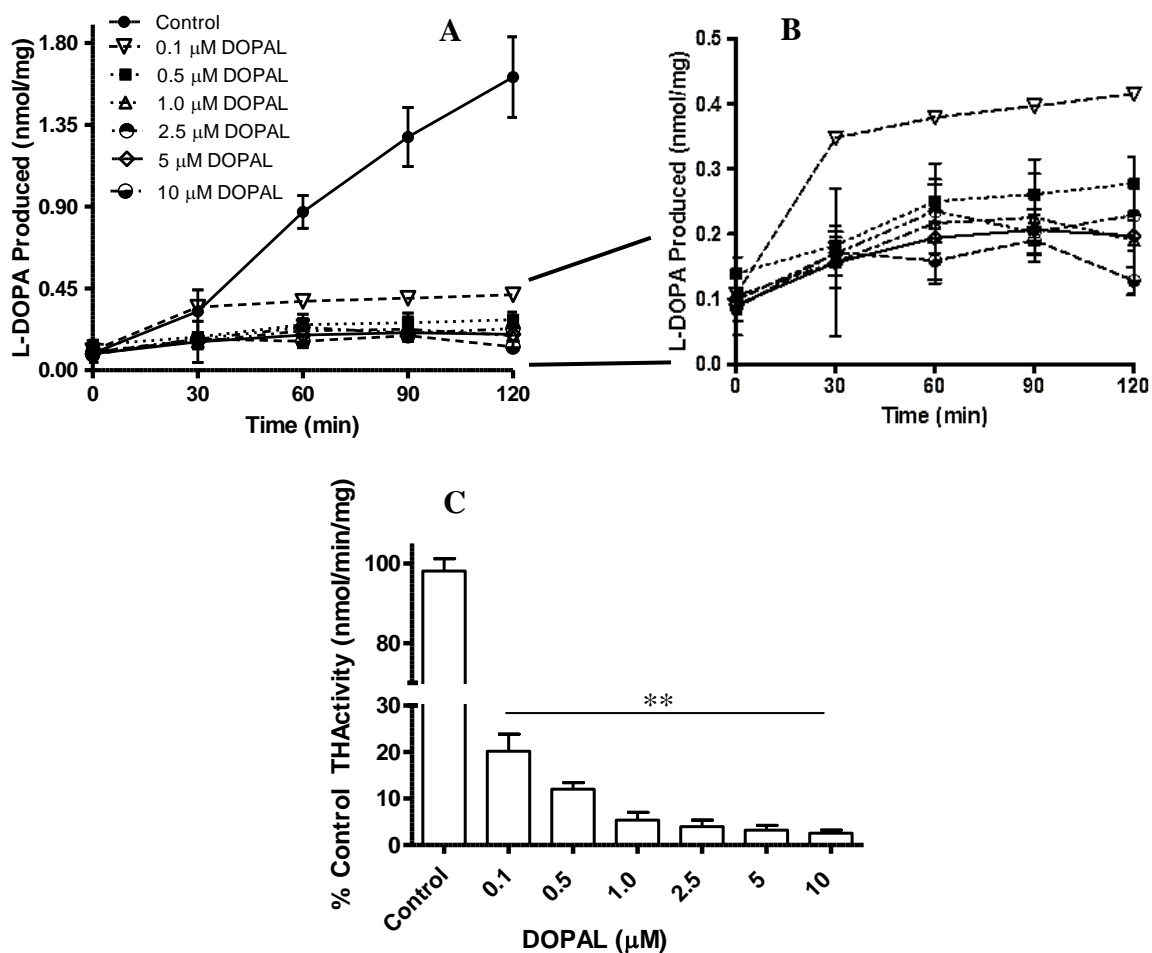


Figure 4.1 Treatment of PC6-3 cell lysate with varying concentrations of DOPAL leads to TH inhibition and a decrease in L-DOPA production. (A) L-DOPA production over 2 h shows significant inhibition by DOPAL. (B) Enhancement of 4.1A showing DOPAL treatment experiments. (C) Comparison of initial linear slopes shows the concentration-dependent decrease in L-DOPA production. Values shown represent the mean \pm SEMs ($n = 4$). **Significantly different from the control ($p < 0.05$). In all graphs: (●) control, (▽) 0.1 μ M DOPAL, (□) 0.5 μ M DOPAL, (▲) 1.0 μ M DOPAL, (◇) 2.5 μ M DOPAL, (◆) 5.0 μ M DOPAL, and (○) 10.0 μ M DOPAL.

Tyrosine Hydroxylase is Inhibited by

DOPAL in PC6-3 Cells

To determine the consequence of elevated DOPAL on TH activity in cells, NGF-differentiated cells were preincubated with HEPES-buffered media (pH 7.4) for 15 min and then 10 μ M tyrosine, 5 μ M MDA, and 5 μ M DOPAL were added for 2 h. Cells were lysed and collected at 30 min time points, and samples were subjected to HPLC analysis of L-DOPA and DA production. 5 μ M DOPAL was chosen as cells do not show significant mitochondrial dysfunction at this concentration, and cell death, while significant compared to control cells, is minimal. At 30 min time points, the supernatant was removed and cells were lysed using 0.1% Triton-X in 10 mM potassium phosphate buffer (pH 7.4). L-DOPA production was analyzed as described via HPLC. As can be seen in the data in Figure 4.2A, there is a decrease in L-DOPA production compared to controls when DOPAL levels were elevated. The DOPAL concentration was found to be between 4-5 μ M intracellularly, and TH activity was decreased ~41% compared to control cells where no DOPAL was present. Furthermore, the graph in 4.2B demonstrates the detrimental effect on DA synthesis as well. When DOPAL levels are elevated and L-DOPA synthesis is decreased, there is a concurrent inhibition in DA synthesis as well (~44%, as compared to control cells). These results indicate that DOPAL elevation in cells leads to significant TH inhibition, resulting in decreased L-DOPA and DA production.

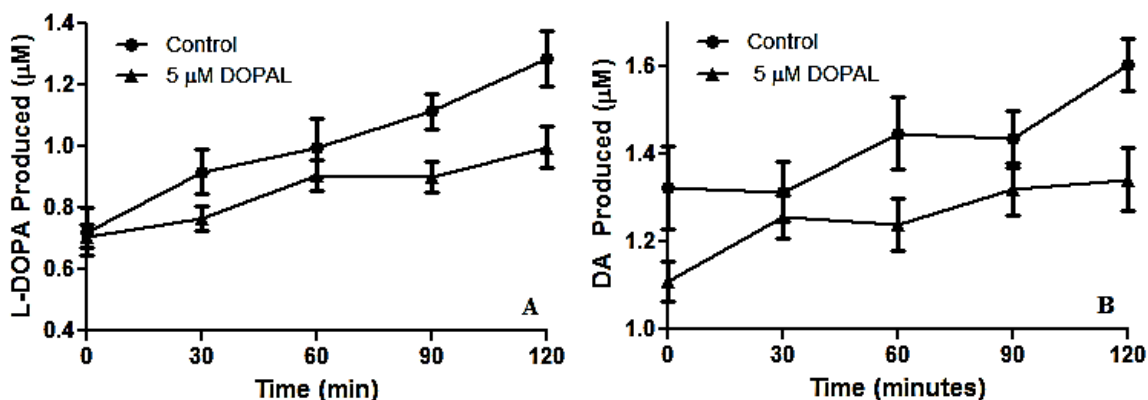


Figure 4.2 NGF-differentiated PC6-3 cells incubated with 10 μM tyrosine and MDA, and 5 μM DOPAL for 2 h. Cells were lysed and subjected to HPLC analysis to determine L-DOPA and DA production. (A) L-DOPA production over time; elevation in DOPAL leads to ~44% TH inhibition. (B) Concomitantly, DA production is decreased by a similar percent due to a decrease in L-DOPA. Values shown represent the mean \pm SEMs ($n = 3$).

DOPAL Inhibition Exhibits

Slow-Irreversible Element

It was of interest to investigate the reversibility of DOPAL-mediated inhibition of TH. These studies were carried out in cell lysate as previously described in the methods section. Briefly, preincubation of DOPAL (5, 10, 20 μM) was carried out for 30, 60, or 90 minutes. Excess DOPAL was then removed and substrate and cofactor were re-introduced. It is important to note that control groups (i.e. no DOPAL) were submitted to the same conditions as DOPAL groups (i.e. samples were also run through a spin-column), and no effect on TH activity was noted. As Figure 4.3A, B, and C demonstrate, recovery of TH activity displays both time- and concentration-dependent elements. Longer preincubations with DOPAL led to a decrease in the recovery of TH activity after

removal of excess DOPAL. Paralleling that trend, higher concentrations of DOPAL also lead to decreased recovery of enzyme activity.

When these data were compared, Figure 4.3D demonstrates the linear decrease in TH recovery as both preincubation time and concentration of DOPAL increases. These results indicate a semi-reversible or slow-irreversible TH inhibition by DOPAL, which is dependent upon both concentration and exposure time, and may have implications for the onset and progression of PD.

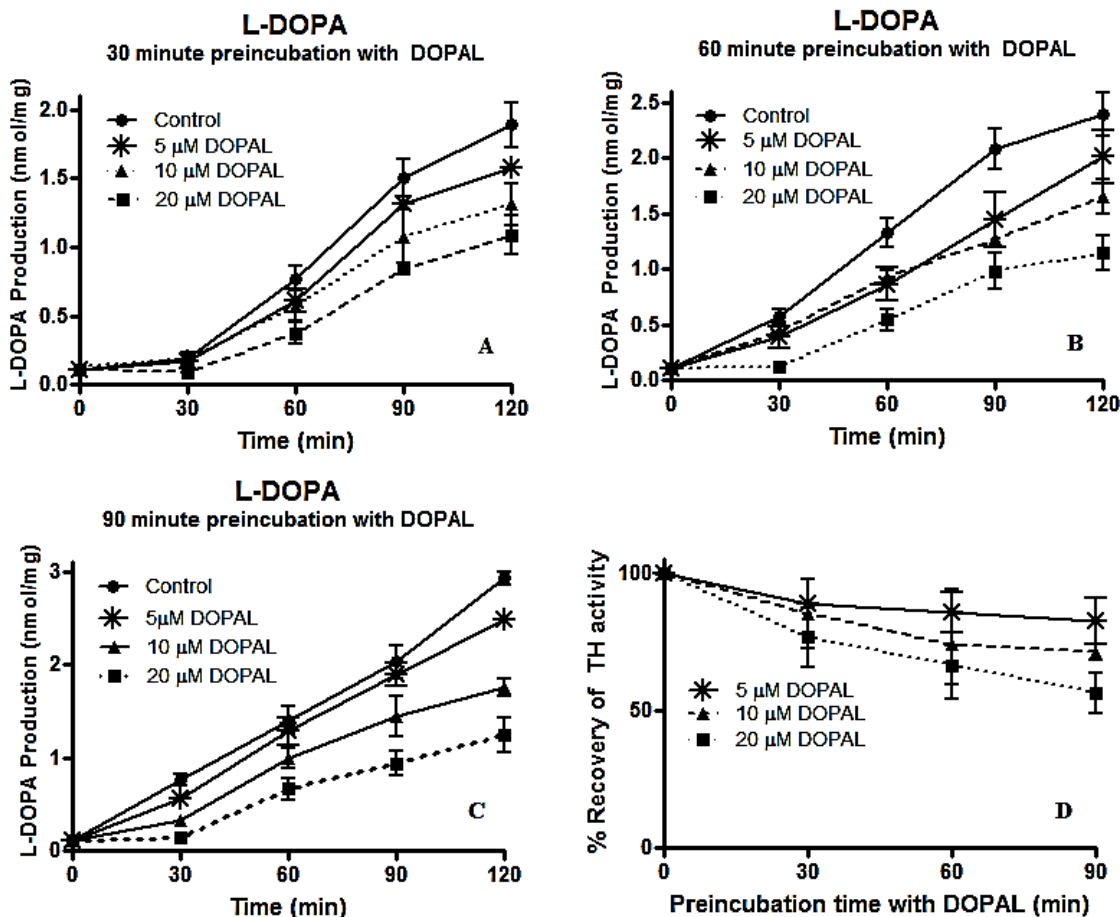


Figure 4.3 TH activity assays to determine recovery of L-DOPA production after inhibition by DOPAL (5, 10, 20 μ M) for 30, 60, or 90 min preincubation. Upon removal of DOPAL, there was re-introduction of tyrosine and BH₄ (100 μ M, 0.5 mM, respectively) and time points were taken as shown in the figure. (A), (B), and (C) demonstrate recovery of activity which displays time and concentration-dependent elements and 30, 60 and 90 min, respectively. (D) Indicates a linear decrease in recovery of TH as preincubation time and DOPAL concentration increase as determined by HPLC analysis. ($n = 3$ for all studies). In all graphs: (●) control, (*) 5 μ M DOPAL, (▲) 10 μ M DOPAL, (■) 20 μ M DOPAL.

Discussion

DOPAL, a reactive intermediate of DA catabolism, is an endogenous neurotoxin known to covalently modify proteins (34, 46, 50) and hypothesized to be a factor in the pathogenesis of PD (47, 67). The work presented here demonstrates the potent inhibition of TH activity after DOPAL modification, leading to a significant decrease in L-DOPA production in both cell lysate and PC6-3 cells. Furthermore, this inhibition appears to have a semi-reversible or slow-irreversible component demonstrating concentration and time-dependent characteristics.

In previous work, DA-quinones and other catecholamine quinones were found to covalently modify TH and inhibit activity (61, 94). Furthermore, results of earlier studies demonstrated the ability of other DA catabolism products, such as DOPAC, to inhibit TH as well (62). Overall, these results establish TH to be susceptible to protein modification via DA-related electrophiles and indicate that a mechanism of toxicity for DA neurons may involve TH. While the mechanism behind toxicity and cell death in the presence of DOPAL is currently unknown, it is hypothesized that toxicity and inhibition of TH are distinct processes which ultimately lead to dopaminergic cell death. Previous data reveal DA can potentially modify other important proteins such as Parkin and α -synuclein which leads to aggregation and overwhelming the capacity of proteasome clearance of aging or modified proteins (2, 53, 95). It is therefore possible that DOPAL could modify several other important proteins found in neurons, causing similar results that may decrease neuronal function in general. It is also of significance that in previously published studies L-DOPA has demonstrated trophic properties; therefore, inhibition of

TH and a decrease in L-DOPA production may lead to a decrease in cell viability (59, 60).

It is important to note the potency of DOPAL as an inhibitor of TH activity (almost 90% at 0.5 μM , Figure 4.1). Several studies have investigated the effect of catechols on TH activity, including L-DOPA, norepinephrine, DOPAC, and DA. Many demonstrated the ability to inhibit TH, with IC_{50} values ranging from 2.3 μM for norepinephrine, to 35 μM for L-DOPA (62, 96). It is clear from the work presented here that DOPAL is a significantly more potent inhibitor than DA or other DA-metabolites. It could be argued that because normal physiologic levels of DOPAL are between 2-3 μM , that TH would be highly inhibited at all times in the cell. It is essential to keep in mind that in these types of experiments DOPAL does not have to traverse cellular membranes, or move from the mitochondrial membrane to the cytosolic fraction where TH is found, thereby allowing higher interaction between DOPAL and TH. Furthermore, in cell lysate experiments involving TH inhibition and reversibility, DOPAL stability was investigated as a control. Preparation of cell lysate for experiments appears to remove cytosolic ALDH and AKR, and HPLC analysis revealed that DOPAL is not metabolized over 2 h, and no significant DA, DOPAC, or DOPET was detected in these control experiments. Due to this, it is significantly more facile for DOPAL to bind and inhibit TH activity when working in a cell lysate model. This model was chosen at first due to ease of experimentation, and the high quantity of lysate that could be obtained after just 4 days of culturing, as opposed to whole PC6-3 cell experiments in which cells must be NGF-differentiated and allowed to grow for a total of 8 days after plating. Overall, these

conditions allow for high DOPAL-TH interaction and modification by DOPAL to occur easily.

This idea is further supported by the dopaminergic PC6-3 cell experiments shown in Figure 4.2. In this system, DOPAL must move into the cell from the extracellular media where it may encounter some metabolism by ALDH and AKR. Furthermore, there are a variety of other possible protein targets for DOPAL to interact with in a whole cell model. Studies conducted in our lab previously identified a number of possible protein targets, including, heat shock protein 1, glutathione-S-transferase mu 1, and ribophorin 1, among others (97). Therefore, when DOPAL intracellular concentrations were 4-5 μM , TH was inhibited ~41%, demonstrating a less inhibition as compared to studies involving cell lysate. As previously discussed, DOPAL concentrations are known to be 2-3 μM (49); therefore, these results demonstrate that even slight shifts in intracellular DOPAL concentration can lead to detrimental effects in the cell in a short period of time.

Reversibility assays revealed that DOPAL incubation with TH exhibited a reversible and irreversible component of TH inhibition. As the data in Figure 4.3 show, there is both a concentration- and time-dependent recovery of TH activity as determined by L-DOPA production. Longer preincubation times with DOPAL (60 or 90 min) coupled with higher concentrations of DOPAL (20 μM) led to decreased TH activity after removal of excess DOPAL and reintroduction of substrate and co-factor. The data in Figure 4.3D show that DOPAL preincubation leads to TH inhibition that is reversible but also has a slow-irreversible component, which accounts for the decrease in recovery of activity after removal of excess DOPAL.

Overall, DOPAL has been shown to demonstrate high inhibition of the protein target, TH. This leads to a significant decrease in the production of L-DOPA in lysate models, and both L-DOPA and DA in PC6-3 cells. These results have implications for Parkinson's disease and exposure time to elevated DOPAL. From the data, it appears that in the presence of slightly elevated DOPAL, TH would be inhibited, leading to decreased L-DOPA production. If exposure to high DOPAL was relatively short (i.e. DOPAL levels were decreased), the reversibility assays demonstrate that TH would recover some of its activity, restoring DA synthesis. On the other hand, the presence of high DOPAL levels for long periods of time is predicted to lead to a decreased ability of the enzyme to recover activity, thus leading to a significant decrease in DA synthesis, a hallmark of PD. As previously discussed, there is evidence that the aging process leads to an increase in the activity of MAO catalyzed metabolism of DA, and products of lipid peroxidation such as malondialdehyde lead to inhibition of ALDH and AKR (33, 86). These combined actions would cause an increase in DOPAL production which, from the results presented here, would lead to potent inhibition of TH activity and a decrease in both L-DOPA and DA. Therefore, not only is DOPAL a toxic and reactive intermediate, but slight changes in cellular levels are predicted to lead to significant TH inhibition, and overall, less DA production.

CHAPTER FIVE
STRUCTURE-ACTIVITY RELATIONSHIP OF DOPAL ANALOGUES:
MECHANISM OF TOXICITY AND ENZYME INHIBITION

Introduction

Parkinson's disease (PD) is a neurodegenerative disorder which affects over a million people in the United States. This progressive disease leads to the selective loss of dopaminergic neurons in the substantia nigra, causing a decrease in the important neurotransmitter dopamine (DA) (2). DA is metabolized by monoamine oxidase (MAO) to the reactive and toxic intermediate 3,4-dihydroxyphenylacetaldehyde (DOPAL), which is further metabolized by aldehyde dehydrogenase (ALDH) and aldehyde reductase (AKR) to 3,4-dihydroxyphenylacetic acid (DOPAC) and 3,4-dihydroxyphenylethanol (DOPET), respectively (67). DOPAL has demonstrated high toxicity (46, 47) and the ability to interact with and modify both model peptides (34, 50), and proteins (88).

Tyrosine hydroxylase (E.C. 1.14.16.2), has been identified in our lab as a protein target of DOPAL modification (88). This leads to potent inhibition of enzyme activity, resulting in a significant decrease in L-DOPA and DA. While it is understood that DOPAL modification is slowly-irreversible (88), the mechanism of TH inhibition is not fully understood. Previous work to investigate the mechanism of DOPAL modification of model peptides revealed it to be dependent upon both the catechol and the aldehyde (50). To further investigate both toxicity and TH inhibition, structure-activity studies (SAR) were undertaken using a number of DOPAL analogues. Phenylacetaldehyde (PAL), a commercially available analogue, investigated the importance of the aldehyde alone. Two analogues were synthesized which determined how masking the catechol changed

toxicity and TH inhibition; 3-methoxy-4-hydroxyphenylacetaldehyde (MOPAL) examined the effect of a single hydroxyl group, while 3,4-dimethoxyphenylacetaldehyde (DMPAL) studied the effect of complete masking of the catechol. Finally, a novel nitrile analogue was synthesized: 3,4-hydroxyphenylacetone nitrile (DHPAN) examined the effect of replacing the aldehyde group with a nitrile. For all four analogues, mitochondrial dysfunction in PC6-3 cells was determined using the MTT assay, and the inhibition of TH was investigated in both cell lysate and whole PC6-3 cells.

While TH has been identified as a protein target of DOPAL modification (88), sites of adduction have not yet been determined. It was therefore of interest to employ mass spectrometry in order to elucidate sites of DOPAL modification to elucidate the mechanism of enzyme inactivation. It was first necessary to clone and purify recombinant TH; therefore, through a novel expression vector and purification procedure, human recombinant TH (hTH) was successfully produced. Using hTH, mass spectrometry studies were undertaken to determine sites of DOPAL adducts. Furthermore, it was possible to develop a novel real-time assay for hTH activity using a plate reader to measure changes in absorbance over time. This assay employed sodium periodate to oxidize L-DOPA formed in the reaction which rapidly converted to dopachrome and was monitored at 475 nm. Initial high-throughput screening (HTS) was performed as well to determine the applicability of this assay for this format.

For the first time, SAR studies were used to determine the importance of the catechol and aldehyde in DOPAL toxicity and inhibition of TH. Furthermore, a novel cloning and purification procedure was developed, and using pure, recombinant hTH, sites of DOPAL modification were identified and a novel plate reader assay for the

activity of hTH was established. Most importantly, using mass spectrometry (MS) and MS/MS, 5 DOPAL adducts were found on hTH, helping to elucidate the reason behind the potent inhibition of TH activity by DOPAL.

Experimental Procedures

Materials

DOPAL was biosynthesized as previously described using enzyme-catalyzed conversion of DA to DOPAL by rat liver MAO (54), and the concentration was determined via an ALDH assay (52) and HPLC analysis as described below. Tyrosine, L-DOPA, DA, DOPAC, phenylacetaldehyde (PAL), and all other chemicals were purchased from Sigma-Aldrich (St. Louis, MO) unless otherwise noted. Malondialdehyde (MDA) was obtained by heating 1,1,3,3-tetraethoxypropane in an aqueous solution containing HCl (91). 3,4-dimethoxyphenylacetaldehyde (DMPAL) was synthesized as described in Appendix A, 3,4-dihydroxyphenylacetonitrile (DHPAN), was synthesized as described in Appendix B, and 3-methoxy-4-hydroxy-phenylacetaldehyde (MOPAL) was biosynthesized as described in Appendix C.

Mitochondrial Dysfunction (MTT assay)

In order to determine the effect on mitochondrial function of the DOPAL analogs in PC6-3 cell cultures, the MTT reduction assay was used as previously described (88). NGF differentiated cells were treated with DOPAL analogs at 0, 5, 10, 25, and 50 μM and incubated for 2 h at 37°C in 5% CO_2 . MTT reagent was then added (0.5 mg/mL) to each well, and incubated for 2 h. The purple crystals were dissolved in DMSO and the

formazan product absorbance at 570 nm was read using a Molecular Devices Spectra-Max plate reader. Absorbance values for the analogs were compared to controls.

Tyrosine Hydroxylase Activity

Assay in Cell Lysate

As previously described in Mexas, *et al.*, cell lysate was collected from PC6-3 cells and assayed for TH activity by allowing cells to grow to confluence and collecting using 10 mM sodium phosphate buffer (pH 6.4). After centrifuging at $100,000 \times g$ for 1 h, lysate was stored at $-80\text{ }^{\circ}\text{C}$ until assays were performed. It is important to note that TH activity is stable up to a year when stored under these conditions (62). As previously reported, cell lysate experiments contained 100 μM tyrosine, 0.25 mM tetrahydrobiopterin (BH_4) and 0.2 mg/mL cell lysate (control), and the addition of either 10 or 20 μM PAL, MOPAL, DMPAL, or DHPAN in experimental conditions. Time points were taken at 0, 30, 60, 90, and 120 min and placed in 5% (v/v) perchloric acid. HPLC analysis was used to determine the production of L-DOPA over time.

Tyrosine Hydroxylase Activity

Assay in PC6-3 Cells

In whole cell assays, NGF-differentiated PC6-3 cells were preincubated in HEPES-buffered media for 15 min, and then 10 μM tyrosine, 5 μM MDA (to inhibit ALDH and AKR) (33), and 20 μM of PAL, MOPAL, DMPAL, or DHPAN were added. At time points of 0, 30, 60, 90, and 120 min, supernatant was removed and cells were lysed using 300 μL of 0.1% Triton-X in potassium phosphate (pH 7.4) buffer. Lysate was analyzed using HPLC analysis as described below for L-DOPA production. It is

important to note that MDA does not inhibit or alter tyrosine hydroxylase activity in studies we completed (data not shown) as well as in previous studies (93).

Relative Protein Reactivity (NBT)

Relative protein reactivity of each compound was determined using BSA. DOPAL, MOPAL, PAL, and DMPAL reactivity was calculated previously (50). In order to determine the reactivity for DHPAN, BSA (1 mg/mL) was incubated with either DOPAL (as a positive control, 100 μ M), or DHPAN (100 μ M) for 4 h at 37°C. Samples (9 μ g) were run on an SDS-PAGE and transferred to a nitrocellulose membrane (20 V, 40 min). As previously shown, nitroblue tetrazolium (NBT) will stain catechol-containing protein adducts (98, 99). The membrane was placed in 0.24 mM NBT in 2 mM potassium glycine buffer (pH 10) and allowed to incubate over night at 4°C. Integration of band density was performed using the NIH program Image J, version 1.37.

HPLC Analysis of Tyrosine Hydroxylase

Activity Assays

HPLC analysis of L-DOPA production in assays was performed using an Agilent 1200 Series Capillary HPLC system with a photodiode array detector measuring absorbance at 202 and 280 nm was used. Samples (15 μ L) were injected and separated using a Phenomenex Luna C18 column. For studies with PAL, DMPAL, MOPAL, and DHPAN a gradient was used as follows: 0-12 min: 3% B, 12-13 min: 15% B, 15-20 min: 15% B, 20-35 min: 3% B, where A consisted of 0.1% trifluoroacetic acid in water, and B was acetonitrile. Retention times were determined to be: 7.5 (L-DOPA), 10.5 (tyrosine), 22 (PAL), 18 (MOPAL), 21 (DMPAL), and 25 min (DHPAN). Conversion of peak area into concentration units was achieved using a calibration curve of standards.

Novel Cloning and Purification of
Human Recombinant Tyrosine Hydroxylase (hTH)

Using *E. coli*.

(In collaboration with Colin A. Higgins in Dr. David L. Roman's laboratory)

Materials for the cloning and purification of human recombinant TH (hTH) are as follows: primers were obtained from Integrated DNA Technologies (Coralville, IA) as dry powder and dissolved in water. Human tyrosine hydroxylase gene was purchased from Harvard PlasmID (Clone ID HsCD00378692) as a glycerol stock of pENTR223-transformed *E. coli* strain DH5 α . DNA purification kits, QIAprep Spin Miniprep and QIAquick Gel Extraction, and Ni-NTA resin were obtained from Qiagen (Valencia, CA). Restriction enzymes SalI and BamHI, T4 ligase, amylose resin were obtained from New England Biolabs (Ipswich, MA). DNaseI and E-64 were purchased Roche Applied Science (Indianapolis, IN). Phenylmethylsulfonyl fluoride (PMSF) was obtained from Research Products International (Mt. Prospect, IL). Lysozyme and pepstatin A were purchased from Thermo Scientific (Waltham, MA). Leupeptin was obtained from EMD Chemicals (Gibbstown, NJ). HiPrep SP FF 16/10 column and AKTApurifier fast protein liquid chromatography (FPLC) system were purchased from GE Healthcare (Piscataway, NJ). Sequencing was performed by the University of Iowa DNA Facility.

Excision of the hTH vector produced and obtained from the Plasmid Database at Harvard and introduction into the expression vector was performed as follows: TH-pENTR223-containing DH5 α stock was streaked onto a plate of LB agar supplemented with 100 μ g/mL spectinomycin, grown for 16 h at 37°C, a single colony was selected and expanded into 8mL LB broth supplemented with 100 μ g/mL spectinomycin, and grown

for 16 h at 37°C. Bacteria were pelleted at 3600 x g for 10 minutes at 4°C. pENTR223 plasmid was purified according to manufacturer's instructions (Qiagen).

The open reading frame containing full-length TH (amino acids MPT...AIG) was amplified with primers containing a 5' BamHI recognition site (5'-CGGATCCATGCCACCCCCGACGCCACCAC-3') and an in-frame 3' engineered stop codon followed by a SalI recognition site (5'-CCCGTCGACCTAGCCAATGGCACTCAGCGCA-3') using Platinum Pfx according to manufacturer's instructions (Life Technologies, Carlsbad, CA). This fragment and pMALc2H₁₀T vector (100) were gel-purified per manufacturer's protocol (Qiagen), double-digested with BamHI and SalI according to manufacturer instructions (New England Biolabs). Digested TH and pMALc2H₁₀T were gel-purified again (Qiagen) and ligated using T4 DNA Ligase according to manufacturer's instructions (New England Biolabs) using a 3:1 insert:vector ratio and incubation overnight at 16°C. The ligated product was transformed into XL10-Gold bacteria according to manufacturer's protocol (Stratagene, La Jolla, CA).

Several colonies were selected, minipreped, and their DNA sequenced to ensure in-frame insertion of TH with forward and reverse with primers: pMAL5'sense GCGGTCGTCAGACTGTCGATGAAG, TH middle antisense GCGCTCCAGCAAAGCAAAGGCC, TH middle sense CCCAGTATATCCGCCACGCG, and pMAL3'antisense GGCGATTAAGTTGGGTAACGCCAGG.

Upon confirmation of proper ligation of the hTH and pMAL vector, expression in *E. coli* was performed. pMALc2H₁₀T-TH (MBP-TH) vector was transformed into

BL21(DE3) *E. coli*, and a single colony was picked and expanded to 10mL in LB supplemented with 100µg/mL ampicillin (amp) and shaken for 16 h at 37°C. This was pelleted at 3600 x g for 10 minutes at 4°C and resuspended in 500µL LB to which was added 500µL 80% (v/v) sterile glycerol and stored at -20°C. To express MBP-TH, 5µL of glycerol stock was expanded in a starter culture of 10mL LB+amp for 8 h shaken at 37°C, which was then expanded to a seed culture of 200mL LB+amp and was shaken overnight at 37°C. On the morning of induction, the seed culture was expanded to 4x1L LB+amp, grown to OD₆₀₀ 0.4 at 37°C, then cooled to 25°C by shaking the flasks in a tub of ice, and grown to OD₆₀₀ 0.6 at 25°C.

In order to induce protein expression, 250µM β-D-1-thiogalactopyranoside (IPTG) was added along with 100 µM FeSO₄, and 0.2% (w/v) glucose for enzyme stability and to prevent the production of bacterial amylases respectively. Induction was carried out for 20 h at 25°C, after which bacteria was pelleted at 3600 x g at 4°C, resuspended in 30mL TH buffer **A** at 4°C (50mM HEPES pH 6.8 100mM NaCl 5mM β-mercaptoethanol) supplemented with protease inhibitors (100µg/mL PMSF, 1 µM Leupeptin, 1 µg/mL Pepstatin, and 1µM E-64) added to buffer immediately before use. The suspended pellet was snap frozen in liquid nitrogen and then the purification of hTH was performed in a 3 step procedure. The pellet was thawed at 37°C, stirred on ice with 0.8mg lysozyme per mL of pellet (not including 30mL of buffer) for 10 min, snap frozen, and thawed again. Following lysis, 10µg/mL DNaseI was stirred into the viscous mixture (10 min on ice), and the lysate was centrifuged for 1 h at 100,000 x g (36500 rpm) in a Sorvall T-647.5 rotor. The supernatant was filtered (0.45 µm) and loaded onto a 10 mL amylose resin column equilibrated with buffer **A**. The resin was washed with 50 mL

buffer A and eluted with 70 mL (5 mL fractions) buffer A containing a competing concentrations of 10 mM maltose. Following SDS-PAGE analysis, MBP-TH fusion protein-containing fractions were pooled and digested with TEV-protease (10:1 molar ratio TH:TEV) for 8 hours at 4°C on a rotating mixer. Digestion was monitored by SDS-PAGE to ensure complete cleavage, after which the sample was diluted 5-fold in TH buffer B (50mM HEPES, pH 6.8, 5mM β ME) and loaded onto a HiPrep Q FF 16/10 column equilibrated with TH buffer B in an AKTApurifier. To elute TH, buffer B plus 1M NaCl was used. The sample was eluted over a gradient of 0-15% B over 1 C.V., 5 C.V. at 15% B, a gradient of 15-30% B over 5 C.V., and then 30-100% B over 5 C.V. The first eluting peak, eluting at 13.5mS/cm, contained pure MBP. The second peak, eluting at 22.5mS/cm, contained 99%+ pure TH.

hTH Activity Assay and HPLC Analysis

In order to assess hTH activity, a similar procedure as used for lysate TH activity was employed. Briefly, 10 μ g of recombinant hTH was incubated with 50 μ M tyrosine, 0.25 mM BH_4 , and 2.5 μ M iron (II) sulfate in 10 mM sodium phosphate buffer (pH 6.4) at 37°C for 20 min. At 5 min time points, aliquots were taken and placed in 5% (v/v) perchloric acid to stop the reaction. L-DOPA production was monitored using an Agilent 1200 Series Capillary HPLC system as described above.

Methanol-Chloroform-Water Precipitation of hTH

Due to the high salt content of the final step of purification of hTH, interference with mass spectrometry analysis was expected. Therefore, a precipitation method involving methanol, chloroform, and water was employed (101). Briefly, 200 μ L of hTH was added to 800 μ L of methanol. After vortexing, the sample was spun at 9000 \times g for

10 sec. Then, 200 μL of chloroform was added and the sample vortexed again. After centrifuging for another 10 sec at $9000 \times g$, 600 μL of water was added, and the sample was again vortexed and spun for 1 min. The upper phase was removed (it is important to note that care was taken to not remove any sample from the bilayer between phases). Another 600 μL of methanol was then added and the sample vortexed again. After spinning at $9000 \times g$ for 4 min, the supernatant was removed and the pellet dried under a stream of air. The sample was then dissolved in 100 μL of 50 mM ammonium bicarbonate (pH 7.4) for incubation with DOPAL and mass spectrometry analysis.

Mass Spectrometry Analysis to Identify

DOPAL Adducts on Tyrosine Hydroxylase

A Shimadzu IT-TOF mass spectrometer was coupled with a Shimadzu HPLC for mass spectrometry (MS) analysis. A Phenomenex Aeris Widepore XB-C18 column (100 x 2.1 mm), with a particle size of 3.6 μm and a pore size of 200 \AA was used to separate peptides. A mobile phase of 0.1% formic acid in water (A) and 0.1% formic acid in ACN (B) was used in gradient with the following time course: 0 min: 5% B, 5-15 min: 5-50% B, 15-30 min: 50-90% B, 31 min: 95% B, 35 min: 50% B, 36 min: 5% B, 40 min: 5% B. Prior to analysis, hTH was incubated with 50 μM DOPAL for 4 h at 37°C. Control samples containing no DOPAL were also incubated at 37°C. Following incubation, samples were run through Bio-Rad spin columns in order to remove excess DOPAL. This was done to ensure adducts were on the whole protein, and not on exposed residues after trypsinization. Finally, the addition of 10% (v/v) ACN, 0.1 mM BME, and a 1:50 ratio of trypsin was incubated for 8 h at 37°C. 15 μL of sample was injected and were run through

the photodiode array detector prior to MS analysis. Scanning was performed from m/z 200 to m/z 2000 in 3.3 seconds.

In MS/MS, the same samples were once again subjected to HPLC-MS analysis from m/z 200 to m/z 2000 followed by MS/MS scanning from m/z 200 to m/z 1000 with a repeat value of 3. Ion accumulation was set to 50, with activating signal conintegrator (ASC) set to 70%, and a collision induced dissociation (CID) setting of 50%. The same gradient was used as described above.

Novel Real-Time Assay to Monitor

Tyrosine Hydroxylase Activity

Utilizing hTH, a novel real-time assay to follow L-DOPA production was developed. This assay employed a plate reader measuring at 475 nm in order to watch the production of dopachrome from L-DOPA, which was catalyzed by sodium periodate. This chemical oxidizes L-DOPA, which then autocyclizes to the chromophore, absorbing at 475 nm. In control activity experiments, TH (10 μ g), BH₄ (0.25 mM), and iron (II) sulfate (2.5 μ M) were pre-mixed to allow for cofactor and iron binding (**A**) for 3-6 min on ice. A second mixture of 10 mM HEPES buffer (pH 6.8) and tyrosine and sodium periodate (50 and 100 μ M, respectively) was made (**B**). The two were combined in a 96-well plate and immediately placed in a Molecular Devices Spectra-Max plate reader with absorbance set to 475 nm. After an initial mix for 3 sec, the plate was read every 10 sec for 30 min at 37°C. In studies with DOPAL, the same concentrations of TH, BH₄, iron sulfate, tyrosine, and sodium periodate were used, with the addition of 5, 10, or 20 μ M DOPAL prior to the addition of mixture B. For plate reader assays, TH activity measured via dopachrome production with $\epsilon=3700 \text{ M}^{-1}\text{cm}^{-1}$ (102), and $b=0.51 \text{ cm}^{-1}$. In negative

control assays, 3-iodo-tyrosine (3IT, 50 μM) or CoCl_2 (100 μM) were used to competitively inhibit tyrosine and iron binding, respectively (103, 104). These were added to **A** immediately prior to the addition of **B**.

Control experiments included the following: exclusion of tyrosine or hTH (to determine background absorbance), and sodium periodate with each component of reaction mixture (to ensure no cross-reactivity). All experiments were done at a final volume of 200 μL and 10 mM HEPES buffer (pH 6.8) and read for 30 min.

High Throughput Screening Assay

To determine if the plate reader assay could be applied to high throughput screening (HTS) for future assessment of possible inhibitors or activators of hTH activity, the real-time assay was scaled down to be performed in a Corning 384-well plate. Samples were read using an EnVision 2104 Multilabel Plate Reader (PerkinElmer) with data collection being performed using the Wallace EnVision Manager Version 1.12 (PerkinElmer). The final sample volume was 100 μL , and in place of BH_4 , 6,7-Dimethyl-5,6,7,8-tetrahydropterine hydrochloride (DMPH_4) was used. This a non-natural cofactor is less active than the natural cofactor, but it allows for higher tyrosine concentrations to be used in the assay (105). The same assay structure was used in the HTS studies, therefore the same concentrations of hTH, iron, and DMPH_4 were preincubated (Mix **A**, 10 μg , 2.5 μM , and 0.25 mM, respectively) for 5-10 min. Mixture **B** contained tyrosine (200 μM), NaIO_4 (400 μM) and HEPES (pH 6.8). **A** was added to the plate, and in order to achieve inhibition in HTS assays, cobalt chloride (CoCl_2 , 100 μM) was used as a competitive inhibitor of Fe binding (104). The 384-well plates were used to determine a Z-factor. 48 wells were used for positive control experiments (maximum signal, no hTH

inhibition), and 48 wells were used for negative control (minimum signal, CoCl₂ inhibition). CoCl₂ was added to the wells immediately prior to the addition of **B**, and plates were then read for 3 h at 60 sec intervals. The Z-factor was determined using the following equation: $Z\text{-factor} = 1 - \frac{3 \times (\sigma_p + \sigma_n)}{|\mu_p - \mu_n|}$, where σ is the standard deviation for the positive (p, no inhibition) and negative (n, CoCl₂ inhibition), and μ is the mean of both of these conditions.

Background absorbance due to CoCl₂ was determined by measuring the absorbance of 100 μ M CoCl₂ in 10 mM HEPES (pH 6.8) and subtracting the measured background from the final absorbance values. All HTS studies were completed at 37°C in 10 mM HEPES (pH 6.8) at a final volume of 100 μ L.

Statistical Analysis

All linear regression and statistical analysis were performed using the software GraphPad Prism 5.0 (Graph Pad Software, San Diego, CA). Data for cells treated with DOPAL or the analogs were compared to the controls and significant differences ($p < 0.05$) were determined using a one-way ANOVA with a Tukey post-test. Data for TH activity and L-DOPA formation was determined using a linear regression. For MS and MS/MS analysis, the University of California, San Francisco (UCSF) Protein Prospector MS-Digest program was used to perform a typical trypsin digest of hTH. A maximum of 2 missed cleavages was used, and variable modifications included the formation of pyroglutamate, and oxidation of methionine and peptide mass was set for m/z 200-4000.


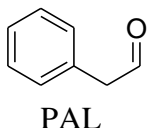
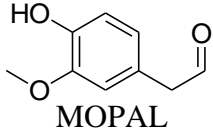
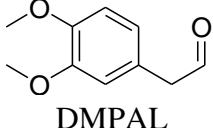
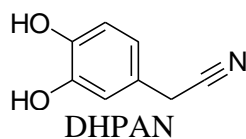
Results

Structure-Activity Relationship Studies

of DOPAL Analogues

In order to study the structure-activity relationship of DOPAL, 4 analogues were used. Shown in Table 5.1 are the structures of each analog and the important feature of DOPAL studied to determine the change in cellular toxicity (i.e. mitochondrial dysfunction), and inhibition of. The relative protein reactivity as determined by NBT staining is also described in the table.

Table 5.1 Summary of key structural features of DOPAL and analogues, and their relative protein reactivity with BSA as determined by the NBT assay.

Compound	Reactive Group	Relative Protein Reactivity (50)
 <p>DOPAL</p>	Catechol and aldehyde	1
 <p>PAL</p>	Aldehyde	<0.1 ^a
 <p>MOPAL</p>	Aldehyde and monomethyl catechol	0.2 ^a
 <p>DMPAL</p>	Aldehyde and dimethyl catechol	<0.2 ^a
 <p>DHPAN</p>	Catechol	ND ^b

^a NaCNBH₃ required for protein reactivity and adduct stability(50).

^b As described in the methods section, no protein reactivity with BSA was determined as compared to DOPAL reactivity by NBT staining.

Phenylacetaldehyde Toxicity and Tyrosine Hydroxylase Inhibition

Using the MTT assay, mitochondrial function was assessed after PC6-3 cell incubation with varying concentrations of phenylacetaldehyde (PAL, 5, 10, 25, 50 μM) for 2 h. Figure 5.1A demonstrates the slight concentration-dependent increase in mitochondrial dysfunction. While these results are significant as compared to the controls, PAL does not display the toxicity of DOPAL (88).

TH activity in both cell lysate as well as whole PC6-3 cells was assessed in the presence of PAL (10 or 20 μM) for 2 h. The data in figures 5.1B and C show that PAL is capable of inhibiting TH activity, leading to decreased L-DOPA production. There is ~44% inhibition of TH activity in cell lysate (20 μM PAL), while ~56% inhibition in PC6-3 cells is observed when 10-12 μM PAL is taken up into cells. These results demonstrate that PAL is capable of inhibiting TH and diffuses into PC6-3 cells, where it leads to some dysfunction and TH inhibition.

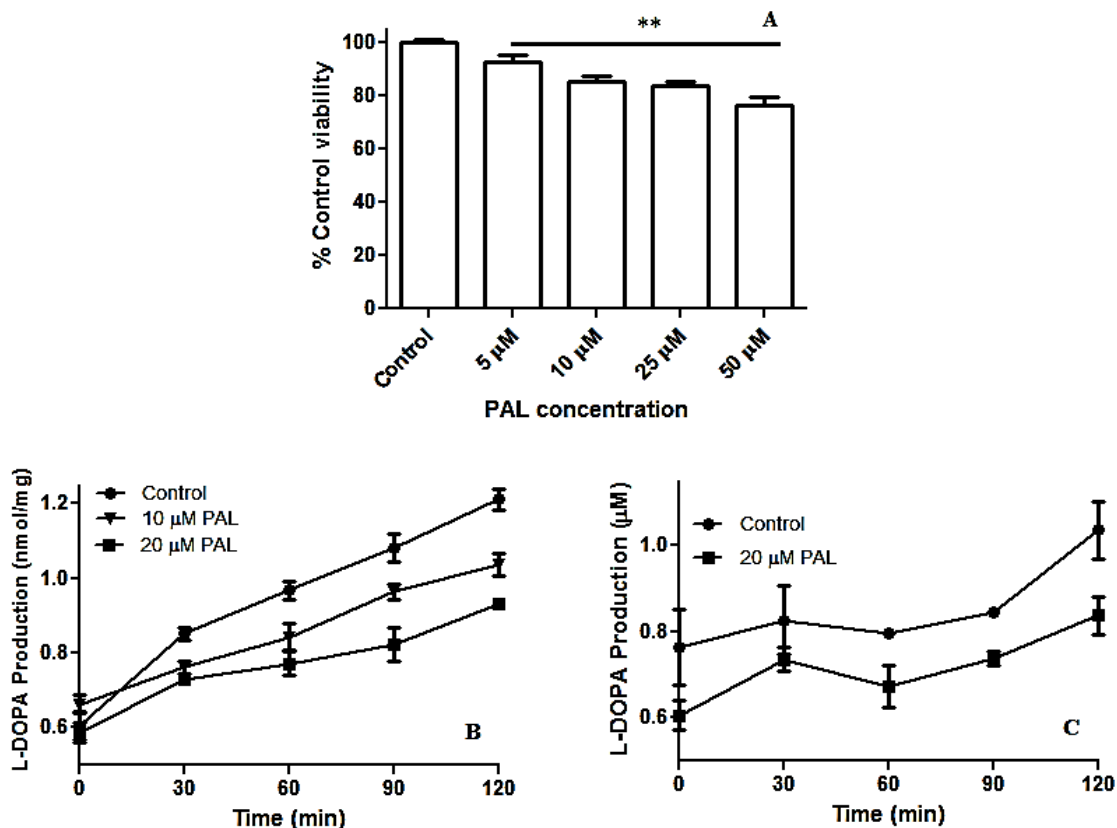


Figure 5.1 PAL toxicity and TH inhibition profile. (A) PC6-3 cells incubated with increasing concentrations of PAL for 2 h. MTT analysis of mitochondrial function showed concentration-dependent increase in dysfunction. (B) Cell lysate activity assay in the presence of PAL; increased PAL demonstrated decreased L-DOPA production. (C) 20 μM PAL on PC6-3 cells lead to ~56% decrease in L-DOPA production. All values shown represent the mean \pm SEMs ($n = 3$). ** indicates significant mitochondrial dysfunction as compared to control cells ($p < 0.05$).

3-Methoxy-4-hydroxyphenylacetaldehyde Toxicity and

Tyrosine Hydroxylase Inhibition

To further study the importance of the catechol group, the DOPAL-metabolite 3-Methoxy-4-hydroxyphenylacetaldehyde (MOPAL) was used. MOPAL is the catechol-o-methyltransferase (COMT) metabolite of DOPAL, which leads to the

selective methylation of the 3-position hydroxyl group (106). These studies may give insight into other mechanisms of protein modification and enzyme inhibition in the cell as this metabolite is also produced from DA metabolism. MOPAL was biosynthesized from 3-methoxytyramine as described in Appendix C. Data in Figure 5.2A demonstrate the result of elevated MOPAL on the mitochondrial function of PC6-3 cells. MOPAL treatment yields some toxicity, but significance from the control is only seen at 50 μ M, making it much less toxic than DOPAL.

To study the effect of MOPAL on TH activity, 20 μ M MOPAL was incubated with PC6-3 cell lysate for 2 h and time points were taken at 30 min intervals. Figure 5.2B indicate MOPAL inhibits TH activity, leading to decreased L-DOPA production. Inhibition was ~44% at 20 μ M MOPAL, indicating it is a less potent inhibitor than DOPAL.

As shown in Figure 5.2C, 20 μ M MOPAL treatment of cells for 2 h demonstrated alteration in TH activity, leading to decreased L-DOPA production. Results indicate TH activity decreased ~50% when MOPAL levels were between 9 and 10 μ M in cells. Overall, these results demonstrate MOPAL to have decreased toxicity and inhibition properties as compared to DOPAL (88).

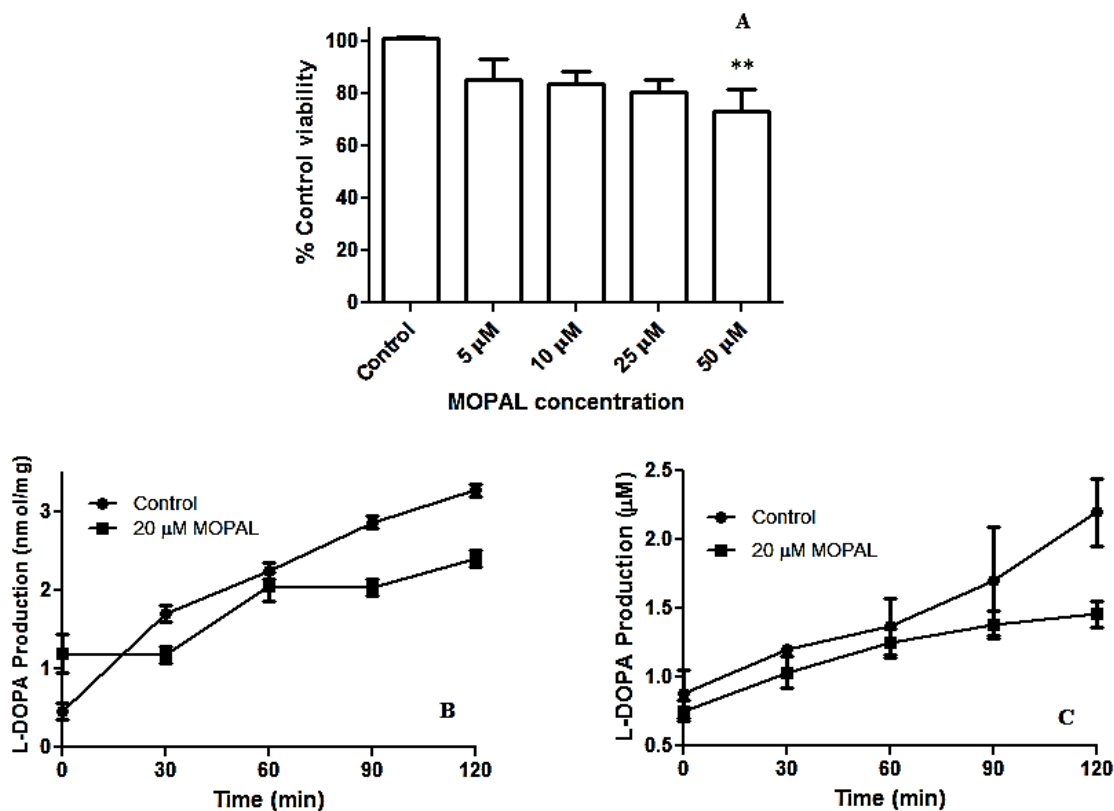


Figure 5.2 MOPAL toxicity and TH inhibition. (A) PC6-3 cells incubated with MOPAL for 2 h demonstrated minimal toxicity, with significance from the controls only seen at 50 μ M. (B) TH inhibition in cell lysate. 20 μ M MOPAL lead to ~44% inhibition. (C) MOPAL lead to ~50% inhibition of TH in PC6-3 cells when 10-12 μ M MOPAL was found intracellularly. All values shown represent the mean \pm SEMs ($n = 3$). **indicates significant mitochondrial dysfunction from control cells ($p < 0.05$).

3,4-Dimethoxyphenylacetaldehyde Toxicity and

Tyrosine Hydroxylase Inhibition

As previously mentioned, 3,4-Dimethoxyphenylacetaldehyde (DMPAL) was also investigated in order to study the importance of the catechol in toxicity and protein modification. DMPAL provides an analogue which contains a “masked” catechol as

compared to DOPAL in order to help assess changes in toxicity and inhibition of TH. The MTT assay revealed a loss of toxicity in PC6-3 cells, with even high concentrations of DMPAL exhibiting no toxicity after 2 h (Figure 5.3A).

PC6-3 cell lysate was incubated with 20 μ M DMPAL and time points were analyzed by HPLC for the production of L-DOPA. Results in Figure 5.3B show that DMPAL leads to ~28% inhibition in cell lysate.

Similarly, Figure 5.3C shows cells incubated with 20 μ M DMPAL lead to just over 30% inhibition of L-DOPA production when 9-10 μ M DMPAL was detected intracellularly. These results indicate DMPAL to be significantly less toxic and exhibit less inhibition of TH activity as compared to DOPAL.

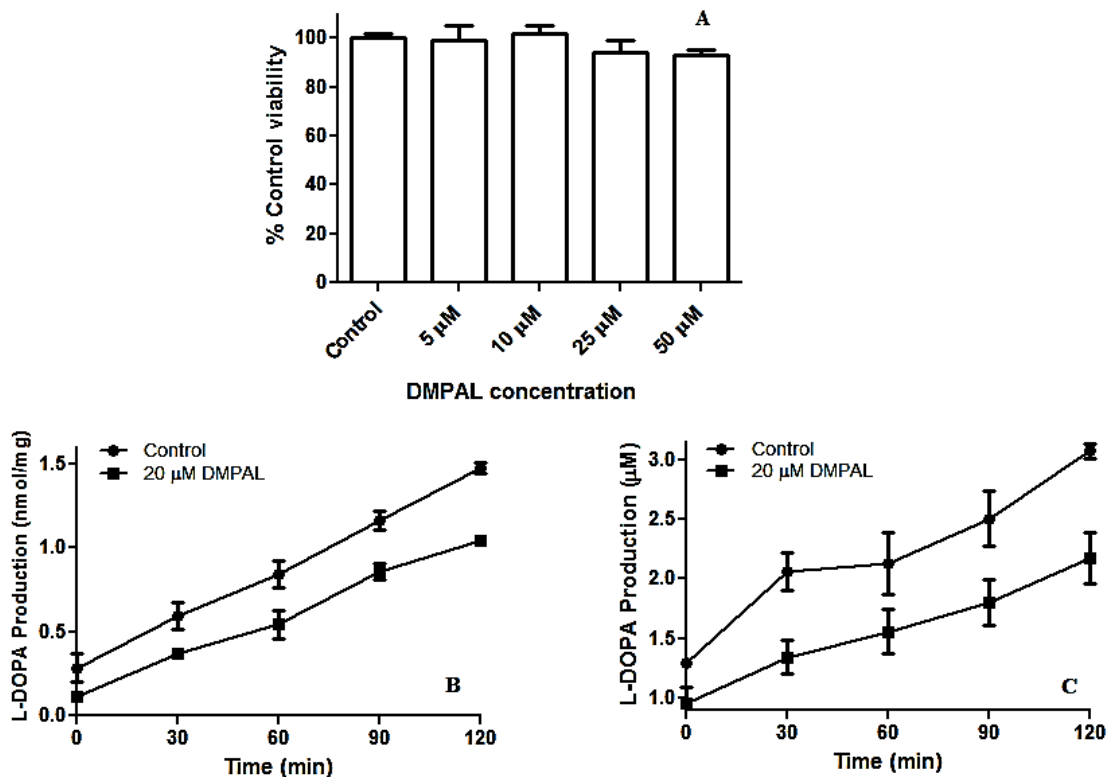


Figure 5.3 DMPAL toxicity and TH inhibition in lysate and PC6-3 cells. (A) MTT results demonstrating no toxicity to PC6-3 cells in the presence of DMPAL after 2 h. (B) TH+ cell lysate incubated with 20 μM DMPAL exhibited ~28% inhibition as compared to controls. (C) PC6-3 cells with 9-10 μM DMPAL intracellularly showed a little over 30% inhibition of TH activity. All values shown represent the mean \pm SEMs ($n = 3$).

3,4-Dihydroxyphenylacetonitrile Toxicity and Tyrosine Hydroxylase Inhibition

The nitrile analog of DOPAL, 3,4-dihydroxyphenylacetonitrile (DHPAN) was synthesized from 3,4-methylenedioxyphenylacetonitrile as described in Appendix B. DHPAN was selected in order to investigate how the replacement of the aldehyde affects toxicity and inhibition of TH. The nitrile functional group is still polar, but predicted to

be much less electrophilic and reactive to nucleophiles. Previous studies support the hypothesis that the aldehyde of DOPAL interacts with amino acid residues containing free amines, such as Lys or Arg residues, leading to covalent modification (50). Replacement of the aldehyde with a nitrile group does not significantly change the electronic or steric properties of the molecule; however, the nitrile will not be as reactive toward nucleophiles as a carbonyl (107).

To compare the mitochondrial dysfunction produced in the presence of elevated DHPAN, the MTT assay was used. After a 2 h incubation with 5, 10, 25 or 50 μM DHPAN, the MTT reagent was added and absorbance measured. As can be seen in Figure 5.4A there is no significant mitochondrial dysfunction. Interestingly, when higher levels of DHPAN were tested in pilot experiments, treatment of cells with 200 μM DHPAN exhibited cellular dysfunction similar to 50 μM DOPAL (Figure 5.4B).

Lysate was incubated with tyrosine, BH_4 , and DHPAN (100 μM , 0.25 mM, and 10 or 20 μM , respectively) for 2 h and time points were taken at 30 min intervals. Upon HPLC analysis, L-DOPA production was decreased ~25% by 20 μM DHPAN as can be seen in Figure 5.4C.

20 μM DHPAN was incubated with PC6-3 cells and wells were lysed at 30 min time points. The production of L-DOPA in Figure 5.4D appeared unaffected by DHPAN with no significant difference between control and DHPAN incubated cells noted. It is important to note that there appeared to be very low levels of DHPAN in the cells at each time point (between 0 and 1 μM), as determined by HPLC analysis. These results suggest the aldehyde plays a role in the trafficking of DOPAL in and out of the cells.

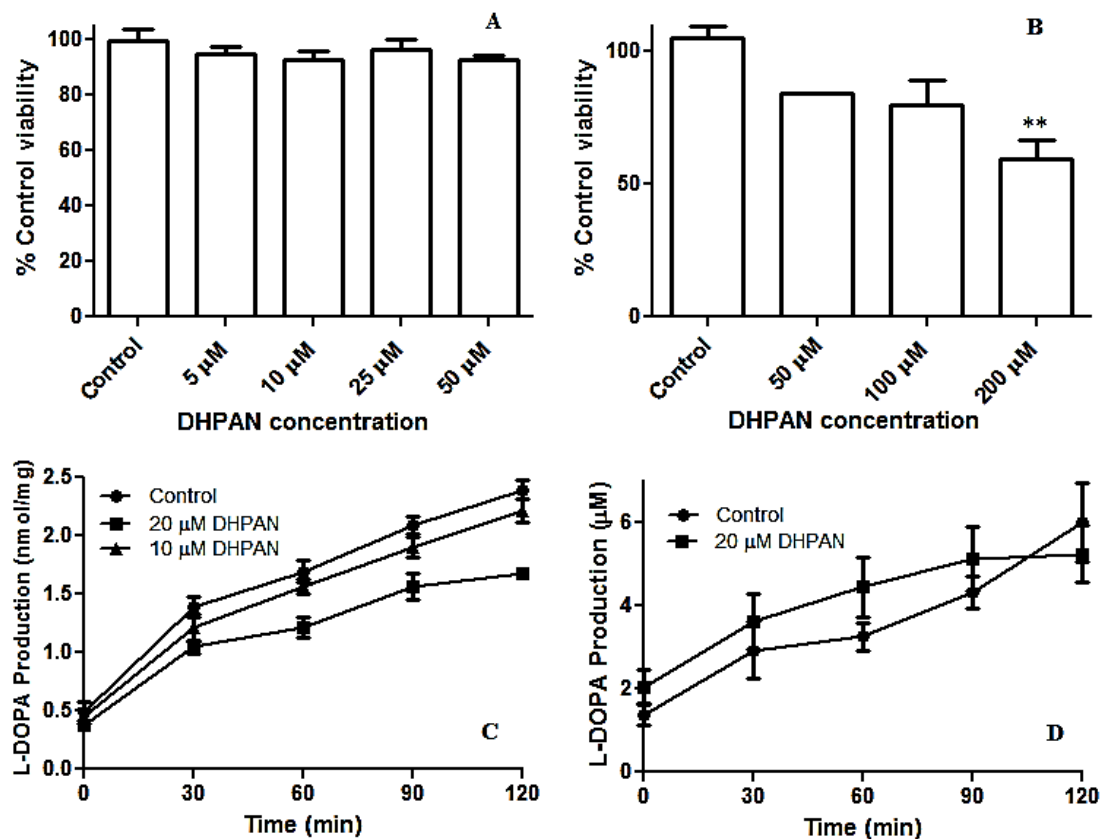


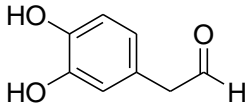
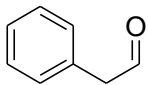
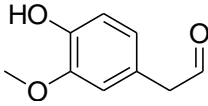
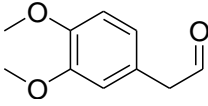
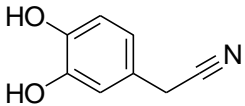
Figure 5.4 DHPAN toxicity and TH inhibition in lysate and cells. (A) MTT results when investigating varying physiologically relevant concentrations of DHPAN after 2 h. Cells show no significant toxicity compared to controls. (B) Pilot studies studying the effect of higher concentrations of DHPAN. 200 μM DHPAN exhibits mitochondrial dysfunction similar to that of 50 μM DOPAL. (C) DHPAN shows inhibition of TH in cell lysate (~25% at 20 μM). (D) DHPAN leads to no significant inhibition in PC6-3 cells. Concentrations of DHPAN were found to be only 0-1 μM intracellularly. All values shown represent the mean ± SEMs ($n = 3$ for A, C and D) ($n = 2$, for B). ** indicates significant mitochondrial dysfunction from the control ($p < 0.05$).

Summary of Structure-Activity Relationship Studies

Table 5.2 summarizes the results from the structure-activity studies with DOPAL analogs. As can be seen, DOPAL is far more toxic to cells and more potently inhibits TH

activity than the analogs. These results demonstrate the importance of both the catechol and aldehyde of DOPAL in terms of toxicity to dopaminergic PC6-3 cells and inhibition of the important enzyme TH.

Table 5.2 Summary of DOPAL and Analogue Toxicity, and TH Inhibition in Lysate and PC6-3 Cells

Compound	Toxicity at 25 μ M (% Cell viability)	TH inhibition (lysate, 20 μ M)	TH inhibition (PC6-3 cells)
 DOPAL	50 ^a (IC ₅₀ = ~80 μ M) ^b	~95% ^b	~56% 5 μ M ^d
 PAL	80 (IC ₅₀ >> 1000 μ M)	~44%	~53% 20 μ M ^d
 MOPAL	80 (IC ₅₀ > 1000 μ M)	~42%	~49% 20 μ M ^d
 DMPAL	NS ^c	~28%	~35% 20 μ M ^d
 DHPAN	NS ^c	~27%	NS ^c

^a Based on trypan blue results as shown in Figure 3.4

^b See reference (88).

^c NS = no significant toxicity or inhibition of TH activity.

^d Concentration of DOPAL or analogue placed exogenously on PC6-3 cells

Furthermore, Figures 5.5 and 5.6 show the summarized TH inhibition in both cell lysate and PC6-3 cells, respectively. It is clear that DOPAL exhibits much higher inhibition of TH activity when compared to the analogues, indicating that even slight changes to structure highly effect the action of DOPAL. While PAL and MOPAL exhibit similar inhibition of TH in PC6-3 cells (Figure 5.6), it requires higher intracellular concentrations than DOPAL (4-5 μM DOPAL versus 9-12 μM for PAL or MOPAL). These results demonstrate the potent inhibition DOPAL exerts on TH is dependent on both functionalities of the compound.

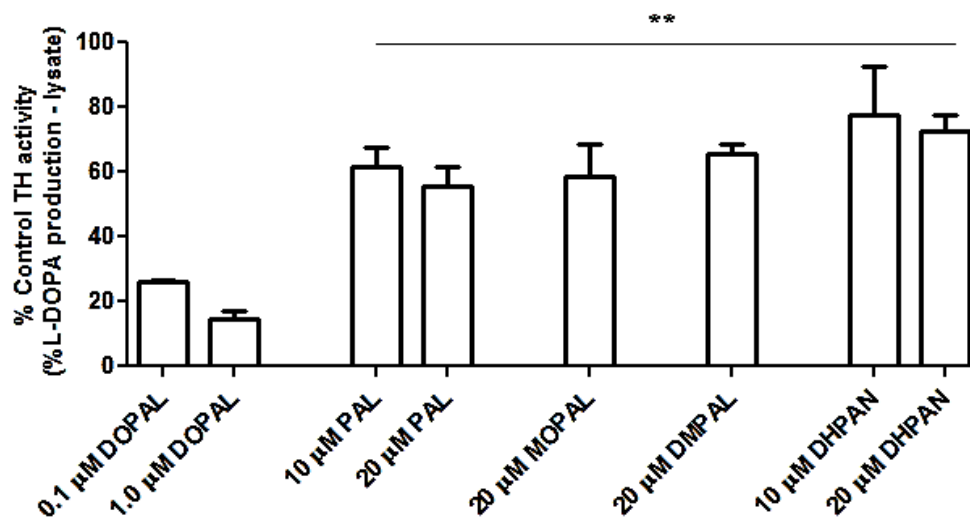


Figure 5.5 TH inhibition by DOPAL and analogues (PAL, MOPAL, DMPAL, and DHPAN) in cell lysate. Analogues show decreased inhibition of TH, indicating DOPAL is a more potent inhibitor of TH activity. All values shown represent the mean \pm SEMs ($n = 3$ for all) ** indicates significant from the control ($p < 0.05$).

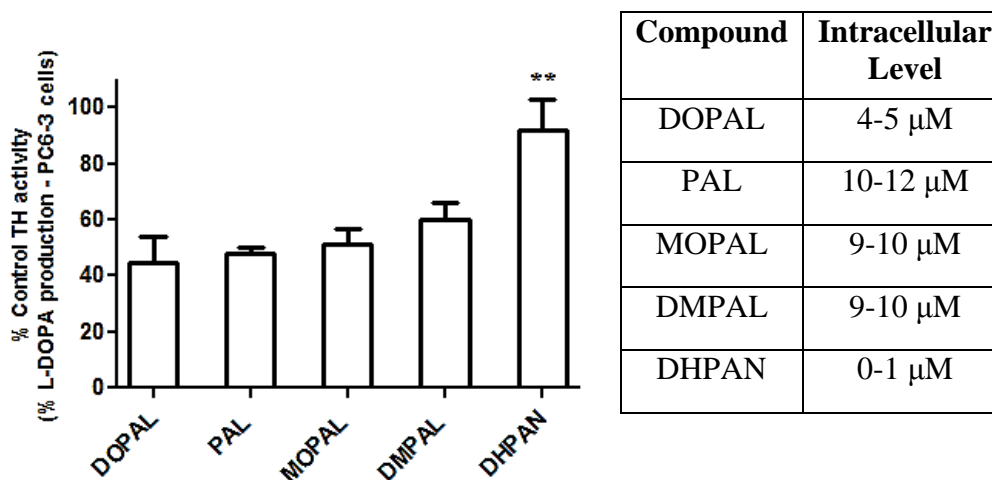


Figure 5.6 TH inhibition in PC6-3 cells by DOPAL and analogues. DOPAL shows more potent inhibition of TH activity than analogues at lower intracellular concentrations. The table shows the levels of each compound in the cells as determined by HPLC analysis. All values shown represent the mean \pm SEMs ($n = 3$ for all) ** indicates significant from DOPAL incubated cells ($p < 0.05$).

Novel Cloning and Purification of hTH

In collaboration with Dr. David L. Roman and Colin A. Higgins

This cloning procedure employed the use of an expression vector containing a maltose-binding protein, which was subsequently used in the purification process after cloning. Each step in the cloning process was verified through the use of the DNA Core Facility at the University of Iowa to ensure the proper sequencing for hTH was obtained. Figure 5.7 shows the hTH construct used for cloning.

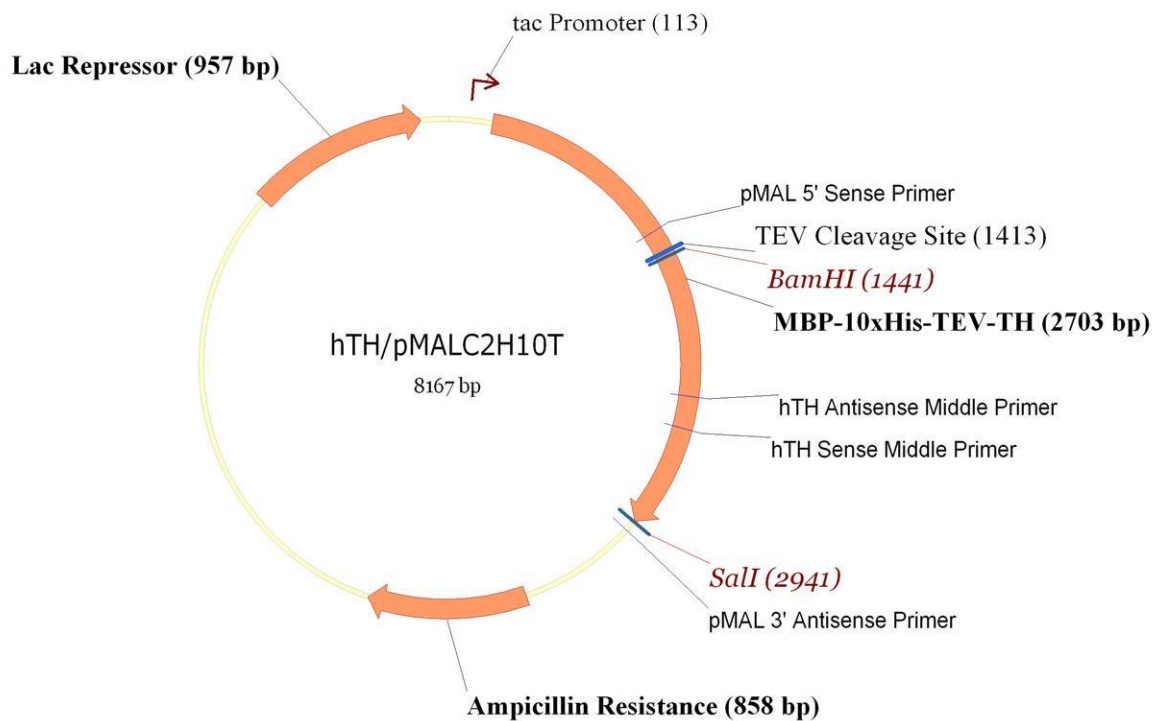


Figure 5.7 Construct used for the cloning of hTH. This pMal vector contained a maltose-binding protein which was used in the purification process later.

A three step purification was employed beginning with an amylose resin column to capture MBP-TH fusion proteins from crude cell lysate. The gel depicted in Figure 5.8A is a representative of the fractions collected. Lane 1 is the molecular weight marker, Lane 2 is the load (crude protein), and lane 3 is the flow (sample that does not bind to resin at all). Lanes 4-6 are the wash fractions. Lanes 7-20 are fractions following the addition of a high concentration of maltose (10 mM), which competitively binds amylose, allowing for the release of the MPB-TH. The band at 100 kDa represents the protein (hTH) bound to MBP. Cleavage of the fusion protein with TEV protease (Figure 5.8B),

leaves MBP and hTH separate and in the same mixture. Lane 2 of Figure 5.8B depicts the two proteins separated by SDS-PAGE, which shows TH at ~60 kDa, and MBP at ~40 kDa. Immediately following confirmation of cleavage, the sample was applied to a HiPrep Q FF 16/10 anionic exchange column and the 2 bands were separated using a salt gradient. Fractions of each peak were collected and analyzed again by SDS-PAGE. The figure in 5.8C depicts a typical gel acquired after use of the anion exchange column. MBP is in lane 2, and TH is in lane 3. Examination of the 2nd peak (TH) via western blot using antibodies specific to TH, confirmed the identity of the protein as TH, which is shown in Figure 5.8D. The 56 kDa band represents the 99% pure TH.

TH activity after each step of the purification using the HPLC method previously described. hTH (15 µg) was incubated with tyrosine, BH₄, and iron (II) sulfate for 20 min and time points were taken at 5 min intervals. HPLC analysis indicated the production of L-DOPA over time. Figure 5.9 shows the production of L-DOPA over time, and the increase in activity of TH as the purification process is completed. The specific activity, protein recovered and fold purification are described in Table 5.3. This novel procedure recovers an average of 24 mg hTH, making it one of the highest yielding procedures currently published for the cloning and purification of this enzyme (108-111).

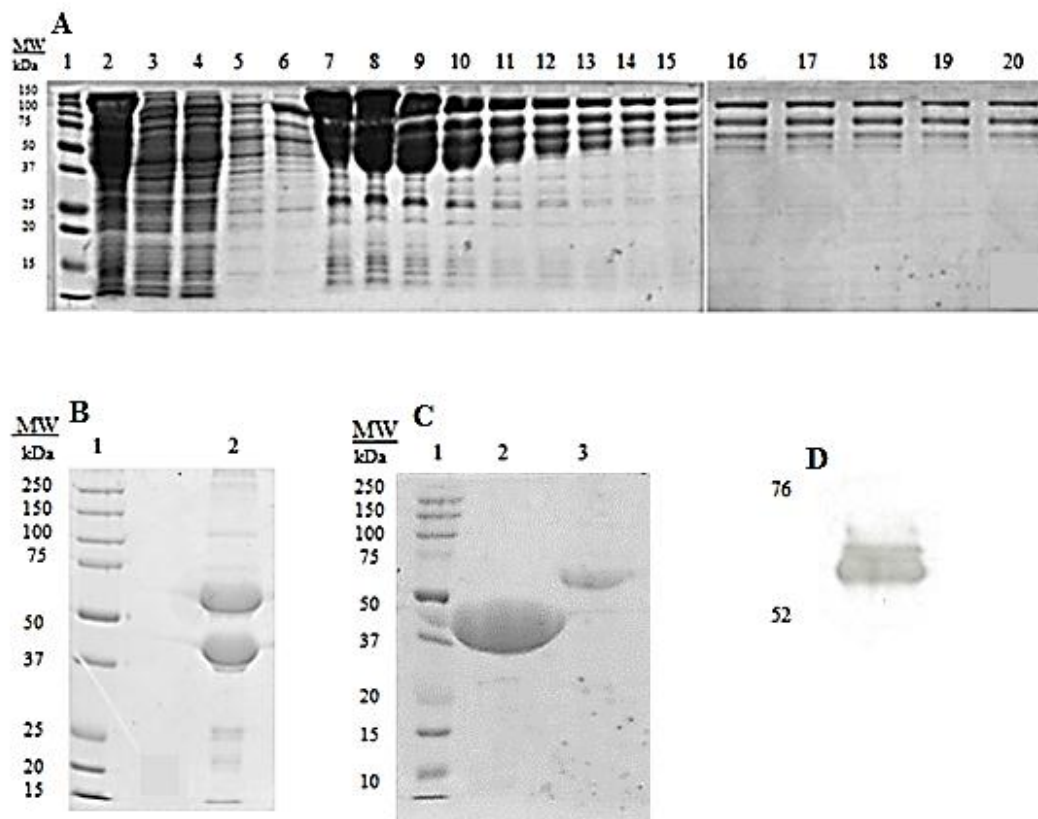


Figure 5.8 SDS-PAGE analysis of each step in the purification of hTH using the novel cloning and purification technique developed. (A) Typical gel obtained after amylose resin. Lane 1: Load (Crude protein); Lane 2: Flow (unbound proteins); Lanes 3-6: Wash, Lanes 7-20: Eluted proteins with competing concentration of maltose. 100 kDa band is indicative of hTH-MBP protein, which was collected. (B) Gel after TEV cleavage for 8 h; upper band is hTH, lower band is MBP. (C) After anion exchange column. MBP elutes first, hTH is second (lane 3). (D) Western blot analysis of pure hTH; band at ~60 kDa is indicative of hTH.

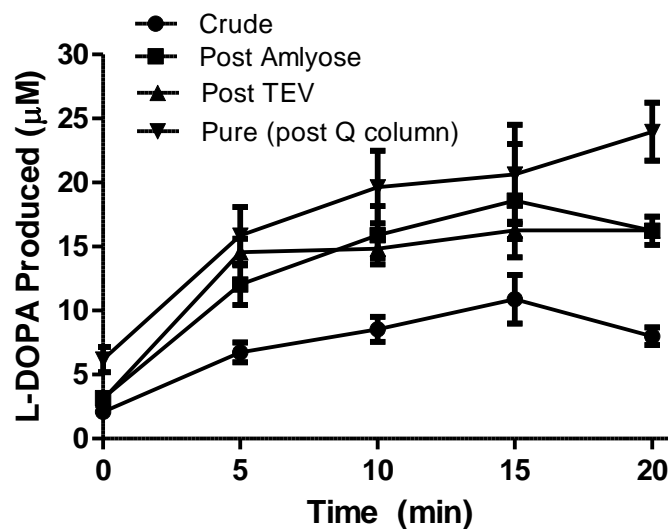


Figure 5.9 TH activity over the purification process using HPLC analysis. L-DOPA production increases as the enzyme is purified, indicating the process does not impede or negatively affect the enzyme, and leads to higher tyrosine turnover as TH is purified.

Table 5.3 hTH protein recovery per step and enzyme characterization.

Purification step	Total protein (mg)	Specific activity (nmol/min/mg)	Total enzyme units (nmol/min)	% Yield ^b	Approx. purity (%)
Crude	89.4	5.40	483	100	33
Amylose	42.6	12.2	520	48	75
TEV	26.0	12.2	317	29	75
Q-column	12.0	16.3	196	13	100

^aWet weight cells 17g

^bOverall yield compared to soluble crude cell lysate

Mass Spectrometry Identification

of DOPAL adducts

MS analysis was performed on trypsinized human recombinant TH (hTH) and hTH incubated with 50 μ M DOPAL for 4 h at 37°C. Prior to trypsin addition, samples were run through a Bio-Rad spin column in order to remove excess DOPAL. This was done to ensure adduction by DOPAL only occurred on the whole protein, and was not due to exposed residues after trypsinization. ACN (10% v/v), 0.1 mM BME, and a 1:50 ratio of trypsin was used for 8 h at 37°C prior to MS analysis. Samples were injected and run through a PDA prior to introduction to the IT-TOF MS. Figure 5.10 depicts typical total ion chromatograms obtained from hTH (A) and hTH+DOPAL (B). The spectra demonstrate a decrease in peaks present, indicating there is some loss of peptides in the DOPAL incubated samples. Sequence analysis revealed 79.8% sequence coverage of hTH samples, while hTH+DOPAL had a calculated sequence coverage of 58.4%. These results indicated there was a loss of sequence coverage when samples were incubated with DOPAL. It was hypothesized that DOPAL may have led to missed cleavages and adducts formed also led to changes in m/z ratio of the peptides.

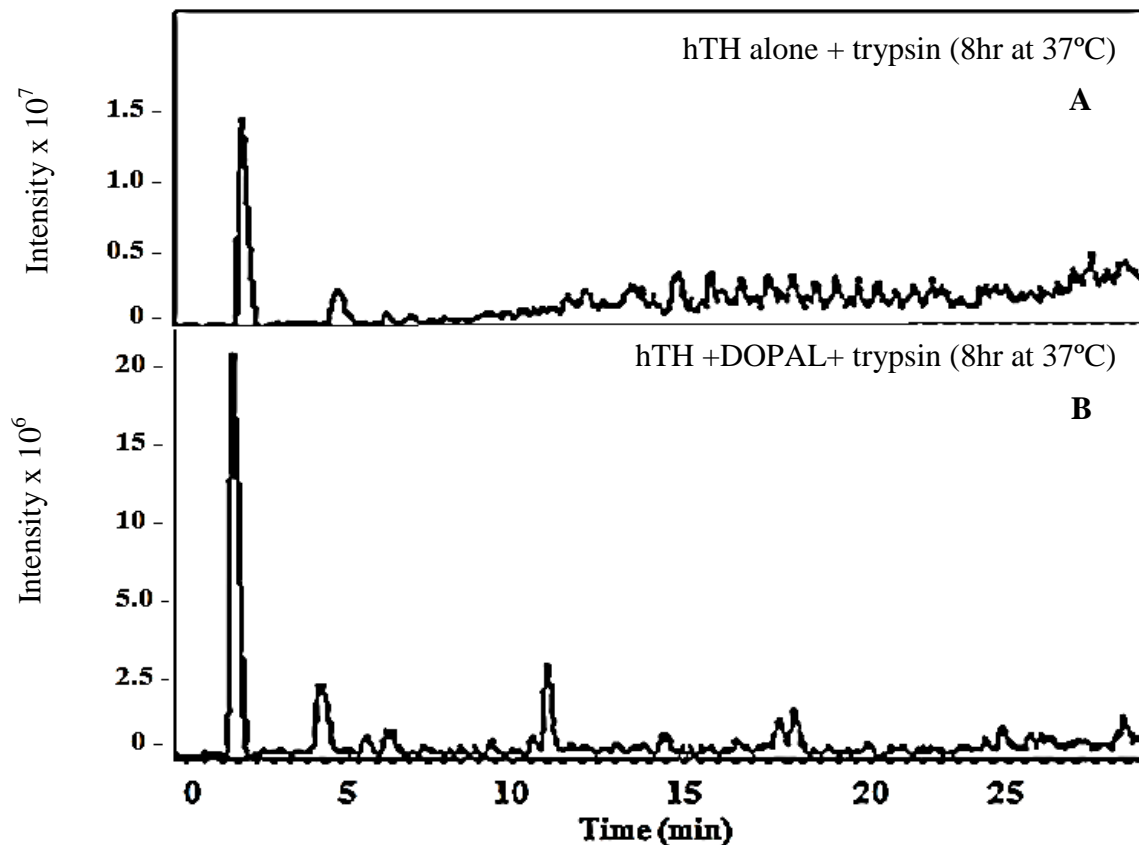


Figure 5.10 Typical MS spectra of hTH digest by trypsin for 8 h at 37°C. (A) depicts hTH with no DOPAL, while (B) is the incubation of hTH with 50 μ M DOPAL for 4 h prior to the addition of trypsin. All samples were run through a Bio-Rad spin column to remove excess DOPAL in order to ensure adducts were on whole hTH. Gradient separation was 40 min, this figure demonstrates the first 30 min of the run; no significant peptides were found after 30 min.

Upon completion of sequence coverage calculations, it was determined there were 11 missing peptides from the hTH+DOPAL samples that were found in hTH alone. A DOPAL adduct corresponding to either 134 Da (Schiff base) or 136 Da (reduced Schiff base) was matched to 5 of the 11 peptides in the hTH+DOPAL MS data. These results

demonstrated 5 DOPAL adducts on hTH. Table 5.4 contains the matched peptides containing a DOPAL adduct.

Table 5.4 hTH+DOPAL adducted peptides determined via mass spectrometry.

Treatment ^a	Peptide ^b	RT (min)	Modified	Unmodified	Adduct ^c
50 μ M DOPAL	220-226	4.5	927.87	791.42	136.45 ^e
	39-51/43 ^d	13.2/14.9	1696.88/1830.89	1560.85	136.03/270.04
	464-481	13.5	2156.91	2020.90	136.01
	312-320	18.6	1291.59	1157.5	134.09
	227-238	20	1573.75	1439.60	134.15

^a Tryptic peptides were obtained and analyzed as described in Materials and Methods.

^b Residue numbers in hTH protein.

^c Adduct mass determined by subtracting mass of unmodified from modified peptide.

^d Peptide found to have mass corresponding to two DOPAL adducts.

^e Mass of DOPAL is approximately 134 or 136 m/z ratio depending on amount of reduction via sodium cyanoborohydride. m/z ratio of 136 refers to complete reduction in which two hydride atoms are present

To better understand the location of each adduct, the NCBI MMDB Protein Structure Summary of hTH was utilized to study the protein. The sequence on NCBI includes the majority of the protein, minus the N-terminal regulatory region (including the location of antibody recognition) (1). Of the above adducts, 4 were visible using this model. The peptide from 39-51 was not present, and is a part of the N-terminal regulatory region. This peptide contains 2 adducts as was determined by MS/MS analysis. As

previous results show (88), the TH antibody demonstrated a concentration-dependent decrease in recognition. Adducts in the antibody-recognition region confirm the hypothesis that antibody can no longer recognize TH upon incubation with DOPAL due to modification. The peptides from 220-226, 312-320, and 227-238 are a part of the catalytic region of TH. Previous studies have demonstrated deletions or truncations of this part of the enzyme lead to an inactive enzyme with poor expression in cloning studies (55). Adducts in this region are predicted to lead to dysfunction of the enzyme, as is supported by the data previously discussed in Chapter 4 in which DOPAL leads to significant inhibition of TH function. The final peptide from 464-481 is the start of the tetramerization domain. Previous crystal structure data reveals this portion of the enzyme to be unnecessary for activity, with truncation or deletion leading to an active monomer (55). It is important to note though, that this part of the enzyme is central to oligomerization of the 4 subunits, and coupled with the other adducts on TH, is predicted to lead to the potent inhibition exhibited by DOPAL. Figure 5.11 demonstrates the location of the 4 of the 5 adducts as modeled in the NCBI MMDB Protein Structure Summary of hTH (missing the N-regulatory domain which was not present in the NCBI sequence).

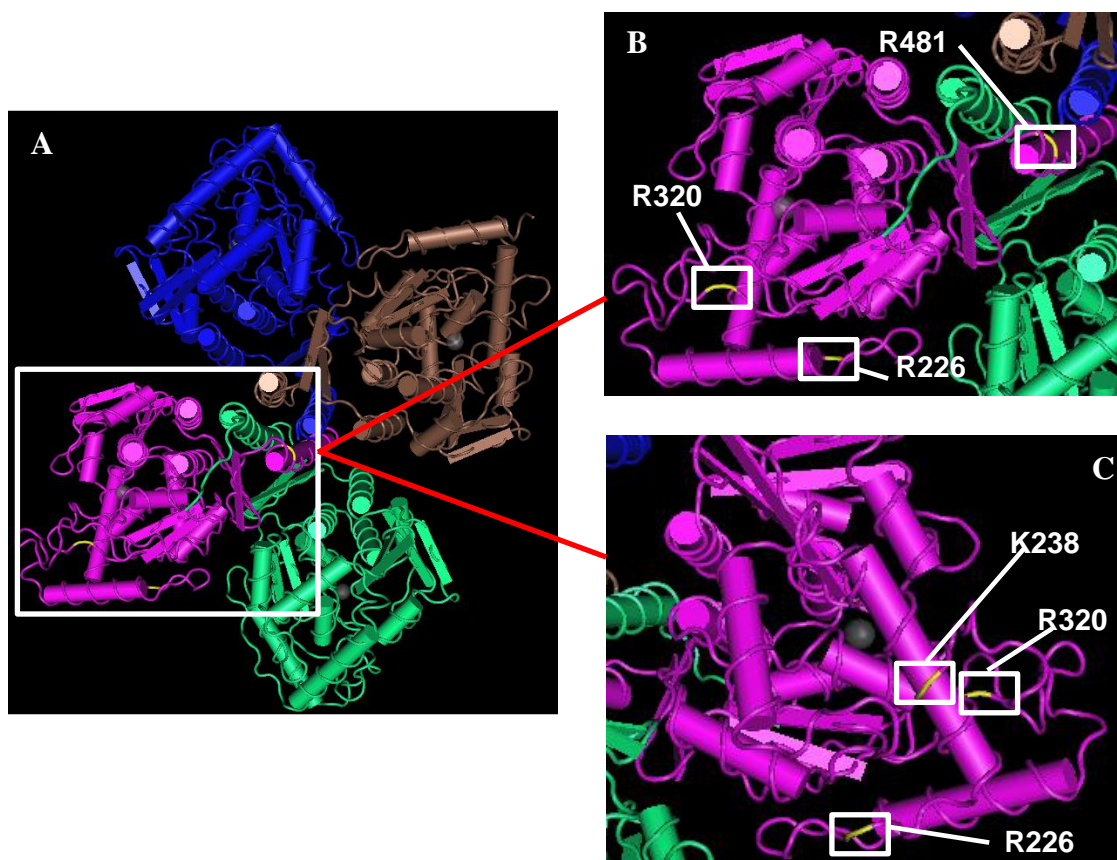


Figure 5.11 NCBI macromolecular structure view of hTH (1) (A). One subunit has been expanded to better visualize the adducts. (B) shows adducts R481, R320, and R226, while (C) shows K238 as well as R320, and R226. As mentioned in the text, this model does not contain the adducts on the peptide from 39-51, which are hypothesized to be the reason behind the decrease in antibody recognition of TH incubated with DOPAL.

MS/MS analysis confirmed the location of adducts on each peptide and mapped the ion fragmentation, which is shown in Figure 5.12. y- and b-ions were matched and further supported the addition of DOPAL adducts on hTH.

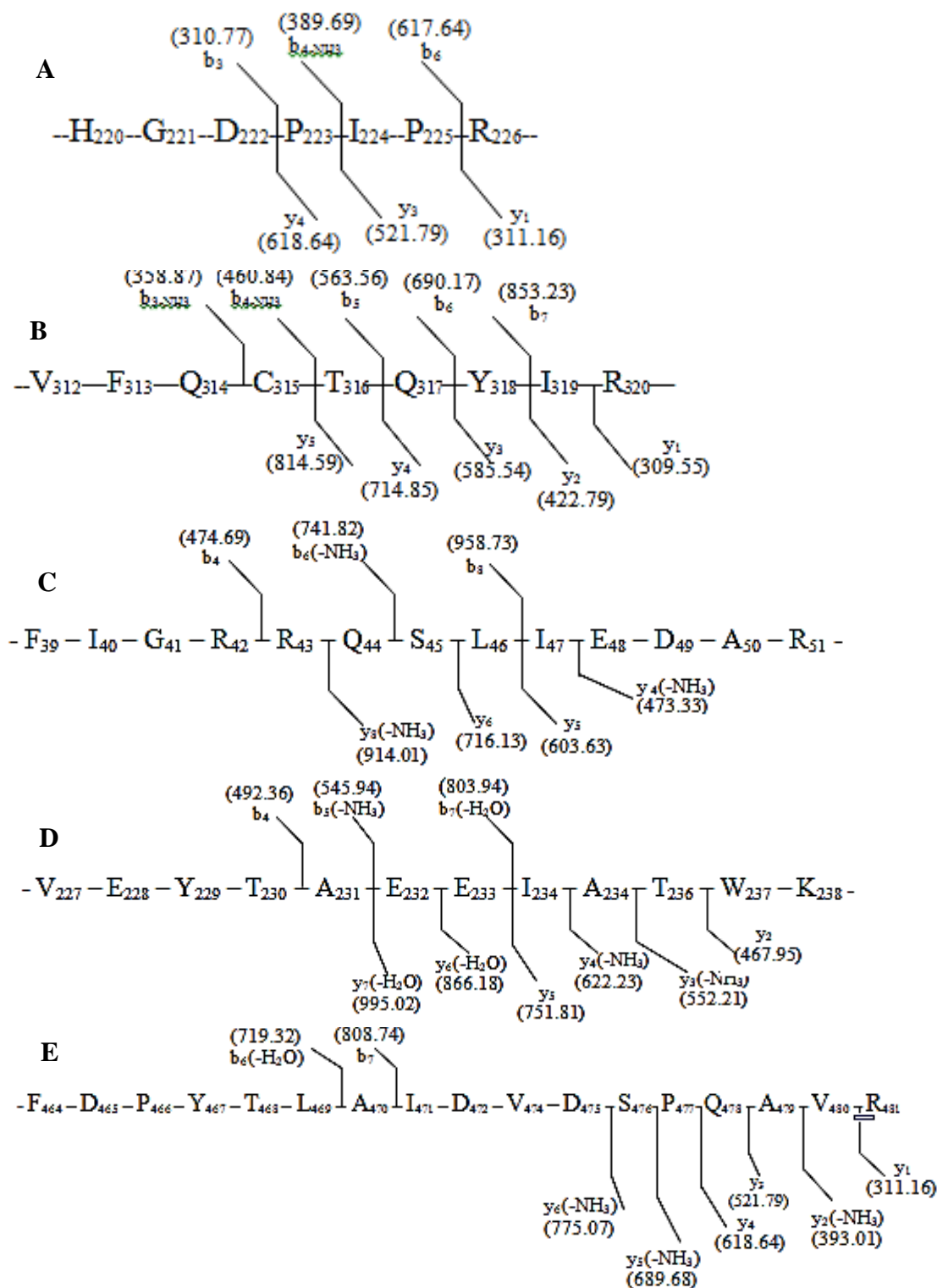


Figure 5.12 Y- and b-ions corresponding to 5 DOPAL adducts found on hTH upon MS/MS analysis of the protein after trypsin. (A) aa220-226 with one DOPAL adduct (R 226). (B) aa312-320 with one DOPAL adduct (R320). (C) aa39-51 with 2 DOPAL adducts (R43, R51). (D) aa227-238 with one DOPAL adduct (K238). (E) aa464-481 with one DOPAL adduct (R481).

The MS and MS/MS results of hTH and hTH+DOPAL revealed five DOPAL adducts, including one in the antibody recognition region of the enzyme, and three in the important catalytic region, helping to explain loss of antibody recognition as well as high inhibition of TH activity by DOPAL. In particular, two of the modifications are hypothesized to play a key role in the potent inhibition of this enzyme by DOPAL. Figure 5.13 shows an enlargement of the adduct location of peptide 220-226. This depiction shows R226 found to be DOPAL-bound, and Leu206, an amino acid that has been shown to be key to the structure stability of hTH. Point mutations of this residue lead to disruption of the helical packing of α -2, thereby destabilizing the protein structure (55). Furthermore, R226 is a part of an important salt bridge connecting α -2 and α -3, and adduction by DOPAL is predicted to not only lead to changes in the structure of this bridge, but, as can be seen from the figure, it is in close proximity to the important Leu residue. Slight alterations to the structure of the protein in this region are hypothesized to lead to destabilization of the enzyme structure, of which DOPAL could be a contributing factor.

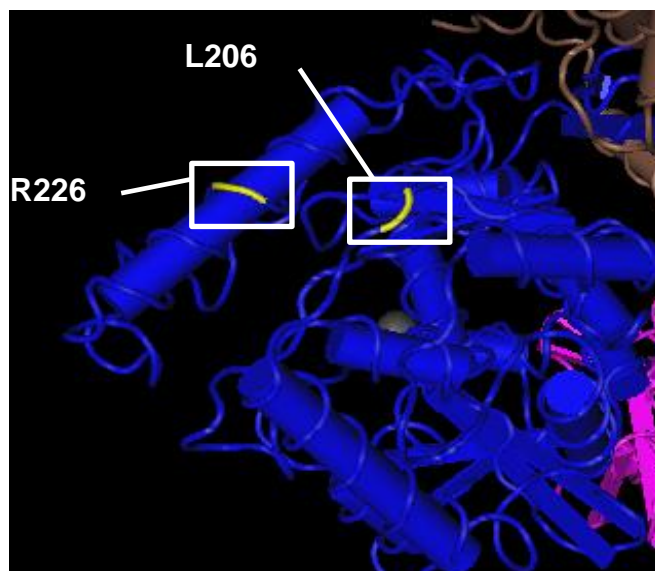


Figure 5.13 Enlarged view of the adduct on peptide 220-226 (1), which contains a DOPAL adduct on R226. Leu206 has been demonstrated to be an important residue to the overall structure of the protein. Furthermore, R226 is a part of an important structural salt bridge and adduction is predicted to lead to destabilization of hTH.

The peptide from 312-320 is depicted in Figure 5.14, and shows R320, where the DOPAL adduct was identified through MS/MS. Two Phe residues are depicted in the figure as well (F300 and F309). Studies have demonstrated these to be important in coordination and binding of the iron (grey ball in figure) to the enzyme subunit, a requirement for TH activity. Due to the proximity of the DOPAL adduct to the site of iron coordination, it is predicted that there are structural alterations in the enzyme which decrease the ability to properly bind the iron. This occurrence would help explain the potent inhibition of enzyme function; if iron cannot bind properly to TH, there would be significant decrease in the turnover of tyrosine.

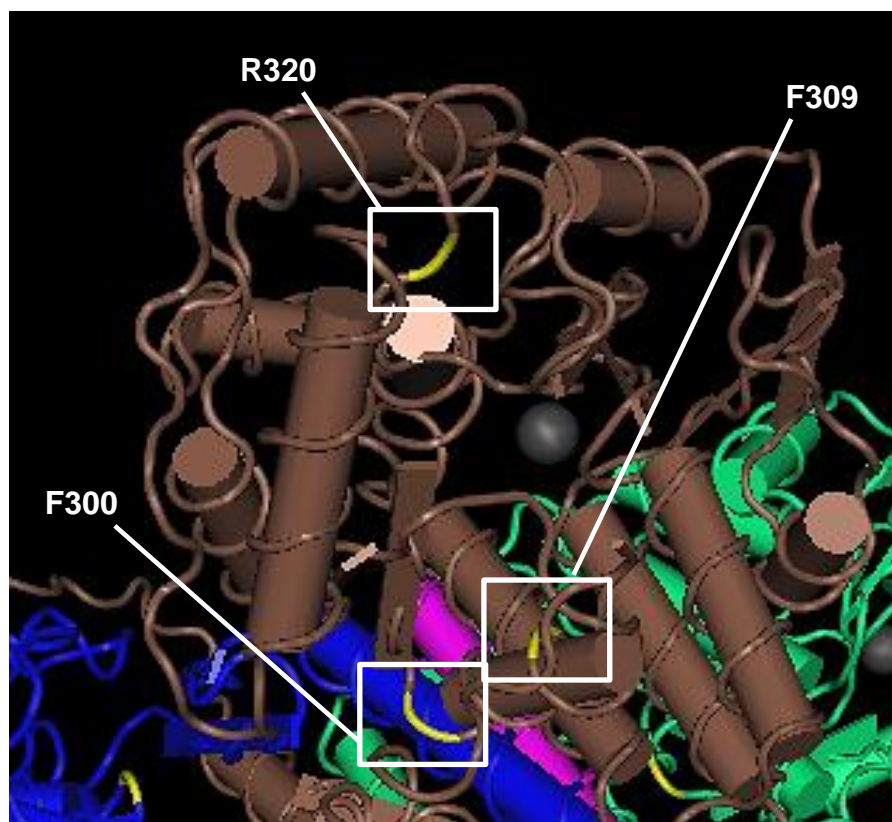


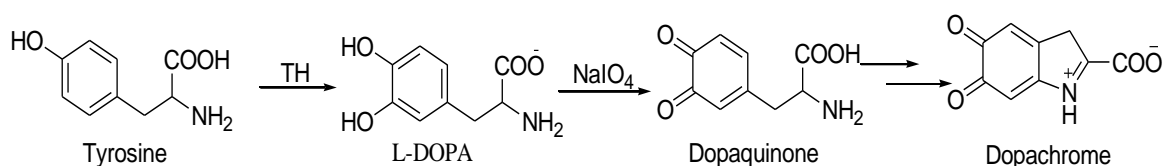
Figure 5.14 An enlargement of the adduct on R320 (1), which is in close proximity to the site of iron binding (gray ball). F300 and F309 are shown due to their importance in the coordinating of the iron atom in each subunit. DOPAL adduction in this location is predicted to lead to structural changes which may cause incomplete or improper binding of iron, partially explaining the dramatic loss of enzyme activity in the presence of DOPAL.

The DOPAL adduct on K238 is a part of another α -helix in the protein, but current literature and previous studies are not yet able explain how this adduct affects enzyme activity. It could be hypothesized that it leads to similar disruption of the packing structure as is predicted with the adduct on R226. As described above, R481 is a part of the tetramerization domain. While not strictly necessary for enzyme function, adduction of this site may lead to decreased oligomerization of the 4 subunits, and coupled with the

other adducts, may cause the potent decrease in TH activity. Finally, the adducts on R42, and R51 are a part of the N-regulatory domain, as well as the antibody recognition region. As previously mentioned, this explains the decrease in antibody recognition of the enzyme when incubated with increasing concentrations of DOPAL. Overall, the combination of these different sites of adduction coupled with the unique structure of TH help explain the potent inhibition by DOPAL. The structural implications are expanded upon further in the discussion.

Novel Plate Reader Assay to Monitor Tyrosine Hydroxylase Activity

The development of a real-time assay to monitor TH activity utilizes sodium periodate to oxidize L-DOPA, which further autocyclizes to dopachrome (Scheme 5.1). This species is absorbed at 475 nm and can be followed using a plate reader.



Scheme 5.1 Tyrosine is metabolized to L-DOPA by TH, which is oxidized by sodium periodate (NaIO_4). This species then autocyclizes to dopachrome, a chromophore species which absorbs at 475 nm.

This assay utilizes hTH obtained as described in the methods section. hTH, BH_4 , and iron were premixed (**A**, 10 μg , 0.25 mM, and 2.5 μM , respectively) and allowed to incubate for 3-6 min on ice while mix **B** was prepared. Mixture **B** consisted of tyrosine, sodium periodate (50, 100 μM , respectively), and 10 mM HEPES (pH 6.8). Mix **A** was added to the plate and immediately after the addition of **B** the plate was placed in a plate reader and monitored for 30 min at 10 sec interval readings. TH activity was measured in the initial linear phase of the experiment, with almost complete tyrosine turnover completed in 20 min. Background absorbance was corrected when calculating L-DOPA production.

hTH was also incubated with varying concentrations of DOPAL (5, 10, 20 μM) and the known competitive inhibitors of tyrosine and iron binding, 3IT and CoCl_2 , respectively. The data in Figure 5.15 displays the decrease in L-DOPA production in the presence of even low micromolar concentrations of DOPAL, which is determined by absorbance measured at 475 nm. Beer's Law [$A = \epsilon bc$], where $\epsilon = 3700 \text{ M}^{-1}\text{cm}^{-1}$, $b = 0.51 \text{ cm}$, $A = \text{absorbance}$ and $c = \text{concentration in molar units}$ was used to determine L-DOPA production. It can be seen that even low levels of DOPAL (5 μM) lead to significant inhibition of hTH activity. DOPAL inhibition follows a concentration-dependent model, with increased levels of DOPAL leading to ~60 and 73% inhibition (10 and 20 μM DOPAL, respectively). Furthermore, control studies with 3IT and CoCl_2 demonstrated significant inhibition of enzyme activity, with 3IT leading to ~50% inhibition, and CoCl_2 causes over 80% inhibition.

L-DOPA Production - Plate Reader

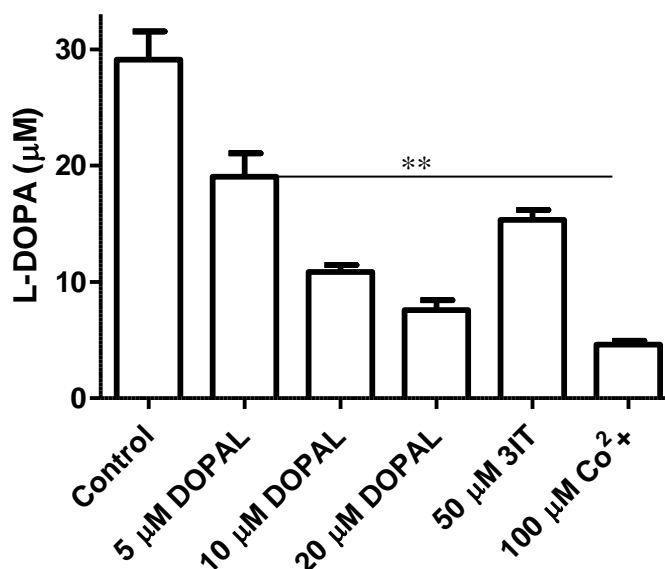


Figure 5.15 L-DOPA production as measured by the plate reader assay. L-DOPA is oxidized by sodium periodate, and then further cyclizes to dopachrome which can be measured at 475 nm. Low micromolar concentrations of DOPAL lead to decreased TH activity, and higher levels of DOPAL 3IT, and CoCl₂ lead to almost complete inhibition of L-DOPA production. All values shown represent the mean \pm SEMs ($n = 5$ for Control, DOPAL, 3IT, $n = 3$ for CoCl₂). **indicates significance from control wells.

In order to fully characterize the plate reader assay and determine the sensitivity (as compared to the HPLC), the specific activity of a number of conditions was determined for the plate reader and compared to the previously published method of HPLC analysis. Table 5.5 shows the values and demonstrates that the plate reader method is comparable to the HPLC in determining L-DOPA production over time.

Table 5.5 Comparison of average specific activities between previously published HPLC method and the plate reader assay

Assay	Control (nmol/min/mg)	10 μ M DOPAL (nmol/min/mg)	20 μ M DOPAL (nmol/min/mg)	50 μ M 3IT (nmol/min/mg)
HPLC	16.2 \pm 1.42	5.06 \pm 0.891	3.31 \pm 0.542	2.13 \pm 1.32
Plate Reader	15.4 \pm 1.13	3.55 \pm 0.670	2.51 \pm 0.776	2.63 \pm 1.48

High-Throughput Screening Assay

Finally, as part of a pilot study to determine if the plate reader assay could be applied to high-throughput screening (HTS), the plate reader assay was scaled down to a 384-well plate and run using CoCl_2 as a negative control. Studies were followed over 3 h at 60 sec read intervals. Comparison of the two conditions (i.e. positive and negative control) elucidated a Z-factor that ranged from 0.825 to 0.925, a robust number well over the accepted threshold of 0.5. Figure 5.16A shows the spectra obtained during the HTS assay. This assay has a high signal to noise ratio, and contains a wide stable screening window. Furthermore, 5.16B demonstrates the consistency of the Z-factor over time, indicating this is a stable assay which has a number of times points that could be monitored for hTH activity. These results demonstrate that the plate reader assay would be successful in an HTS format. A variety of conditions and possible inhibitors of hTH activity could be investigated easily and quickly; possibly resulting in data currently unknown about the structure and function of hTH and how it is affected by both endogenous and exogenous toxins that humans may encounter throughout their lives.

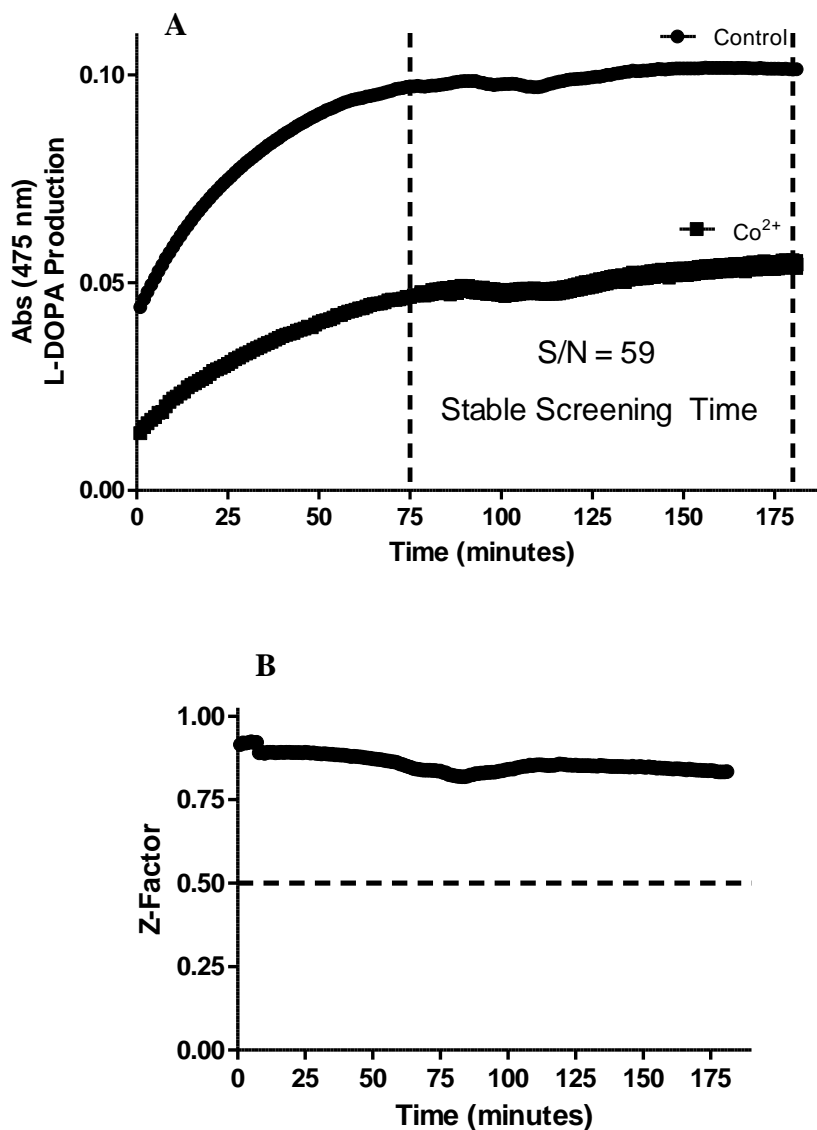


Figure 5.16 High-throughput screening (HTS) of hTH plate reader assay. 48 wells were used for positive (no inhibition) and 48 wells used for negative control (100 μM CoCl_2). Assay was performed for 180 min at 90 sec read intervals. (A) depicts spectra obtained, exhibiting high signal-to-noise (S/N) ratio, and a long stable screening time (between 75-180 min). (B) Z-factor over time of assay shows stability over the course of the assay well above the accepted threshold of 0.5. Z-factor values ranged between 0.825 and 0.925, a robust value which makes this ideal for HTS.

Discussion

DOPAL, the endogenously produced metabolite of DA is known to exhibit toxic effects in cells and lead to the potent inhibition of tyrosine hydroxylase in both a lysate and a dopaminergic cell model (88). It has been shown that modification of DOPAL structure leads to decreased reactivity with Lys residues, indicating protein reactivity is dependent upon both the catechol and the aldehyde (50). This study furthers such results by investigating the importance of these functional groups in the inhibition of a known protein target of DOPAL modification, the enzyme TH. Furthermore, this work demonstrates the importance of DOPAL structure for cytotoxicity through mitochondrial dysfunction. The data presented in this work also elucidates site of modification on hTH using MS analysis, as well as employs recombinant TH to develop a novel plate reader assay which follows L-DOPA production.

The following order for toxicity and potency in regards to TH inhibition was found: DOPAL >> PAL=MOPAL > DMPAL=DHPAN. Interestingly, the nitrile analog DHPAN exhibited only slight TH inhibition in cells and HPLC analysis of the cell lysate indicates intracellular DHPAN is very low event after 2 h treatment (Figure 5.4C, table in Figure 5.6). These results have implications for the uptake and trafficking of DOPAL in a cell.

For the first time, the importance of the aldehyde is studied using an analog in which a nitrile group replaces the aldehyde. As noted above in Figure 5.4A, toxicity was decreased significantly for the nitrile analog. Results indicate that there is inhibition of TH in cell lysate, but such a finding was not observed for PC6-3 cells treated with DHPAN (Figure 5.4C and D, respectively), indicating that DHPAN did not enter the cell.

While trafficking of DA and DOPAC are established (78, 112, 113), it is currently unknown how DOPAL movement is mediated in the cell. When PC6-3 cells are treated exogenously with DOPAL and time points taken over 2 h, the acid and alcohol metabolites (i.e., DOPAC and DOPET, respectively) are observed in the extracellular media (Chapter 3). This indicates that DOPAL is taken up into the cell and metabolized. It is conceivable that DHPAN is able to traverse the cellular membrane, but then interacts with and binds to other proteins via reversible thiol modification (114), precluding its ability to inhibit TH. Furthermore, it is possible there is an undiscovered mechanism for DOPAL transport, which facilitates the movement of DOPAL in and out of the cell. In this case, the nitrile analog would be unrecognized by the transporter and would not be able to enter the cell. More work is needed to identify the means via which DOPAL and the analogs are taken up by cells and exported.

In regards to TH inhibition, it is also important to note that while protein reactivity is decreased significantly upon the replacement of the aldehyde with the nitrile group, there is the possibility for interaction of the nitrile with Cys residues, as studies have indicated (107, 115). Such could possibly explain the loss of TH activity in cell lysate as well as the known inhibition of the enzyme by catechol-containing compounds such as DOPAC and L-DOPA (61, 62) DHPAN shares many structural characteristics with DA (i.e., catechol, nitrile analogous to amine), indicating DHPAN could interact with the DA-binding site of TH, thus inhibiting the enzyme. Further work is also needed to fully understand the inhibition of TH by DHPAN.

MOPAL, a DOPAL-metabolite generated via COMT activity (116) exhibited toxicity and inhibition of TH. While significantly less than that for DOPAL, these results

indicate the potential for other metabolites of DA to exhibit harmful cellular consequences. It is important to note though, that while MOPAL is generated simultaneously with DOPAL (116) and therefore has the ability to compete with DOPAL for protein binding sites, the results here, as well as previously published data show DOPAL is significantly more protein reactive (63, 88).

Mass spectrometry analysis of hTH incubated with DOPAL revealed 5 adducts on a variety of important parts of the enzyme. Most notably, the peptide from 220-226, and 312-320 are in areas of the catalytic region of hTH that if altered in some way (i.e. through an adduct), this may lead to the destabilization of the protein. Previous crystal structure studies have demonstrated that the structure of TH is unique and found nowhere else in nature. Of important note, the catalytic domain of the enzyme family of TH shows no sequence or structure homology to other proteins, indicating this is unique to this enzyme (117). Furthermore, the structure of TH is very loosely packed; the only tightly bound portion of the enzyme is in the catalytic domain closest to the tetramerization domain (α -8, α -9, and α -13), with α -8 and α -9 being a part of the active site cleft (55). Otherwise, the structure of TH is based on loose helical packing, which may explain why DOPAL adducts have such a potent inhibitory effect. Slight changes to the structure of TH through DOPAL modification are predicted to lead to destabilization of the AKReady loose packing, thus leading to the inability of the substrate, co-factor or iron to bind, all of which are necessary for proper function of the enzyme.

It is important to note that previous work has shown DOPAL to be highly reactive with Lys residues, while there have been fewer studies demonstrating the reactivity with Arg. The MS results presented here elucidated that four of the five DOPAL modifications

were found on Arg residues, including the two predicted to be key in the inhibition of TH. While it was initially surprising to find these results, there have been multiple studies showing reactivity of bifunctional molecules with Arg that help support the data described here. A number of studies published have shown that the bifunctional molecules phenylglyoxal and 4-hydroxy-2-nonenal (4-HNE) are reactive with Arg residues (118, 119). Using ESI-MS, these studies demonstrated adduction of these bifunctional chemicals to Arg residues. Proposed ion structures included the production of a ring structure between the phenylglyoxal or 4-HNE and Arg residue. Based on this, it is hypothesized a similar mechanism of adduction may be occurring between Arg and DOPAL. It could be further hypothesized that DOPAL adduction occurs through two separate binding sites on the Arg; including, the formation of a Schiff base-like structure (as expected with Lys residues), as well as a Michael addition at the two position of the phenyl ring. Overall, this adduct would cause the m/z ratio to be either 134 or 136 higher, depending on the reduction state of the adduct (as demonstrated in Table 5.4). This hypothesis requires further studies to help elucidate the exact structure of the DOPAL-Arg adduct.

Finally, this chapter discusses the development of a novel real-time assay for monitoring the activity of TH. This assay utilizes sodium periodate, which leads to the formation of dopachrome from L-DOPA. Using a plate reader at absorbance 475 nm, TH activity can be observed over time. Furthermore, the potential for the use of HTS was investigated, with the assay showing promise for translation into screening high volumes of compounds in the future. Not only could this be used to investigate the inhibition of

TH, but also look at the activation of the enzyme, which may potentially lead to better therapeutics for sufferers of PD, who exhibit low DA levels.

Of important note, Table 5.5 compares the specific activities gained in both the HPLC assay, which is previously published (88), and the new plate reader assay, with results showing continuity between the two methods. Furthermore, a variety of control experiments were carried out to ensure that the absorbance change over time was due to the production of L-DOPA. These include: absence of both tyrosine and hTH, in order to determine background absorbance that occurs in this assay; incubation of each component with sodium periodate, to confirm no cross-reactivity was observed; as well as the use of known competitive inhibitors (3IT and CoCl_2) of TH activity, to demonstrate a working model of TH inhibition that could be compared to DOPAL. In the absence of tyrosine (substrate) or hTH, some background absorbance was observed; therefore, all results were corrected to ensure proper calculation of L-DOPA concentration. When each assay component (i.e. iron, co-factor, or substrate) was incubated with sodium periodate, there no significant change in absorbance observed. These results indicate that sodium periodate does not cross-react with these components and therefore does not contribute to changes in absorbance over time. Finally, the use of known inhibitors of TH activity helped confirm inhibition of TH and was used to compare to the inhibition observed in the presence of DOPAL.

There are several noteworthy advantages to the use of this assay compared to previously published TH activity assays. First, it is significantly faster; there is no major lag time between sample preparation and data analysis. Currently, it is common to use the tritium-release method of determining TH activity. This assay employs tritiated tyrosine

and using liquid scintillation, the amount of tritiated water released is measured (120). This method requires extensive post-run work up in order to separate the tritiated water from the reaction mixture. Another favored assay is $^{14}\text{CO}_2$ trapping which necessitates an apparatus to trap the compound, as well as liquid scintillation counting. Finally, the method employed previously in our lab used the HPLC to measure L-DOPA production at time points during the activity assay. This can be a time consuming process, which entails waiting a minimum of 20 min for each sample to run on the HPLC. Overall, this real-time assay allows for fast production of data, with no post-run work up or sample preparation required.

It is also important to note that in the 96-well (or greater in HTS studies) format, a large number of multiples of each condition can be run at once. This decreases variability, and increasing the number of experimental conditions that can be tested in a single assay. Sodium periodate does not interfere with TH activity, or interact with any other components in the assay, making it an idea method for converting L-DOPA to the chromophore. Furthermore, this assay allows for observation of TH activity as the reaction proceeds, giving insight into what occurs between time points in the previously described stop-kinetic assays.

The large array of data presented in this chapter leads to the major conclusion that DOPAL is a highly toxic and potent inhibitor of TH activity. SAR studies revealed a decrease in toxicity and inhibition as structural modifications were made to DOPAL. Furthermore, MS analysis of DOPAL-bound hTH demonstrated that 5 adducts were found on TH. These results help elucidate the mechanism behind the potent inhibition of TH activity due to DOPAL modification. Finally, the development of a new assay for

activity was described, with results demonstrating a faster method for determining L-DOPA production in real-time.

CHAPTER SIX

RESEARCH SUMMARY

Restatement of Hypothesis

Parkinson's disease (PD) is a progressive neurodegenerative disorder which affects the dopaminergic neurons in the substantia nigra, leading to their selective death. This causes a decrease in the important neurotransmitter, dopamine (DA) (2). The pathogenesis behind PD is unknown; however, it has been hypothesized that there are both environmental causes (such as pesticides and metals) as well as endogenously produced causes (such as reactive oxygen species or reactive intermediates of metabolism) (5, 12, 65). DA is metabolized by monoamine oxidase (MAO) to 3,4-dihydroxyphenylacetaldehyde (DOPAL), which is further catabolized by aldehyde dehydrogenase (ALDH) and aldehyde reductase (AKR) to 3,4-dihydroxyphenylacetic acid (DOPAC) and 3,4-dihydroxyphenylethanol (DOPET), respectively (49). While DA has been shown to be reactive with proteins and lead to cellular toxicity, DOPAL was found to be several orders of magnitude more toxic (46, 63). Normal physiological concentrations of DOPAL have been measured to be 2-3 μM , and slight elevations from this (6.6 μM) demonstrated a decrease in tyrosine hydroxylase positive cells, which indicates dopaminergic cell death (47, 48). Furthermore, DOPAL has previously been implicated in protein modification, and studies have shown the ability of DOPAL to covalently modify Lys and Arg residues via the aldehyde, forming a Schiff base-like structure predicted to interfere with normal protein function (34, 50-52). Tyrosine hydroxylase (TH) is the rate-limiting step in DA-synthesis, oxidizing tyrosine to L-DOPA, which is further metabolized to DA (40). Studies have demonstrated this

enzyme to be tightly controlled, with phosphorylation, feedback inhibition, and proper binding order of substrate and cofactor all playing a role in its activation and activity (58, 121, 122). Furthermore, evidence has shown TH to be inhibited by other catechols, including norepinephrine, L-DOPA, and DOPAC (62).

Based on this, it was hypothesized that **the endogenously produced neurotoxin 3,4-dihydroxyphenylacetaldehyde covalently modifies and inhibits tyrosine hydroxylase, leading to a decrease in L-DOPA and dopamine production.**

Discussion of Specific Aims

Specific Aim 1: Investigate DOPAL as a Neurotoxin and Identify Protein Targets of Modification

As demonstrated in Figures 3.1 and 3.2, DOPAL-exposed PC6-3 cells exhibited a number of morphological changes; including, loss of uniform cell shape, blebbing, and evidence of apoptotic bodies. Furthermore, the data in Figure 3.3 and 3.4 show that cells begin to have mitochondrial dysfunction, as well as significant cell death at very low micromolar concentrations of DOPAL. These results are in line with previous studies that demonstrated the ability of DOPAL to cause dopaminergic cell death when levels are raised (46, 47). There is also significant evidence that DOPAL interacts with and modifies model proteins through Lys and Arg residues, forming Schiff base-like adducts (34, 50). Indirect evidence for this by western blot analysis in Figure 3.6 demonstrated DOPAL interfered with antibody recognition of TH. Furthermore, through the assessment of reactive oxygen species production using flow cytometry, it was determined that DOPAL lead to other cellular consequences. Cells demonstrated significant elevation in superoxide anion in the presence of just 10 μ M DOPAL. It was interesting to note a

decrease in hydrogen peroxide in the presence of elevated DOPAL, but previous studies demonstrated that inhibition of TH in rat brains led to similar results due to a decrease in DA turnover by MAO (81). Combined, these results support the hypothesis that TH is modified by DOPAL.

Specific Aim 2: Determine the Effect of DOPAL on Tyrosine Hydroxylase Activity

A number of experiments were done in both cell lysate and PC6-3 cells to determine the effect of DOPAL modification of TH. It was hypothesized that DOPAL would lead to a decrease in TH activity, leading to decreased L-DOPA production. The data in Figure 4.1 demonstrates potent inhibition of TH in cell lysates, with results exhibiting almost 95% inhibition at concentrations of just 1 μM . It was predicted that due to the cell lysate environment, where no metabolizing enzymes of DOPAL are present, and DOPAL is able to freely interact with TH, the inhibition was much greater than what would be exhibited in a PC6-3 cell model. As the data in Figure 4.2A shows, TH inhibition occurs in whole cells, but is significantly less potent than cell lysate. Intracellular levels of 4-5 μM DOPAL produced over 40% inhibition of TH activity, which also led to ~40% inhibition of DA synthesis (Figure 4.2B). It is important to note that normal, physiologic levels of DOPAL are between 2-3 μM (49); therefore, these results demonstrate how even slight changes to DOPAL levels can lead to detrimental consequences for dopaminergic cells. Finally, it was determined that DOPAL exhibits slow-irreversible inhibition of TH, which is time- and concentration-dependent. Figure 4.3A, B, and C display the reversibility data for TH inhibition by DOPAL. It is clear that exposure to increased concentrations of DOPAL for longer periods of time leads to a

decreased ability of the enzyme to recover normal activity. This has implications for TH inhibition and its relationship to the onset and progression of PD. These data demonstrate that short exposure to low levels of DOPAL (i.e. normal physiologic concentrations) will lead to less than significant inhibition of the enzyme, as well as the ability of the enzyme to recover activity if DOPAL levels are restored to normal. Conversely, if there is inhibition of DOPAL metabolism or other alterations to DOPAL synthesis/catabolism and levels increase to even 4-5 μM , TH activity would be markedly decreased. Furthermore, longer exposure to elevated DOPAL would be predicted to lead to a decreased ability of the enzyme to recover normal activity, thus decreasing DA levels, a hallmark of PD.

Specific Aim 3: Elucidate Mechanisms by Which DOPAL

Inhibits Tyrosine Hydroxylase

A number of approaches were used to study this aim; including, structure-activity studies (SAR) as well as mass spectrometry to positively identify adducts on TH. The data presented in Figures 5.1-5.4 display the SAR results. Overall, it was determined that slight modifications to the structure of DOPAL lead to significant decreases in toxicity and inhibition of TH, both in cell lysate and PC6-3 cells. SAR studies of TH inhibition are summarized in Figures 5.5 and 5.6. The DOPAL metabolite 3-methoxy-4-hydroxyphenylacetaldehyde (MOPAL), containing only one masked hydroxyl group, exhibited a decreased ability to cause mitochondrial dysfunction and inhibition of TH. While there was some decrease in TH activity, it required concentrations double that of DOPAL to achieve similar results (4-5 μM intracellularly for DOPAL versus 9-10 μM for MOPAL). The SAR studies confirmed the previously

published results involving model proteins, and extend these data by investigating how structural changes affect inhibition of a known protein target of DOPAL (50).

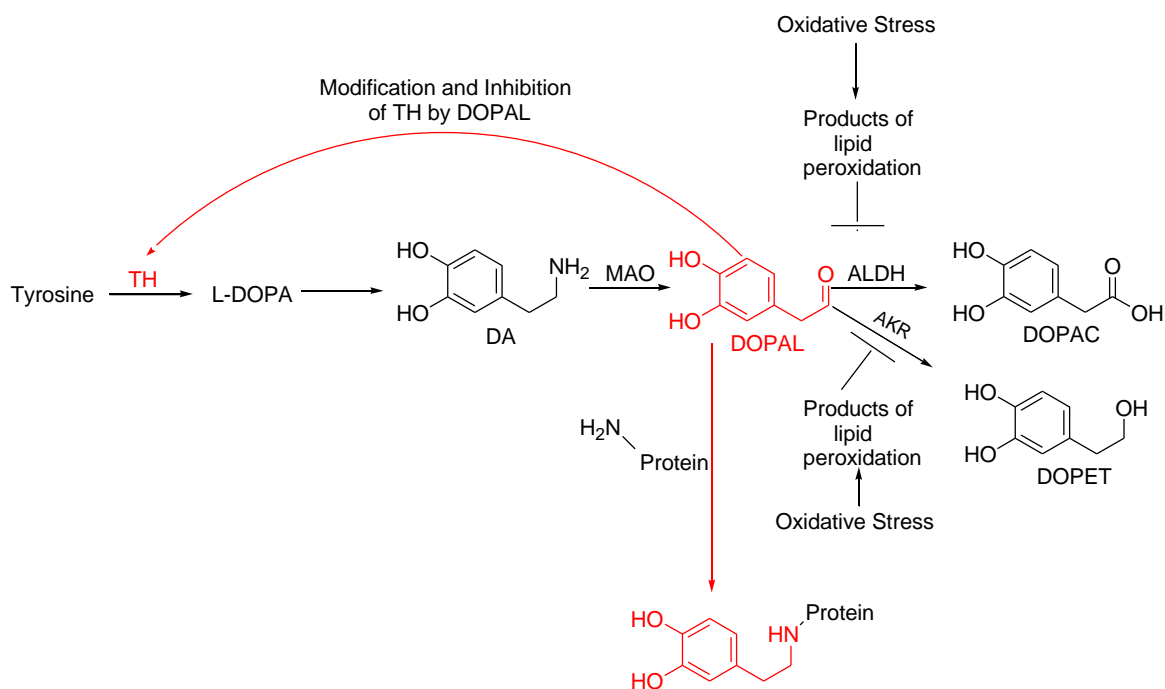
Cloning and purification of human recombinant TH (hTH) was completed in order to obtain mass spectrometry analysis of DOPAL adducts. This novel procedure produced high quantities of pure, active TH, as the data in Figures 5.8 and 5.9 demonstrate the purification process and activity of hTH, respectively. Furthermore, the activity over the course of the purification is expressed in terms of specific activity in Table 5.3. Mass spectrometry analysis revealed 5 DOPAL adducts on TH, including two predicted to be highly detrimental to enzyme activity (Table 5.4, Figures 5.13 and 5.14).

Finally, a novel plate reader assay was developed using hTH, in which real-time analysis of activity can take place. This assay has a number of advantages which could prove useful when studying TH activity; including, fast set up and analysis time, decreased post-run workup, and the ability to study enzyme activity real-time. Furthermore, high throughput screening was assessed and the assay exhibited favorable results for further use in this format in the future.

Conclusions and Implications for Parkinson's Disease

PD is characterized by a selective loss of dopaminergic neurons in the substantia nigra, which leads to a decrease in the important neurotransmitter, DA. Patients typically exhibit a variety of motor problems, including, bradykinesia, muscle stiffness, and resting tremor (2). While it is not currently known what the pathogenesis behind this disease is, there is evidence the aldehyde metabolite of DA, DOPAL plays a role in the onset and progression. DOPAL has been shown to be reactive with model peptides, as well as model proteins, such as BSA. Furthermore, the data presented here demonstrate

modification of TH, an important enzyme in the production of the neurotransmitter DA. These results have many implications for the onset of PD. There is evidence that MAO activity increases with age, as well as products of lipid peroxidation leading to inhibition of ALDH and AKR, both metabolizing enzymes of DOPAL (5, 33, 86). Combined, these occurrences would lead to elevation in DOPAL levels, and from the data presented here, it is predicted that modification and inhibition of TH would occur. Furthermore, DOPAL has been shown to be toxic and negatively affect mitochondrial function, as presented in Chapter 3, indicating an increase in DOPAL would also be detrimental to overall cell viability. As these data suggest, and outlined in Scheme 6.1, DOPAL is a neurotoxin capable of protein modification and inhibition. This work helps further the knowledge of the pathogenesis behind PD and may direct future research for novel therapeutics for this debilitating disease. Such studies may lead to better treatments for PD, or possibly a way to prevent the onset and progression of the selective dopaminergic cell death.



Scheme 6.1 DOPAL is hypothesized to be a neurotoxin, capable of causing mitochondrial dysfunction and cell death. Oxidative stress may lead to inhibition of DOPAL metabolism. The data presented here predicts elevated DOPAL would modify and inhibit intracellular TH (and possibly other proteins), leading to a decrease in DA production.

Future Direction of the Project

Circular Dichroism Studies of Structural Changes

There are still several approaches that should be investigated to further the TH and DOPAL story. It would be of interest to study the structure of TH in the presence of DOPAL. Due to sites of adduction found through MS analysis (Table 5.4, Figures 5.11, 5.12, 5.13, and 5.14), it is predicted that structural changes to TH lead to the potent inhibition exhibited. While the active site is not directly bound by DOPAL, several other

important sites are modified, and based on previous data, are predicted to cause destabilization of enzyme structure. Circular dichroism can be employed to further study the effect DOPAL has on the overall structure of TH, and determine if DOPAL modification leads to the hypothesized destabilization.

Investigation of DOPAL Trafficking

It would also be of interest to further investigate the trafficking of DOPAL in and out of the cell. As the data in Chapter 5 demonstrated, the nitrile analogue of DOPAL, DHPAN, exhibited altered trafficking in the cell. HPLC analysis showed that there was little uptake of the compound. Due to the replacement of the aldehyde moiety with a nitrile group, these results indicate the aldehyde plays some role in trafficking of DOPAL. It has been established that DOPAL moves into the cell when placed exogenously, is metabolized and DOPAC and DOPET are trafficked out the cell, but the mechanism behind this is not fully understood. Currently, it is assumed DOPAL moves through passive diffusion, but these results indicate there may be an unknown transport mechanism. Studies investigating the DA and DOPAC transporters would be a starting point to determine if DOPAL utilizes these as a means of moving in and out of the cell.

Effect of Tyrosine Hydroxylase Phosphorylation on DOPAL-Mediated Inhibition

As described earlier, TH activity is tightly controlled by a number of mechanisms, including phosphorylation of three key Ser residues located at Ser19, 31, and 40. Phosphorylation of these residues (particularly Ser40) lead to a rapid increase in TH activity, due to decreasing the negative feedback inhibition by DA (and other catechols) (90, 122). It would be of interest to study the effect phosphorylation of TH has after

inhibition by DOPAL. It is possible that phosphorylation, which would not occur actively in cell lysate or recombinant enzyme systems, could alleviate or decrease the inhibition of TH by altering the structure upon phosphorylation. These studies could help further determine how DOPAL inhibition of TH may be decreased or eliminated in order to help restore DA synthesis.

Determine the Structure of the DOPAL Adduct

It has been established that DOPAL modifies and inhibits TH, but the structure of the adduct is still unknown. While a cyclic structure with Arg was proposed in the preceding chapter, and while it has been hypothesized DOPAL forms a Schiff base with Lys residues, the exact structure has not been elucidated. Mass spectrometric analysis using fragmentation could be of use in determining the structure of both adducts formed on TH. This information would further the knowledge of the mechanism behind DOPAL's covalent modification of TH, leading to its potent inhibition.

Identification of Other DOPAL Protein Targets

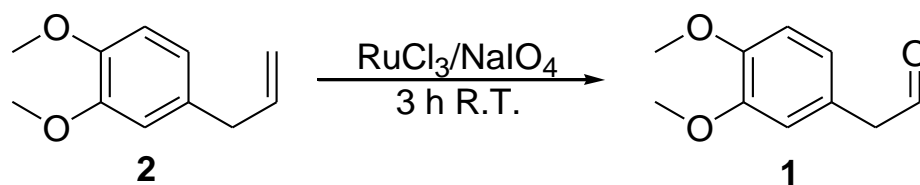
While TH has been identified as a protein target of DOPAL modification, there are a number of other possible targets which may play a role in the onset of PD. Current literature identifies proteins such as DJ-1, vesicular monoamine transporter 2 (VMAT2), and α -synuclein as playing an important role in Parkinson's disease. DJ-1 has been shown to have protective effects in preserving cell viability (123), while VMAT2 deficient mice demonstrate Parkinson-like symptoms (124). Finally, α -synuclein is a major component of Lewy bodies, which are protein aggregates found in the post-mortem brains of PD patients (31).

In conclusion, all of these studies would further the story of TH inhibition by DOPAL, shedding light on this neurotoxin and the mechanism of action behind protein modification. These results, coupled with the data described here may help lead to better treatments or new therapeutics in the treatment of PD.

APPENDIX A
THE SYNTHESIS OF
3,4-DIMETHOXYPHENYLACETALDEHYDE

Introduction

3,4-Dimethoxyphenylacetaldehyde (DMPAL) is a structural analogue of 3,4-dihydroxyphenylacetaldehyde (DOPAL). This analogue was used as part of the structure-activity studies in order to determine the effect of “masking” the catechol of DOPAL using methyl groups. It was predicted that DMPAL would have decreased toxicity and TH inhibition as compared to DOPAL due to previously published results demonstrating decreased reactivity with N-acetyl-Lys (50). We employed a synthetic scheme previously outlined in the literature (125) with some minor modifications, which is detailed below in Scheme A.1.



Scheme A.1 1-step synthesis of DMPAL (1) using 4-allyl-1,2-dimethoxybenzene (2).

Experimental Procedure

Materials

4-allyl-1-2-dimethoxybenzene, ruthidium chloride (RuCl_3), sodium periodate (NaIO_4) and all other chemicals were purchased from Sigma-Aldrich (St. Louis, MO) unless otherwise noted. NMR spectrum of DMPAL was run in CDCl_3 using a Bruker 300 MHz spectrometer (Appendix D, Figure D.1). DMPAL concentration was determined using an aldehyde dehydrogenase (ALDH) assay which follows the change in absorbance at 340 nm as NAD is converted to NADH when ALDH oxidizes the aldehyde to an acid product. Standards used were dilutions of DOPAL at known concentrations.

Synthesis Method

4-allyl-1-2-dimethoxybenzene (**2**) (0.096 μL (~100 mg), 5.5 mmol) was dissolved in 35 mM RuCl_3 (0.561 mL, 3.5 mol%) and 4 mL 6:1 ACN : H_2O (125). Following this, NaIO_4 was added slowly over a 5 min period (0.4798 g, 5 eq). This stirred for 3 h at room temperature and then was quenched with 8 mL saturated sodium thiosulphate. Using a separatory funnel, compound **1** was extracted into ethyl acetate (3 x 5 mL). After drying the organic layer with MgSO_4 , it was evaporated using a rotary evaporator. The resulting product was further purified using column chromatography on silica gel, eluting the product using a 2:1 mixture of hexanes and ethyl acetate. The product (**1**) was obtained as a brownish-yellow oil in a ~18% yield (~18 mg).

^1NMR (CDCl_3) δ 3.6 (d, 2H), 5.93 (s, 2H), 6.65-6.82 (m, 3H), 9.71 (t, 1H).

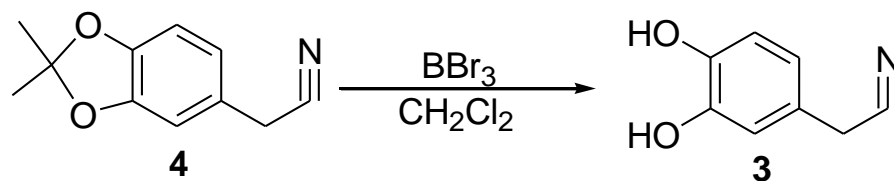
Results

As Scheme A.1 demonstrates, the synthesis of DMPAL is a one-step reaction requiring oxidation of the allyl-moiety to the aldehyde. This synthesis resulted in a 26.5% yield, similar to previously published results (50, 125). NMR confirmation of the product can be found in Appendix D.

APPENDIX B
THE SYNTHESIS OF
3,4-DIHYDROXYPHENYLACETONITRILE

Introduction

3,4-dihydroxyphenylacetonitrile (DHPAN) is a second analogue of 3,4-dihydroxyphenylacetaldehyde (DOPAL) which was used to study the importance of the aldehyde in toxicity and tyrosine hydroxylase (TH) inhibition in both cell lysate and PC6-3 cells. Previously, studies have focused on the importance of the catechol found on DOPAL, and this is the first time the aldehyde role has been investigated. The replacement of the aldehyde with a nitrile group does not significantly change the electronic or steric properties of the molecule; however, the nitrile will not be as reactive toward nucleophiles as a carbonyl (107). DHPAN is synthesized in a one-step procedure which is allowed to stir overnight. Scheme B.1 outlines the synthesis. It is very important to note boron tribromide is extremely reactive with air and water, and using proper protective clothing is necessary. Furthermore, the reaction must be done in dry conditions to minimize the risk of boron tribromide reaction with water.



Scheme B.1 Synthesis of DHPAN (3) from 3,4-methylenedioxyphenylacetonitrile (4).

Experimental Procedure

Materials

3,4-methylenedioxyphenylacetonitrile (**4**), boron tribromide (BBr₃), and all other chemicals were purchased from Sigma-Aldrich (St. Louis, MO) unless otherwise noted. NMR spectrum of DHPAN was run in CDCl₃ using a Bruker 300 MHz spectrometer (Appendix D, Figure D.2).

Synthesis Method

3,4-methylenedioxyphenylacetonitrile (**4**, 500 mg) was added to dry 20 mL CH₂Cl₂. The round bottom flask was then placed in a dry ice bath (-80°C) and while under N₂, 2 equivalents of BBr₃ (0.219 mL) was added drop-wise. This was allowed to stir for 15 min and then removed from the ice bath and allowed to warm slowly to room temperature. The reaction stirred at room temperature for 1.5 h under N₂, and then was quenched using 15 mL H₂O. After stirring for 45 min, the product (**3**) was extracted using ethyl acetate (3 x 10 mL). After drying on a rotovap, the sample was further purified using column separation with silica gel employing a 5:1 petroleum ether : ethyl acetate mobile phase. The remaining starting material eluted slowly, and in order to remove the product methanol was used to strip the column, with a percent yield of ~9% (42.3 mg).

¹NMR (DMSO-d₆): 3.67 (d, 2H), 6.65-6.68 (m, 3H), 8.99 (s, 1H), 9.1 (s, 1H) (126, 127).

Results

As Scheme B.1 demonstrates, the synthesis of DHPAN is a one-step reaction requiring oxidation of the allyl-moiety to the aldehyde. This synthesis resulted in an

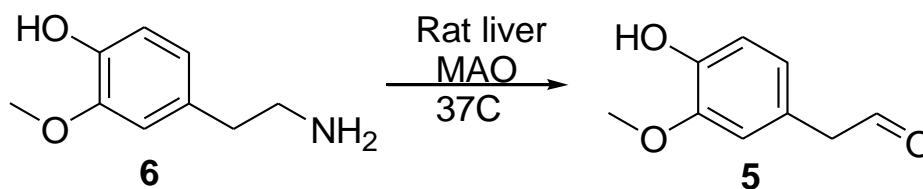
18.6% yield of white powder after rotary evaporation. NMR confirmation of the product can be found in Appendix D.

APPENDIX C
THE BIOSYNTHESIS OF
3-METHOXY-4-HYDROXYPHENYLACETALDEHYDE

(In collaboration with Laurie L. Eckert)

Introduction

3-Methoxy-4-hydroxyphenylacetaldehyde (MOPAL) is the catechol-o-methyltransferase metabolite of DOPAL (106). Studying this compound will give insight into other mechanisms of protein modification and enzyme inhibition in the cell as this metabolite is produced from dopamine (DA) metabolism as well. The biosynthesis of MOPAL is completed using rat liver monoamine oxidase (MAO), similarly to the biosynthesis of DOPAL from DA. Scheme C.1 shows the conversion of 3-methoxytyramine to MOPAL in a one-step biosynthesis at 37°C. The bisulfited product is then extracted using a procedure described below.



Scheme C.1 Biosynthesis of MOPAL (5) from 3-methoxytyramine (6).

Experimental Procedure

Materials

3-methoxytyramine was purchased from Sigma Aldrich (St. Louis, MO). Rat monoamine oxidase was isolated from rat liver and used as described below.

Synthesis Method

0.004 g of 3-methoxytyramine was added to 9.5 mL of potassium phosphate buffer (pH 7.5) and 1.0 mL of 100 mM sodium bisulfite. Rat liver MAO was added (via a membrane pellet after preparation from rat liver), and the mixture was thoroughly vortexed and incubated at 37°C for 4 h with cap loosened, but not off. Approximately every half-hour oxygen was introduced into the mixture and vortexed once again. The reaction was then terminated by centrifugation at 100,000 \times g for 30 min. The supernatant was removed and frozen until the extraction procedure.

MOPAL Extraction

The bisulfited-MOPAL was extracted using Supelco Discovery DSC-18 Solid Phase Extraction (SPE) Tubes. The SPE column was prepped by running 3 mL methanol and then 3 mL of water through it. Next, the MOPAL sample (1.5 mL) was passed through the column and the fraction was saved in order to run on HPLC later for comparison. 3 mL of a 6% acetonitrile/0.01% TFA solution was then run through the column. 0.5 mL fractions were collected as the sample passed through the column and run on HPLC to check for purity.

HPLC analysis showed MOPAL eluting at 3 min, while starting material (3-methoxytyramine) eluted at 7 min. Clean MOPAL fractions were pooled after HPLC

analysis and placed in a glass conical tube with stopper. 0.5 mL of 50 mM sodium pyrophosphate (pH 8.8) was added for every 0.5 mL of MOPAL. ~4 mL of ether was added and the tube was shaken for ~30 sec. After separation, the top layer was removed and saved in separate tubes. The extraction with sodium pyrophosphate and ether was repeated 4 times. At the end of the extraction, 8 tubes of ether are made. To the ether fractions 1-6, 200 μ L of 1 mM HCL was added. Fractions 1-5 are dried separately, while 6-8 are pooled and dried. The ether was allowed to dry off, taking care not to dry the sample completely as this decreases yield and increases polymer formation. Diluted samples were run on HPLC to check for purity and loss of bisulfite.

HPLC analysis

HPLC analysis was carried out using an Agilent 1200 Series HPLC with a Phenomenex Luna C18 column (1 x 150 mm, 100 Å). A gradient was used employing 0.1% TFA in water (A) and ACN (B), following this time line: 0-12 min: 3% B, 12-13 min: 10% B, 13-23 min: 10% B, 23-24 min: 3% B, 24-35 min: 3% B. Flow rate was 50 μ L/min and MOPAL eluted at ~9 min under these conditions.

Results

As Scheme C.1 demonstrates, MOPAL can be biosynthesized in one step using rat liver MAO to oxidize 3-methoxytyramine. Following synthesis, MOPAL is extracted and the bisulfite used to stabilize the product is removed. HPLC analysis was used to successfully determine purity and concentration.

REFERENCES

- (1) Madej, T., Address, K. J., Fong, J. H., Geer, L. Y., Geer, R. C., Lanczycki, C. J., Liu, C., Lu, S., Marchler-Bauer, A., Panchenko, A. R., Chen, J., Thiessen, P. A., Wang, Y., Zhang, D. and Bryant, S. H. (2012) MMDB: 3D structures and macromolecular interactions. *Nucleic Acids Res* 40, D461-464.
- (2) Lees, A. J., Hardy, J. and Revesz, T. (2009) Parkinson's disease. *Lancet* 373, 2055-2066.
- (3) Dauer, W. and Przedborski, S. (2003) Parkinson's disease: mechanisms and models. *Neuron* 39, 889-909.
- (4) Salawu, F. K., Danburam, A. and Olokoba, A. B. (2010) Non-motor symptoms of Parkinson's disease: diagnosis and management. *Niger J Med* 19, 126-131.
- (5) Andersen, J. K. (2004) Oxidative stress in neurodegeneration: cause or consequence? *Nat Med* 10 Suppl, S18-25.
- (6) Goetz, C. G., Poewe, W., Rascol, O. and Sampaio, C. (2005) Evidence-based medical review update: pharmacological and surgical treatments of Parkinson's disease: 2001 to 2004. *Mov Disord* 20, 523-539.
- (7) Shannon, K. M., Bennett, J. P., Jr. and Friedman, J. H. (1997) Efficacy of pramipexole, a novel dopamine agonist, as monotherapy in mild to moderate Parkinson's disease. The Pramipexole Study Group. *Neurology* 49, 724-728.
- (8) Kanthasamy, A. G., Kitazawa, M., Kanthasamy, A. and Anantharam, V. (2005) Dieldrin-induced neurotoxicity: relevance to Parkinson's disease pathogenesis. *Neurotoxicology* 26, 701-719.
- (9) Sharma, H., Zhang, P., Barber, D. S. and Liu, B. (2010) Organochlorine pesticides dieldrin and lindane induce cooperative toxicity in dopaminergic neurons: role of oxidative stress. *Neurotoxicology* 31, 215-222.
- (10) Bates, M. N., Buckland, S. J., Garrett, N., Ellis, H., Needham, L. L., Patterson, D. G., Jr., Turner, W. E. and Russell, D. G. (2004) Persistent organochlorines in the serum of the non-occupationally exposed New Zealand population. *Chemosphere* 54, 1431-1443.
- (11) Corrigan, F. M., Murray, L., Wyatt, C. L. and Shore, R. F. (1998) Diorthosubstituted polychlorinated biphenyls in caudate nucleus in Parkinson's disease. *Exp Neurol* 150, 339-342.
- (12) Fleming, L., Mann, J. B., Bean, J., Briggles, T. and Sanchez-Ramos, J. R. (1994) Parkinson's disease and brain levels of organochlorine pesticides. *Ann Neurol* 36, 100-103.

- (13) Sharma, R. P., Winn, D. S. and Low, J. B. (1976) Toxic, neurochemical and behavioral effects of dieldrin exposure in mallard ducks. *Arch Environ Contam Toxicol* 5, 43-53.
- (14) Miller, G. W., Kirby, M. L., Levey, A. I. and Bloomquist, J. R. (1999) Heptachlor alters expression and function of dopamine transporters. *Neurotoxicology* 20, 631-637.
- (15) Kitazawa, M., Anantharam, V. and Kanthasamy, A. G. (2001) Dieldrin-induced oxidative stress and neurochemical changes contribute to apoptotic cell death in dopaminergic cells. *Free Radic Biol Med* 31, 1473-1485.
- (16) Kitazawa, M., Anantharam, V. and Kanthasamy, A. G. (2003) Dieldrin induces apoptosis by promoting caspase-3-dependent proteolytic cleavage of protein kinase Cdelta in dopaminergic cells: relevance to oxidative stress and dopaminergic degeneration. *Neuroscience* 119, 945-964.
- (17) Allen, E. M., Anderson, D. G., Florang, V. R., Khanna, M., Hurley, T. D. and Doorn, J. A. (2010) Relative inhibitory potency of molinate and metabolites with aldehyde dehydrogenase 2: implications for the mechanism of enzyme inhibition. *Chem Res Toxicol* 23, 1843-1850.
- (18) Quistad, G. B., Sparks, S. E. and Casida, J. E. (1994) Aldehyde dehydrogenase of mice inhibited by thiocarbamate herbicides. *Life Sci* 55, 1537-1544.
- (19) Jewell, W. T. and Miller, M. G. (1999) Comparison of human and rat metabolism of molinate in liver microsomes and slices. *Drug Metab Dispos* 27, 842-847.
- (20) Youdim, M. B., Ben-Shachar, D. and Riederer, P. (1991) Iron in brain function and dysfunction with emphasis on Parkinson's disease. *Eur Neurol* 31 Suppl 1, 34-40.
- (21) Ben-Shachar, D., Riederer, P. and Youdim, M. B. (1991) Iron-melanin interaction and lipid peroxidation: implications for Parkinson's disease. *J Neurochem* 57, 1609-1614.
- (22) Rasia, R. M., Bertocini, C. W., Marsh, D., Hoyer, W., Cherny, D., Zweckstetter, M., Griesinger, C., Jovin, T. M. and Fernandez, C. O. (2005) Structural characterization of copper(II) binding to alpha-synuclein: Insights into the bioinorganic chemistry of Parkinson's disease. *Proc Natl Acad Sci U S A* 102, 4294-4299.
- (23) Olanow, C. W. (2004) Manganese-induced parkinsonism and Parkinson's disease. *Ann N Y Acad Sci* 1012, 209-223.
- (24) Gasser, T. (2001) Genetics of Parkinson's disease. *J Neurol* 248, 833-840.
- (25) Dawson, T. M. and Dawson, V. L. (2010) The role of parkin in familial and sporadic Parkinson's disease. *Mov Disord* 25 Suppl 1, S32-39.

- (26) Brice, A. (2005) Genetics of Parkinson's disease: LRRK2 on the rise. *Brain* 128, 2760-2762.
- (27) Healy, D. G., Falchi, M., O'Sullivan, S. S., Bonifati, V., Durr, A., Bressman, S., Brice, A., Aasly, J., Zabetian, C. P., Goldwurm, S., Ferreira, J. J., Tolosa, E., Kay, D. M., Klein, C., Williams, D. R., Marras, C., Lang, A. E., Wszolek, Z. K., Berciano, J., Schapira, A. H., Lynch, T., Bhatia, K. P., Gasser, T., Lees, A. J. and Wood, N. W. (2008) Phenotype, genotype, and worldwide genetic penetrance of LRRK2-associated Parkinson's disease: a case-control study. *Lancet Neurol* 7, 583-590.
- (28) Wszolek, Z. K., Pfeiffer, R. F., Tsuboi, Y., Uitti, R. J., McComb, R. D., Stoessl, A. J., Strongosky, A. J., Zimprich, A., Muller-Mysok, B., Farrer, M. J., Gasser, T., Calne, D. B. and Dickson, D. W. (2004) Autosomal dominant parkinsonism associated with variable synuclein and tau pathology. *Neurology* 62, 1619-1622.
- (29) Martin, I., Dawson, V. L. and Dawson, T. M. Recent advances in the genetics of Parkinson's disease. *Annu Rev Genomics Hum Genet* 12, 301-325.
- (30) Davidson, W. S., Jonas, A., Clayton, D. F. and George, J. M. (1998) Stabilization of alpha-synuclein secondary structure upon binding to synthetic membranes. *J Biol Chem* 273, 9443-9449.
- (31) Winslow, A. R., Chen, C. W., Corrochano, S., Acevedo-Aroza, A., Gordon, D. E., Peden, A. A., Lichtenberg, M., Menzies, F. M., Ravikumar, B., Imarisio, S., Brown, S., O'Kane, C. J. and Rubinsztein, D. C. (2010) alpha-Synuclein impairs macroautophagy: implications for Parkinson's disease. *J Cell Biol* 190, 1023-1037.
- (32) Grimsrud, P. A., Xie, H., Griffin, T. J. and Bernlohr, D. A. (2008) Oxidative stress and covalent modification of protein with bioactive aldehydes. *J Biol Chem* 283, 21837-21841.
- (33) Jinsmaa, Y., Florang, V. R., Rees, J. N., Anderson, D. G., Strack, S. and Doorn, J. A. (2009) Products of oxidative stress inhibit aldehyde oxidation and reduction pathways in dopamine catabolism yielding elevated levels of a reactive intermediate. *Chem Res Toxicol* 22, 835-841.
- (34) Rees, J. N., Florang, V. R., Anderson, D. G. and Doorn, J. A. (2007) Lipid peroxidation products inhibit dopamine catabolism yielding aberrant levels of a reactive intermediate. *Chem Res Toxicol* 20, 1536-1542.
- (35) Doorn, J. A., Hurley, T. D. and Petersen, D. R. (2006) Inhibition of human mitochondrial aldehyde dehydrogenase by 4-hydroxynon-2-enal and 4-oxonon-2-enal. *Chem Res Toxicol* 19, 102-110.
- (36) Dexter, D. T., Carter, C. J., Wells, F. R., Javoy-Agid, F., Agid, Y., Lees, A., Jenner, P. and Marsden, C. D. (1989) Basal lipid peroxidation in substantia nigra is increased in Parkinson's disease. *J Neurochem* 52, 381-389.

- (37) Yoritaka, A., Hattori, N., Uchida, K., Tanaka, M., Stadtman, E. R. and Mizuno, Y. (1996) Immunohistochemical detection of 4-hydroxynonenal protein adducts in Parkinson disease. *Proc Natl Acad Sci U S A* 93, 2696-2701.
- (38) Eruslanov, E. and Kusmartsev, S. (2010) Identification of ROS using oxidized DCFDA and flow-cytometry. *Methods Mol Biol* 594, 57-72.
- (39) Sayre, L. M., Perry, G. and Smith, M. A. (2008) Oxidative stress and neurotoxicity. *Chem Res Toxicol* 21, 172-188.
- (40) Nagatsu, T., Levitt, M. and Udenfriend, S. (1964) Tyrosine Hydroxylase. The Initial Step in Norepinephrine Biosynthesis. *J Biol Chem* 239, 2910-2917.
- (41) Hastings, T. G., Lewis, D. A. and Zigmond, M. J. (1996) Reactive dopamine metabolites and neurotoxicity: implications for Parkinson's disease. *Adv Exp Med Biol* 387, 97-106.
- (42) Spencer, J. P., Jenner, P., Daniel, S. E., Lees, A. J., Marsden, D. C. and Halliwell, B. (1998) Conjugates of catecholamines with cysteine and GSH in Parkinson's disease: possible mechanisms of formation involving reactive oxygen species. *J Neurochem* 71, 2112-2122.
- (43) Van Laar, V. S., Dukes, A. A., Cascio, M. and Hastings, T. G. (2008) Proteomic analysis of rat brain mitochondria following exposure to dopamine quinone: implications for Parkinson disease. *Neurobiol Dis* 29, 477-489.
- (44) Graham, D. G. (1978) Oxidative pathways for catecholamines in the genesis of neuromelanin and cytotoxic quinones. *Mol Pharmacol* 14, 633-643.
- (45) Stokes, A. H., Hastings, T. G. and Vrana, K. E. (1999) Cytotoxic and genotoxic potential of dopamine. *J Neurosci Res* 55, 659-665.
- (46) Burke, W. J., Li, S. W., Williams, E. A., Nonneman, R. and Zahm, D. S. (2003) 3,4-Dihydroxyphenylacetaldehyde is the toxic dopamine metabolite in vivo: implications for Parkinson's disease pathogenesis. *Brain Res* 989, 205-213.
- (47) Kristal, B. S., Conway, A. D., Brown, A. M., Jain, J. C., Ulluci, P. A., Li, S. W. and Burke, W. J. (2001) Selective dopaminergic vulnerability: 3,4-dihydroxyphenylacetaldehyde targets mitochondria. *Free Radic Biol Med* 30, 924-931.
- (48) Mattammal, M. B., Haring, J. H., Chung, H. D., Raghu, G. and Strong, R. (1995) An endogenous dopaminergic neurotoxin: implication for Parkinson's disease. *Neurodegeneration* 4, 271-281.
- (49) Burke, W. J., Chung, H. D. and Li, S. W. (1999) Quantitation of 3,4-dihydroxyphenylacetaldehyde and 3, 4-dihydroxyphenylglycolaldehyde, the monoamine oxidase metabolites of dopamine and noradrenaline, in human tissues by microcolumn high-performance liquid chromatography. *Anal Biochem* 273, 111-116.

- (50) Rees, J. N., Florang, V. R., Eckert, L. L. and Doorn, J. A. (2009) Protein reactivity of 3,4-dihydroxyphenylacetaldehyde, a toxic dopamine metabolite, is dependent on both the aldehyde and the catechol. *Chem Res Toxicol* 22, 1256-1263.
- (51) Helander, A. and Tottmar, O. (1989) Reactions of biogenic aldehydes with hemoglobin. *Alcohol* 6, 71-75.
- (52) Ungar, F., Tabakoff, B. and Alivisatos, S. G. (1973) Inhibition of binding of aldehydes of biogenic amines in tissues. *Biochem Pharmacol* 22, 1905-1913.
- (53) LaVoie, M. J., Ostaszewski, B. L., Weihofen, A., Schlossmacher, M. G. and Selkoe, D. J. (2005) Dopamine covalently modifies and functionally inactivates parkin. *Nat Med* 11, 1214-1221.
- (54) Nilsson, G. E. and Tottmar, O. (1987) Biogenic aldehydes in brain: on their preparation and reactions with rat brain tissue. *J Neurochem* 48, 1566-1572.
- (55) Goodwill, K. E., Sabatier, C., Marks, C., Raag, R., Fitzpatrick, P. F. and Stevens, R. C. (1997) Crystal structure of tyrosine hydroxylase at 2.3 Å and its implications for inherited neurodegenerative diseases. *Nat Struct Biol* 4, 578-585.
- (56) McCulloch, R. I., Daubner, S. C. and Fitzpatrick, P. F. (2001) Effects of substitution at serine 40 of tyrosine hydroxylase on catecholamine binding. *Biochemistry* 40, 7273-7278.
- (57) Wu, J., Filer, D., Friedhoff, A. J. and Goldstein, M. (1992) Site-directed mutagenesis of tyrosine hydroxylase. Role of serine 40 in catalysis. *J Biol Chem* 267, 25754-25758.
- (58) Gordon, S. L., Quinsey, N. S., Dunkley, P. R. and Dickson, P. W. (2008) Tyrosine hydroxylase activity is regulated by two distinct dopamine-binding sites. *J Neurochem* 106, 1614-1623.
- (59) Datla, K. P., Blunt, S. B. and Dexter, D. T. (2001) Chronic L-DOPA administration is not toxic to the remaining dopaminergic nigrostriatal neurons, but instead may promote their functional recovery, in rats with partial 6-OHDA or FeCl₃ nigrostriatal lesions. *Mov Disord* 16, 424-434.
- (60) Murer, M. G., Dziewczapolski, G., Menalled, L. B., Garcia, M. C., Agid, Y., Gershanik, O. and Raisman-Vozari, R. (1998) Chronic levodopa is not toxic for remaining dopamine neurons, but instead promotes their recovery, in rats with moderate nigrostriatal lesions. *Ann Neurol* 43, 561-575.
- (61) Xu, Y., Stokes, A. H., Roskoski, R., Jr. and Vrana, K. E. (1998) Dopamine, in the presence of tyrosinase, covalently modifies and inactivates tyrosine hydroxylase. *J Neurosci Res* 54, 691-697.

- (62) Laschinski, G., Kittner, B. and Brautigam, M. (1986) Direct inhibition of tyrosine hydroxylase from PC-12 cells by catechol derivatives. *Naunyn Schmiedeberg's Arch Pharmacol* 332, 346-350.
- (63) Burke, W. J. (2003) 3,4-dihydroxyphenylacetaldehyde: a potential target for neuroprotective therapy in Parkinson's disease. *Curr Drug Targets CNS Neurol Disord* 2, 143-148.
- (64) Anderson, D. G., Mariappan, S. V., Buettner, G. R. and Doorn, J. A. (2011) Oxidation of 3,4-dihydroxyphenylacetaldehyde, a toxic dopaminergic metabolite, to a semiquinone radical and an ortho-quinone. *J Biol Chem* 286, 26978-26986.
- (65) Jenner, P. (2003) Oxidative stress in Parkinson's disease. *Ann Neurol* 53 Suppl 3, S26-36; discussion S36-28.
- (66) Graham, D. G., Tiffany, S. M., Bell, W. R., Jr. and Gutknecht, W. F. (1978) Autoxidation versus covalent binding of quinones as the mechanism of toxicity of dopamine, 6-hydroxydopamine, and related compounds toward C1300 neuroblastoma cells in vitro. *Mol Pharmacol* 14, 644-653.
- (67) Burke, W. J., Li, S. W., Chung, H. D., Ruggiero, D. A., Kristal, B. S., Johnson, E. M., Lampe, P., Kumar, V. B., Franko, M., Williams, E. A. and Zahm, D. S. (2004) Neurotoxicity of MAO Metabolites of Catecholamine Neurotransmitters: Role in Neurodegenerative Diseases. *Neurotoxicology* 25, 101-115.
- (68) Strack, S. (2002) Overexpression of the protein phosphatase 2A regulatory subunit Bgamma promotes neuronal differentiation by activating the MAP kinase (MAPK) cascade. *J Biol Chem* 277, 41525-41532.
- (69) Pittman, R. N., Wang, S., DiBenedetto, A. J. and Mills, J. C. (1993) A system for characterizing cellular and molecular events in programmed neuronal cell death. *J Neurosci* 13, 3669-3680.
- (70) Hirata, Y., Adachi, K. and Kiuchi, K. (1998) Activation of JNK pathway and induction of apoptosis by manganese in PC12 cells. *J Neurochem* 71, 1607-1615.
- (71) Shafer, T. J. and Atchison, W. D. (1991) Transmitter, ion channel and receptor properties of pheochromocytoma (PC12) cells: a model for neurotoxicological studies. *Neurotoxicology* 12, 473-492.
- (72) Seegal, R. F., Brosch, K., Bush, B., Ritz, M. and Shain, W. (1989) Effects of Aroclor 1254 on dopamine and norepinephrine concentrations in pheochromocytoma (PC-12) cells. *Neurotoxicology* 10, 757-764.
- (73) Strober, W. (2001) Trypan blue exclusion test of cell viability. *Curr Protoc Immunol Appendix 3*, Appendix 3B.
- (74) Hegstrand, L. R., Simon, J. R. and Roth, R. H. (1979) Tyrosine hydroxylase:--examination of conditions influencing activity in pheochromocytoma, adrenal medulla and striatum. *Biochem Pharmacol* 28, 519-523.

- (75) Jimenez, C. R. H., L.; Qui, Y.; and Burlingame, A.L. (1998) *Current Protocols in Protein Science*, John Wiley and Sons, New York.
- (76) Nesvizhskii, A. I., Keller, A., Kolker, E. and Aebersold, R. (2003) A statistical model for identifying proteins by tandem mass spectrometry. *Anal Chem* 75, 4646-4658.
- (77) Marchitti, S. A., Deitrich, R. A. and Vasiliou, V. (2007) Neurotoxicity and metabolism of the catecholamine-derived 3,4-dihydroxyphenylacetaldehyde and 3,4-dihydroxyphenylglycolaldehyde: the role of aldehyde dehydrogenase. *Pharmacol Rev* 59, 125-150.
- (78) Elsworth, J. D. and Roth, R. H. (1997) Dopamine synthesis, uptake, metabolism, and receptors: relevance to gene therapy of Parkinson's disease. *Exp Neurol* 144, 4-9.
- (79) Bairoch, A. and Apweiler, R. (2000) The SWISS-PROT protein sequence database and its supplement TrEMBL in 2000. *Nucleic Acids Res* 28, 45-48.
- (80) Volchenboum, S. L., Kristjansdottir, K., Wolfgeher, D. and Kron, S. J. (2009) Rapid validation of Mascot search results via stable isotope labeling, pair picking, and deconvolution of fragmentation patterns. *Mol Cell Proteomics* 8, 2011-2022.
- (81) Kulagina, N. V. and Michael, A. C. (2003) Monitoring hydrogen peroxide in the extracellular space of the brain with amperometric microsensors. *Anal Chem* 75, 4875-4881.
- (82) Harada, S., Misawa, S., Agarwal, D. P. and Goedde, H. W. (1980) Liver alcohol dehydrogenase and aldehyde dehydrogenase in the Japanese: isozyme variation and its possible role in alcohol intoxication. *Am J Hum Genet* 32, 8-15.
- (83) Badawy, A. A., Bano, S. and Steptoe, A. (2011) Tryptophan in alcoholism treatment II: inhibition of the rat liver mitochondrial low Km aldehyde dehydrogenase activity, elevation of blood acetaldehyde concentration and induction of aversion to alcohol by combined administration of tryptophan and benserazide. *Alcohol Alcohol* 46, 661-671.
- (84) Doorn, J. A. (2010) Dopamine catabolism and Parkinson's disease: Role of a reactive aldehyde intermediate, In *Endogenous Toxins: Targets for Disease Treatment and Prevention* (O'Brien, P. J. B., W.R., Ed.), Wiley-VCH Verlag GmbH & Co., Weinheim.
- (85) Turner, A. J., Illingworth, J. A. and Tipton, K. F. (1974) Simulation of biogenic amine metabolism in the brain. *Biochem J* 144, 353-360.
- (86) Oreland, L. and Gottfries, C. G. (1986) Brain and brain monoamine oxidase in aging and in dementia of Alzheimer's type. *Prog Neuropsychopharmacol Biol Psychiatry* 10, 533-540.

- (87) Goldstein, D. S., Sullivan, P., Holmes, C., Kopin, I. J., Basile, M. J. and Mash, D. C. (2010) Catechols in post-mortem brain of patients with Parkinson disease. *Eur J Neurol* 18, 703-710.
- (88) Mexas, L. M., Florang, V. R. and Doorn, J. A. (2011) Inhibition and covalent modification of tyrosine hydroxylase by 3,4-dihydroxyphenylacetaldehyde, a toxic dopamine metabolite. *Neurotoxicology*.
- (89) Fitzpatrick, P. F. (1991) Steady-state kinetic mechanism of rat tyrosine hydroxylase. *Biochemistry* 30, 3658-3662.
- (90) Nakashima, A., Hayashi, N., Kaneko, Y. S., Mori, K., Sabban, E. L., Nagatsu, T. and Ota, A. (2009) Role of N-terminus of tyrosine hydroxylase in the biosynthesis of catecholamines. *J Neural Transm* 116, 1355-1362.
- (91) Esterbauer, H., Schaur, R. J. and Zollner, H. (1991) Chemistry and biochemistry of 4-hydroxynonenal, malonaldehyde and related aldehydes. *Free Radic Biol Med* 11, 81-128.
- (92) Clift-O'Grady, L., Linstedt, A. D., Lowe, A. W., Grote, E. and Kelly, R. B. (1990) Biogenesis of synaptic vesicle-like structures in a pheochromocytoma cell line PC-12. *J Cell Biol* 110, 1693-1703.
- (93) Stone, D. M., Stahl, D. C., Hanson, G. R. and Gibb, J. W. (1986) The effects of 3,4-methylenedioxymethamphetamine (MDMA) and 3,4-methylenedioxyamphetamine (MDA) on monoaminergic systems in the rat brain. *Eur J Pharmacol* 128, 41-48.
- (94) Kuhn, D. M., Arthur, R. E., Jr., Thomas, D. M. and Elferink, L. A. (1999) Tyrosine hydroxylase is inactivated by catechol-quinones and converted to a redox-cycling quinoprotein: possible relevance to Parkinson's disease. *J Neurochem* 73, 1309-1317.
- (95) Conway, K. A., Rochet, J. C., Bieganski, R. M. and Lansbury, P. T., Jr. (2001) Kinetic stabilization of the alpha-synuclein protofibril by a dopamine-alpha-synuclein adduct. *Science* 294, 1346-1349.
- (96) Udenfriend, S., Zaltzman-Nirenberg, P. and Nagatsu, T. (1965) Inhibitors of purified beef adrenal tyrosine hydroxylase. *Biochem Pharmacol* 14, 837-845.
- (97) Rees, J. N. (2009) Protein reactivity of 3,4-dihydroxyphenylacetaldehyde, an endogenous, potential neurotoxin relevant to Parkinson's disease, In *Medicinal and Natural Products Chemistry* p 186, The University of Iowa, Iowa City.
- (98) Paz, M. A., Fluckiger, R., Boak, A., Kagan, H. M. and Gallop, P. M. (1991) Specific detection of quinoproteins by redox-cycling staining. *J Biol Chem* 266, 689-692.

- (99) Akagawa, M., Ishii, Y., Ishii, T., Shibata, T., Yotsu-Yamashita, M., Suyama, K. and Uchida, K. (2006) Metal-catalyzed oxidation of protein-bound dopamine. *Biochemistry* 45, 15120-15128.
- (100) Kristelly, R., Gao, G. and Tesmer, J. J. (2004) Structural determinants of RhoA binding and nucleotide exchange in leukemia-associated Rho guanine-nucleotide exchange factor. *J Biol Chem* 279, 47352-47362.
- (101) Wessel, D. and Flugge, U. I. (1984) A method for the quantitative recovery of protein in dilute solution in the presence of detergents and lipids. *Anal Biochem* 138, 141-143.
- (102) Winder, A. J. and Harris, H. (1991) New assays for the tyrosine hydroxylase and dopa oxidase activities of tyrosinase. *Eur J Biochem* 198, 317-326.
- (103) Fitzpatrick, P. F. (1991) Studies of the rate-limiting step in the tyrosine hydroxylase reaction: alternate substrates, solvent isotope effects, and transition-state analogues. *Biochemistry* 30, 6386-6391.
- (104) Martinez, A., Abeygunawardana, C., Haavik, J., Flatmark, T. and Mildvan, A. S. (1993) Interaction of substrate and pterin cofactor with the metal of human tyrosine hydroxylase as determined by ¹H-NMR. *Adv Exp Med Biol* 338, 77-80.
- (105) Fujisawa, H., Okuno, S. (1987) [8] Tyrosine 3-monooxygenase from rat adrenals. *Methods Enzymol* 142, 63-71.
- (106) Guldberg, H. C. and Marsden, C. A. (1975) Catechol-O-methyl transferase: pharmacological aspects and physiological role. *Pharmacol Rev* 27, 135-206.
- (107) Oballa, R. M., Truchon, J. F., Bayly, C. I., Chauret, N., Day, S., Crane, S. and Berthelette, C. (2007) A generally applicable method for assessing the electrophilicity and reactivity of diverse nitrile-containing compounds. *Bioorg Med Chem Lett* 17, 998-1002.
- (108) Le Bourdelles, B., Horellou, P., Le Caer, J. P., Deneffe, P., Latta, M., Haavik, J., Guibert, B., Mayaux, J. F. and Mallet, J. (1991) Phosphorylation of human recombinant tyrosine hydroxylase isoforms 1 and 2: an additional phosphorylated residue in isoform 2, generated through alternative splicing. *J Biol Chem* 266, 17124-17130.
- (109) Gahn, L. G. and Roskoski, R., Jr. (1991) Tyrosine hydroxylase purification from rat PC12 cells. *Protein Expr Purif* 2, 10-14.
- (110) Haavik, J., Le Bourdelles, B., Martinez, A., Flatmark, T. and Mallet, J. (1991) Recombinant human tyrosine hydroxylase isozymes. Reconstitution with iron and inhibitory effect of other metal ions. *Eur J Biochem* 199, 371-378.
- (111) Kuhn, D. M. and Billingsley, M. L. (1987) Tyrosine hydroxylase: purification from PC-12 cells, characterization and production of antibodies. *Neurochem Int* 11, 463-475.

- (112) Lamensdorf, I., Hrycyna, C., He, L. P., Nechushtan, A., Tjurmina, O., Harvey-White, J., Eisenhofer, G., Rojas, E. and Kopin, I. J. (2000) Acidic dopamine metabolites are actively extruded from PC12 cells by a novel sulfonylurea-sensitive transporter. *Naunyn Schmiedebergs Arch Pharmacol* 361, 654-664.
- (113) Leviel, V. Dopamine release mediated by the dopamine transporter, facts and consequences. *J Neurochem* 118, 475-489.
- (114) Hanzlik, R. P., Zygmunt, J. and Moon, J. B. (1990) Reversible covalent binding of peptide nitriles to papain. *Biochim Biophys Acta* 1035, 62-70.
- (115) MacFaul, P. A., Morley, A. D. and Crawford, J. J. (2009) A simple in vitro assay for assessing the reactivity of nitrile containing compounds. *Bioorg Med Chem Lett* 19, 1136-1138.
- (116) Eisenhofer, G., Aneman, A., Hooper, D., Holmes, C., Goldstein, D. S. and Friberg, P. (1995) Production and metabolism of dopamine and norepinephrine in mesenteric organs and liver of swine. *Am J Physiol* 268, G641-649.
- (117) Goodwill, K. E., Sabatier, C. and Stevens, R. C. (1998) Crystal structure of tyrosine hydroxylase with bound cofactor analogue and iron at 2.3 Å resolution: self-hydroxylation of Phe300 and the pterin-binding site. *Biochemistry* 37, 13437-13445.
- (118) Zhang, Q., Crosland, E. and Fabris, D. (2008) Nested Arg-specific bifunctional crosslinkers for MS-based structural analysis of proteins and protein assemblies. *Anal Chim Acta* 627, 117-128.
- (119) Saraiva, M. A., Borges, C. M. and Florencio, M. H. (2006) Non-enzymatic model glycation reactions--a comprehensive study of the reactivity of a modified arginine with aldehydic and diketonic dicarbonyl compounds by electrospray mass spectrometry. *J Mass Spectrom* 41, 755-770.
- (120) Nagatsu, T., Levitt, M. and Udenfriend, S. (1964) A Rapid and Simple Radioassay for Tyrosine Hydroxylase Activity. *Anal Biochem* 9, 122-126.
- (121) Almas, B., Le Bourdelles, B., Flatmark, T., Mallet, J. and Haavik, J. (1992) Regulation of recombinant human tyrosine hydroxylase isozymes by catecholamine binding and phosphorylation. Structure/activity studies and mechanistic implications. *Eur J Biochem* 209, 249-255.
- (122) Fujisawa, H. and Okuno, S. (2005) Regulatory mechanism of tyrosine hydroxylase activity. *Biochem Biophys Res Commun* 338, 271-276.
- (123) Lev, N., Roncevic, D., Ickowicz, D., Melamed, E. and Offen, D. (2006) Role of DJ-1 in Parkinson's disease. *J Mol Neurosci* 29, 215-225.
- (124) Taylor, T. N., Caudle, W. M. and Miller, G. W. (2011) VMAT2-Deficient Mice Display Nigral and Extranigral Pathology and Motor and Nonmotor Symptoms of Parkinson's Disease. *Parkinsons Dis* 2011, 124165.

- (125) Yang, D. and Zhang, C. (2001) Ruthenium-catalyzed oxidative cleavage of olefins to aldehydes. *J Org Chem* 66, 4814-4818.
- (126) Mzengeza, S., Whitney, R.A. (1988) Asymmetric Induction in Nitronc Cycloadditions. *J. Org. Chem* 53, 4074-4081.
- (127) Nguyen, N. H., Cougnon, C. and Gohier, F. (2009) Deprotection of arenediazonium tetrafluoroborate ethers with BBr₃. *J Org Chem* 74, 3955-3957.